Southeastern Geology: Volume 44, No. 4
February 2007

Editor in Chief: S. Duncan Heron, Jr.

Abstract

Academic journal published quarterly by the Department of Geology, Duke University.

SOUTHEASTERN GEOLOGY

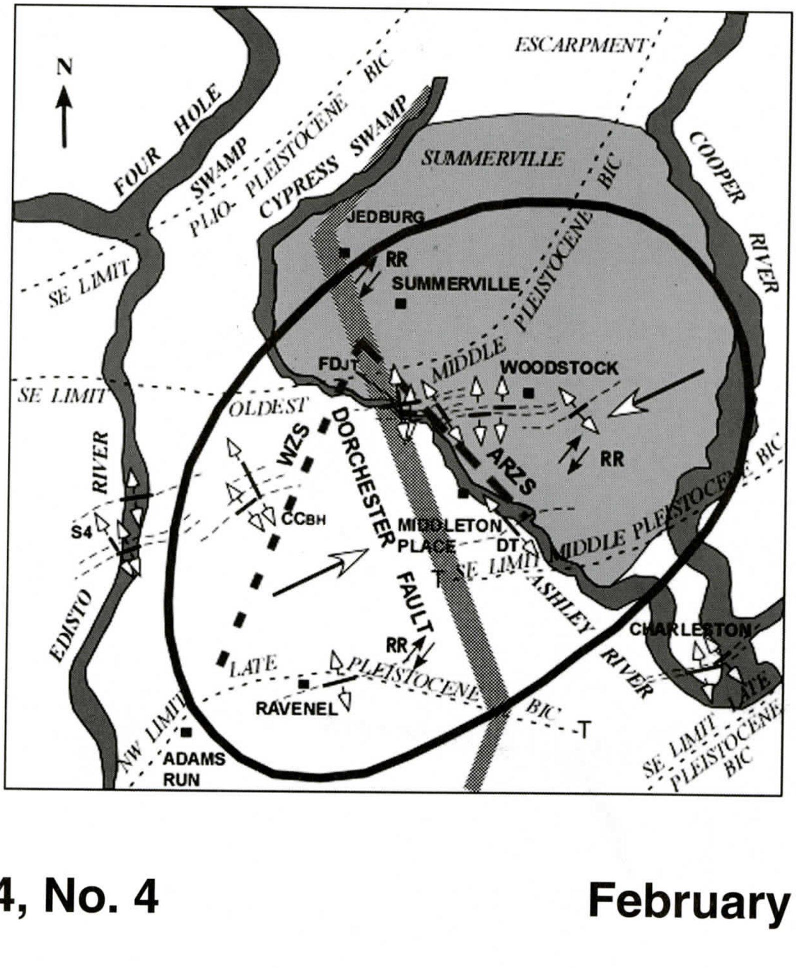

Vol. 44, No. 4 February 2007

SOUTHEASTERN GEOLOGY

PUBLISHED

at

DUKE UNIVERSITY

Duncan Heron

Editor in Chief

David M. Bush

Editor

This journal publishes the results of original research on all phases of geology, geophysics, geochemistry and environmental geology as related to the Southeast. Send manuscripts to **David Bush, Department of Geosciences, University of West Georgia, Carrollton, Georgia 30118, for Fed-X, etc. 1601 Maple St.,** Phone: 678-839-4057, Fax: 678-839-4071, Email: dbush@westga.edu. Please observe the following:

1) Type the manuscript with double space lines and submit in duplicate, or submit as an Acrobat file attached to an email.
2) Cite references and prepare bibliographic lists in accordance with the method found within the pages of this journal. Data citations examples can be found at http://www.geoinfo.org/TFGeosciData.htm
3) Submit line drawings and complex tables reduced to final publication size (no bigger than 8 x 5 3/8 inches).
4) Make certain that all photographs are sharp, clear, and of good contrast.
5) Stratigraphic terminology should abide by the North American Stratigraphic Code (American Association Petroleum Geologists Bulletin, v. 67, p. 841-875).
6) Email Acrobat (pdf) submissions are encouraged.

Subscriptions to *Southeastern Geology* for volume 44 are: individuals - $24.00 (paid by personal check); corporations and libraries - $35.00; foreign $45. Inquires should be sent to: **SOUTHEASTERN GEOLOGY, DUKE UNIVERSITY, DIVISION OF EARTH & OCEAN SCIENCES, BOX 90233, DURHAM, NORTH CAROLINA 27708-0233**. Make checks payable to: *Southeastern Geology*.

Information about **SOUTHEASTERN GEOLOGY** is on the World Wide Web including a searchable author-title index 1958-2001 (Acrobat format). The URL for the Web site is: http://www.southeasterngeology.org

SOUTHEASTERN GEOLOGY is a peer review journal.

ISSN 0038-3678

SOUTHEASTERN GEOLOGY

Table of Contents

Volume 44, No. 4 February 2007

1. THE WALLS OF COLONIAL FORT DORCHESTER: A RECORD OF STRUCTURES CAUSED BY THE AUGUST 31, 1886 CHARLESTON, SOUTH CAROLINA, EARTHQUAKE AND ITS SUBSEQUENT EARTHQUAKE HISTORY
MERVIN J. BARTHOLOMEW AND FREDRICK J. RICH. 147

2. CRADLE-OF-FORESTRY-IN-AMERICA FAULT, AN ACADIAN AND ALLEGHANIAN DEXTRAL STRIKE-SLIP FAULT WITHIN THE EASTERN BLUE RIDGE, TRANSYLVANIA COUNTY, NORTH CAROLINA
JAMES A. DOCKAL. 171

3. THE STRATIGRAPHIC UTILITY OF THE TRACE FOSSIL *PTERIDICHNITES BISERIATUS* IN THE UPPER DEVONIAN OF EASTERN WEST VIRGINIA AND WESTERN VIRGINIA, USA
RONALD R. MCDOWELL, KATHARINE L. AVARY, DAVID L. MATCHEN AND JAMES Q. BRITTON 191

4. QUATERNARY COASTAL DEVELOPMENT IN NW FLORIDA: MISCONCEPTIONS RELATED TO EOLIAN PROCESSES: DISCUSSION OF A PAPER BY CARL R. FROEDE, JR., BRIAN R. RUCKER AND RICHARD L. GILLAM
ERVIN G. OTVOS 203

5. REPLY TO ERVIN G. OTVOS: "QUATERNARY COASTAL DEVELOPMENT IN NW FLORIDA: MISCONCEPTIONS RELATED TO EOLIAN PROCESSES"
CARL R. FROEDE, JR., BRIAN R. RUCKER AND RICHARD L. GILLIAM 206

SOUTHEASTERN GEOLOGY
V. 44, No. 4, February 2007, p. 147-169

THE WALLS OF COLONIAL FORT DORCHESTER: A RECORD OF STRUCTURES CAUSED BY THE AUGUST 31, 1886 CHARLESTON, SOUTH CAROLINA, EARTHQUAKE AND ITS SUBSEQUENT EARTHQUAKE HISTORY

MERVIN J. BARTHOLOMEW

Department of Earth Sciences
University of Memphis
Memphis, TN 38152-3550
Jbrthlm1@memphis.edu

FREDRICK J. RICH

Department of Geology and Geography
Georgia Southern University
Statesboro, GA, 30460-8149
frich@georgiasouthern.edu

ABSTRACT

Orthogonal sets of both joints and conjugate normal faults formed in tabby walls of colonial (1757) Fort Dorchester during the 1886 Charleston, South Carolina, earthquake. The principal joint set (080° +/-20°) is identical to joints (080°) observed in wells in 1886 and is subparallel to both 063° SH_{MAX} and late Quaternary joints (065° +/-20°). The orthogonal joint set (170° +/-20°) is subparallel to: joints (~330°) observed in 1886; the dominant trend of borehole-breakouts (~335°); and orthogonal late Quaternary joints (335° +/-20°). Intersections of mean planes for each set of conjugate normal faults are subparallel to the orthogonal joint sets and plunge 7° at 255° and 8° at 342°. Post-1886 earthquake activity resulted in mode I opening (joint-reactivation) of some of these normal faults with subhorizontal separation of hanging and footwalls rather than shearing, hence, only five faults with minimal displacement-vectors were used to determine the 1886 orthogonal planes of slip of 069°, 74° and 159°, 89° preserved in the walls. Coeval orthogonal joint/fault sets require orthogonal tensile stresses, inferred to have resulted from slight arching of the area beneath the fort in 1886, consistent with (1) previously documented uplift of the epicentral area east of the Ashley River, (2) deflection of Cypress Swamp and Cooper River on opposing flanks of this uplift, and (3) deflections and terminations of Pleistocene coastal features which are consistent with uplift east of the Ashley River and subsidence to the west.

These orthogonal planes of slip approximate the attitudes of two reverse faults which could have caused the arching and produced the strike-parallel and cross-strike joint/fault sets. Most FPS define the nearby south-southeast-trending, steeply southwest-dipping, Ashley River zone of seismicity (4-8 km depth) characterized by reverse faulting. These FPS, though, have a wide range of orientations which are generally unfavorably oriented to severely misoriented with respect to the 063° SH_{MAX}, and hence, are likely reactivated pre-existing surfaces. Orientations of FPS are strikingly similar to normal fault orientations in the fort walls, suggesting FPS-reactivated surfaces originated as normal faults (c.f., a southeast-trending, Late Eocene, growth-fault analogue near Williston, South Carolina). There, orthogonal sets of normal faults, developed in an arch above the main reverse-fault, were reactivated as reverse faults during subsequent growth. We suggest that the source fault, herein named the Dorchester fault, was probably a nearly

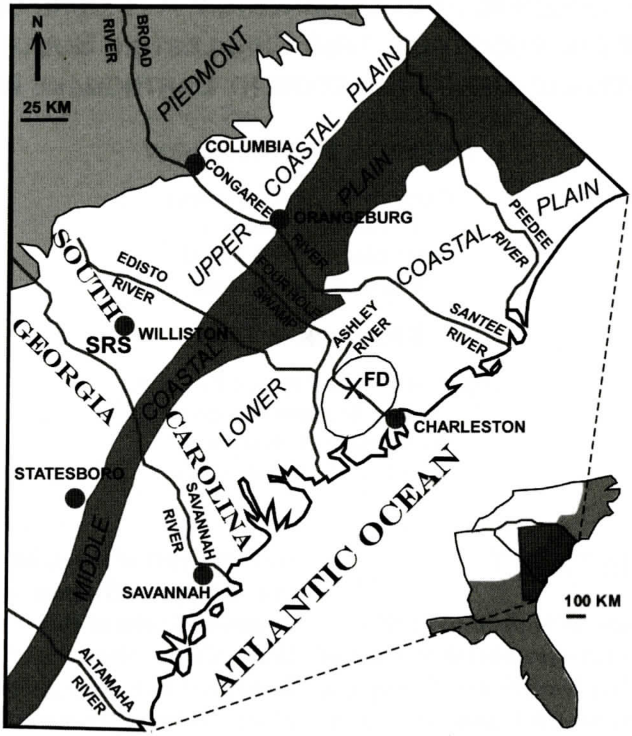

Figure 1. Map showing location of Fort Dorchester (FD) along the Ashley River within the epicentral area with Modified Mercalli Intensity (MMI) of X (shaded) of 1886 Charleston earthquake (Bollinger, 1977). Subdivisions of the Atlantic Coastal Plain are modified from Willoughby and others (1999), Colquhoun (1965, 1969), and Hoyt and Hails (1974).

vertical, northwest-trending, oblique (right-lateral) reverse fault that extends downward (8 to 13+ km) from the base of the Ashley River zone of seismicity and that it is seismically dormant since seismic monitoring began long after its strain release in 1886. The Dorchester fault had a rupture length and depth consistent with the large moment magnitude (M 7.3) for the 1886 Charleston earthquake, whereas the Ashley River zone of seismicity represents post-1886 strain-accommodation in the arched shallow crust.

INTRODUCTION

The Charleston, South Carolina, earthquake of August 31, 1886 (Figure 1) produced no obvious surface rupture (Dutton, 1889). Therefore, as with many other large earthquakes of the pre-instrument era, the location, orientation, and displacement of the actual fault that moved are unknown. Research conducted over the last three decades by the U.S. Geological Survey and other researchers (e.g., Rankin, 1977; Gohn, 1984; Dewey, 1985; Amick and others, 1990; Johnston, 1996), has helped to constrain possible locations, types, and orientations of faults that might be the source fault for the 1886 earthquake. However, authors disagree on whether the source fault activated in 1886 is 1) a northeast-striking, right-lateral, strike-slip fault of great length (Talwani, 1982, 2000; Marple, 1994; Marple and Talwani, 1993), 2) a northeast-striking, dip-slip fault of great length (e.g., Marple and Talwani, 2000), 3) a relatively short, northwest-striking, near-vertical, reverse fault (e.g., Tarr, 1977; Tarr and Rhea, 1983), or 4) some combination of two faults (Madabhushi and Talwani, 1993; Weems and Lewis, 2002). We believe that a re-examination of strain features that formed during the 1886 earthquake (Dutton, 1889) helps to clarify which of these alternatives is most likely. Specifically, we suggest that a northwest-striking oblique reverse fault, herein named the Dorchester fault, (e.g., Tarr, 1977; Tarr and Rhea, 1983) is most consistent with the data. We analyze orthogonal sets of joints and normal faults developed in the walls of Fort Dorchester during the 1886 earthquake. We compare the orientations of these fracture sets to: 1) regional Late Pleistocene/ Holocene joint sets in lower Coastal Plain strata; 2) *in situ* stress measurements; 3) the regional stress field determined from modern fault-plane solutions (FPS); and 4) other fractures that developed in the ground during the 1886 earthquake (Dutton, 1889). Slip-vectors on most of the normal faults in the fort do not lie on their respective fault-surfaces but are subhorizontal indicating that post-1886 movement has reactivated these shear surfaces by opening them as joints. We compare these slip-vectors with FPS from the modern seismicity to determine the role of modern seismicity in the opening of these fractures. Finally, we use five of these normal faults, whose slip-vectors lie on or very near their respective fault-surfaces, to determine two orthogonal planes of slip during the 1886 earthquake. These two planes approximate the orientations of near-vertical reverse faults that could have caused the fracture sets in the fort. One plane could also have produced the relative sense of regional uplift and subsidence associated with deflections of river channels and coastal features (Bartholomew and Rich, 2001, 2002) in the epicentral area of the 1886 earthquake.

PREVIOUS WORK

Dutton and Sloan (plates 26 and 27, respectively, *in* Dutton, 1889) originally defined the epicentral area of the 1886 Charleston earthquake largely from deformation of railroad lines and destruction of buildings using the Rossi-Forel scale. They had two epicenters, one a little northeast of Woodstock, South Carolina, and the other along Caw Caw Swamp north of Ravenel, South Carolina (Figure 2). They also considered the area near colonial Dorchester as a possible third epicenter, but later rejected it and attributed the intense deformation there to landsliding adjacent to the Ashley River. Bollinger (1977) used Dutton's descriptions of many features to redefine the epicentral area based on the Modified Mercalli Intensity (MMI) scale and established a MMI of X for this area and an estimated body-wave magnitude of 6.8 – 7.1 for the earthquake. Johnston (1996) calculated a moment magnitude of **M** 7.3 for the earthquake and modeled rupture lengths of 30-80 km for depths of 16-25 km. The center of Bollinger's epicentral map is near colonial Fort Dorchester, which is located along the Ashley River about halfway between Summerville and Middleton Place, South Carolina (Figure 2).

Improved velocity models (e.g., Talwani, 1977; Stihler, 1985) allowed relocation of some pre-1974 earthquakes into the Summerville-Middleton Place seismic zone (e.g., Dewey, 1983), which is defined by microearthquake activity recorded since 1974 (e.g., Tarr and Rhea, 1983; Madabhushi and Talwani, 1993; Talwani, 2000). Microearthquakes define two relatively shallow zones of seismic activity that vie as the proposed source of the 1886 earthquake. These two seismically defined zones (Figure 2) are 1) the Ashley River and 2) Woodstock zones of Talwani (1982). Madabhushi and Talwani (1993) established SH_{MAX} of 063° for the region from recent earthquakes, but, since this value comes from the same data set, it is also consistent with both zones of seismicity. The Ashley River zone is inferred to be a southeast-striking, steeply southwest-dipping zone of reverse faulting at 4-8 km depth. The Woodstock zone is inferred to be a southwest-striking, northwest-dipping, right-lateral strike-slip fault at 9-13 km depth (Talwani, 1982, 2000). The Ashley River zone is relatively well constrained and thus has been placed in the same approximate location and orientation as new data have accumulated (Figure 2). In contrast, the Woodstock zone is defined from dispersed events and its more poorly defined interpreted location has

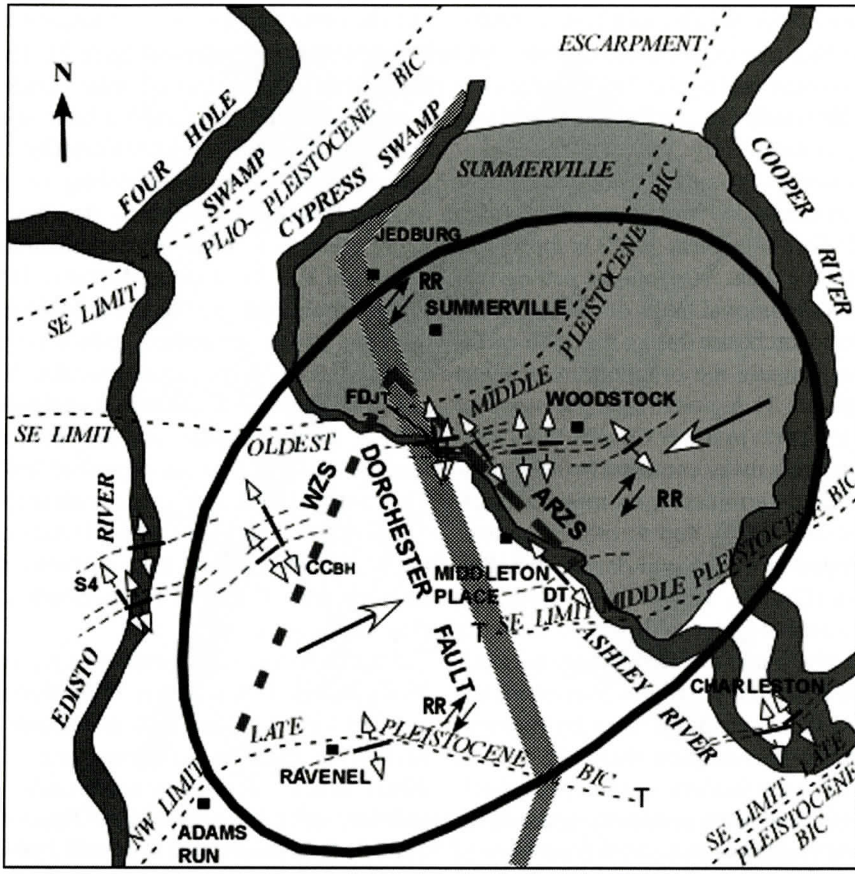

Figure 2. Map showing location of Fort Dorchester (FD) within epicentral area of MMI of X (heavy line) (Bollinger, 1977) of 1886 Charleston earthquake. Heavy bars with arrows showing extension directions show joint trends: from this study (FDJT); from Dutton (1889) (Table 1); at Stop 4 (S4) of Bartholomew and others (2000) along the Edisto River; at Drayton Tomb (DT) (Talwani, 2000); and of in situ stress measurements in Clubhouse Crossroads well (CCBH) (Zoback and others, 1978). Black arrows show relative strike-slip displacements of deformed railroad tracks (RR) (Dutton, 1889). Dashed lines are surface projections of the Ashley River and Woodstock zones of seismicity (Talwani, 1982; Talwani, 1989, respectively). Large open arrows- compression direction indicated by recent seismicity from Middleton Place to Summerville (Madabhushi and Talwani,1993). Shaded area- approximate uplifted area identified by Rhea (1989) and defined by deflections of the Cooper and Ashley Rivers. Limits of barrier island complexes (BIC) adapted from Colquhoun (1969) and Marple and Talwani (2000); T represents termination of a BIC. Dark shaded area- approximate trend of source fault inferred from this study.

shifted as new data have accumulated (Talwani, 1982, 2000; Madabhushi and Talwani, 1993). Recently, Weems and Lewis (2002) postulated that movement on two buried, larger reverse faults, the northwest-trending Charleston and south-trending Adams Run faults, which are both aseismic and peripheral to the region of seismicity, were responsible for the 1886 Charleston Earthquake.

THE WALLS OF 1757 FORT DORCHESTER

According to historical records for the Dorchester State Park, the fort was built in 1757 to protect the powder magazine (Figure 3) at the colonial town of Dorchester (Smith, 1905; Johnson, 1905). Johnson (1905) mapped the ruins of the fort in 1903 and indicated that the

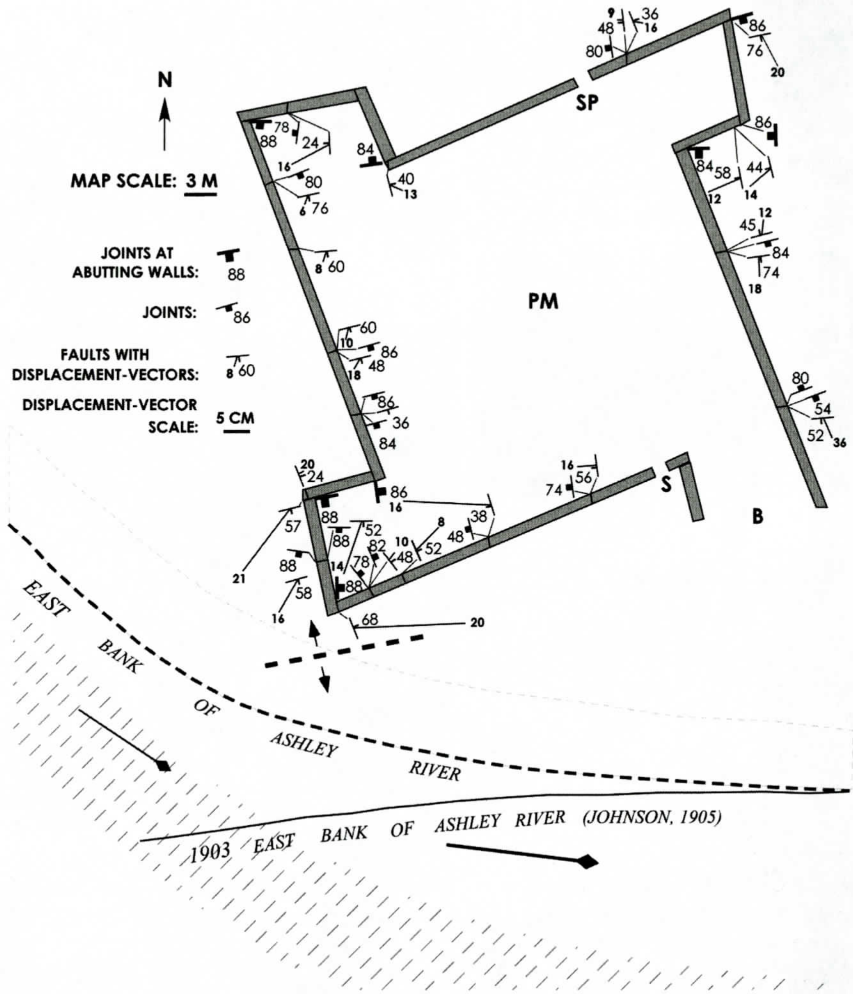

Figure 3. Map of 1757 Fort Dorchester (modified after Johnson, 1905) showing strike and dip of joints and normal faults; heavy bars on joint-strikes indicate joint-reactivation of contact between abutting walls; trend and plunge of joint-reactivation displacement-vectors on faults have displacement indicated by length of arrow. Heavy black dashed line is inferred location of fractures mentioned by Dutton (1889) (Table 1) as parallel to river (inferred to be parallel to the 1903 bank) with large arrows showing extension direction; long arrows indicate direction of flow of Ashley River. PM- powder magazine; B- breach in wall; SP- sally port; S- breach with stairs.

south wall had been leveled at the breach (Figure 3) sometime before that date in order to remove bricks from the old magazine and load them onto a boat. He also showed a small sally port (Figure 3) in the northeast corner. The small port with stairs just west of the breach was not on Johnson's 1905 map, and hence, it is inferred to have been opened after his mapping in 1903. For our purposes, we assume that Johnson's (1905) map, which was made 17 years after the earthquake, is a close approximation of what the fort looked like at the time of the 1886 earthquake. However, the location of the bank of the Ashley River relative to the fort on Johnson's 1905 map was different then from what it is today (Figure 3). This inferred older location is consistent with apparent differences between the modern river and its former course shown on Dutton's (1889) small-scale map as well. The trend of the riverbank is important be-

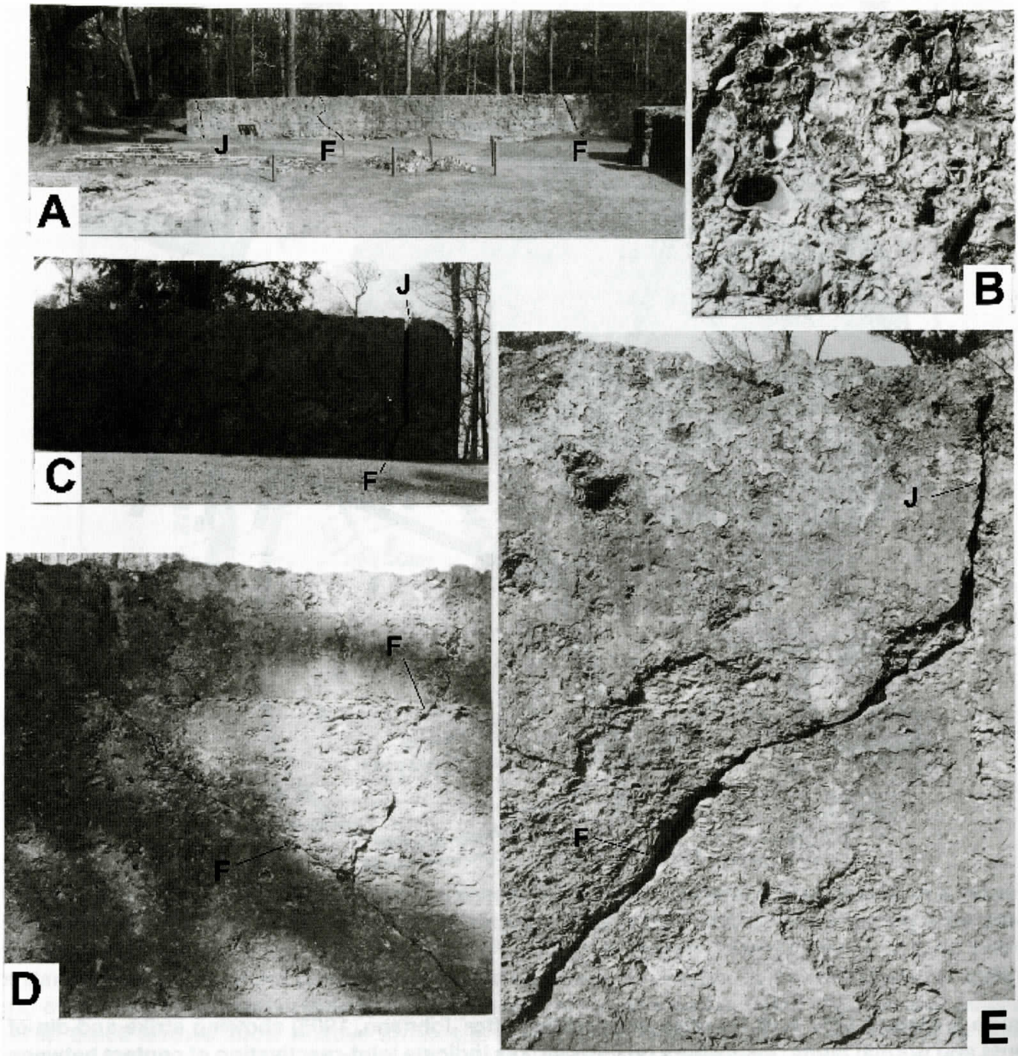

Figure 4. Photographs of systematic joints and faults in walls of 1757 Fort Dorchester. A) View of Fort looking east, across rubble of brick-lined powder magazine, at eastern wall showing faults (F) and a joint (J) at abutting walls. B) Closeup of wall showing oyster shell "tabby" concrete. C) View looking west at exterior wall of the northeastern corner showing joint-separation of abutting walls above a normal fault. D) Normal faults in interior northern wall in the northeastern corner where Dutton (1889) indicated the most severe damage was in 1889; fault on right terminates upward into tail joint. E) interior wall showing normal fault terminating upward into tail joint. F) (next page) Interior wall showing low-angle displacement vectors (arrows mark matching points) on normal faults that experienced joint-reactivation. G) Interior wall of northwestern corner showing fracture inferred by Talwani (2000) to represent 10cm of left-lateral strike –slip displacement; separation is due to joint-reactivation of west-dipping normal fault (below lens cap) that originally terminated upward into large near-vertical tail joint; trend and plunge of displacement vector is similar to two in the eastern wall (Figure 3) but not similar to that of the supposed correlative fracture in the southern wall. H) exterior wall showing normal fault, with about 0.5cm displacement, that has minimal separation of hanging and footwalls.

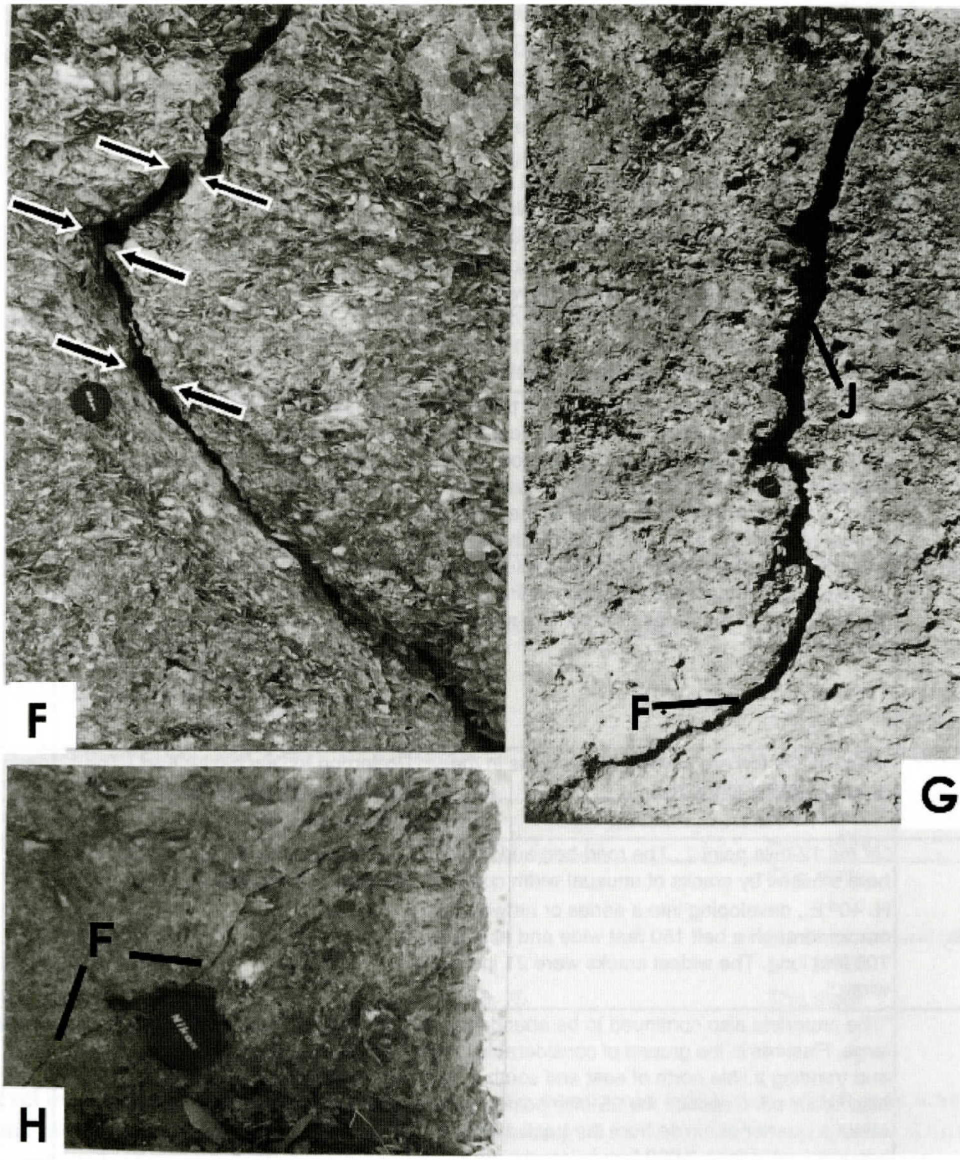

cause Dutton (1889) described fractures in the ground near the Fort as parallel to the riverbank.

Dutton (1889) described the walls of the fort (Figures 3 and 4A) as made from "...a peculiar concrete, consisting of oyster shells embedded in a lime-mortar obtained by burning and calcining oyster shells..." which according to Smith (1905) was known as "Tabby." Dutton (1889) noted that it was still "...fresh and hard as newly cut granite" when he was there, and we must add that it is still quite resistant to weathering today after nearly two and a half centuries!

Each wall-segment was started with a footer embedded in the ground. The ground level is the same both inside and outside the fort along the north wall and the northern part of the west wall. Outside the fort, the ground surface slopes southward toward the river. Inside the fort today, the ground surface is slightly hummocky, but relatively level, suggesting that the colonists had filled the southern part in order to have

Table 1. Strain features noted by Dutton (1889)

page	quotation	comments	strike
297	"Proceeding onward about a mile to the southwest, the line of section entered upon a.... 'Belt of craterlets bearing S. 80º W., N. 80º E. – Along this ridge many dry cracks have occurred, as well as long cracks connecting series of craterlets. We here find wells cracked in vertical planes through the axis of the wells with azimuth N. 80º E., the cracks extending from the tops to the bottoms of the wells. ..... We find, extending through a field for a distance of 700 feet, a fissure from eight to fourteen inches wide, connecting a series of large craterlets..."	referring to a traverse by Mr. Sloan from Woodstock to Dorchester Fort	080º
298 plate XXIII	" Strongly individualized and instructive traces are few until the Ashley River is reached. Here the bank of the river is a rounded clay terrace, which was shaken southward towards the stream, opening a series of wide cracks parallel to the river, as represented in Pl. XXIII. The sliding of the bank riverward uprooted several large trees, which fell over into the water. Almost directly opposite this point on the other side of the Ashley stands Gregg's Phosphate Works."	referring to the east side of the Ashley River just south of the mouth of Eagle Creek about a mile east of Dorchester Fort. Dutton's map shows the phosphate works opposite the mouth of Eagle Creek not two km downstream near the modern Greggs Landing. Thus the location of the large fissure illustrated by Dutton is along the 6-7m-high bluff adjacent to the northwestern half of 0.8 km-long straight stretch of the Ashley River which trends 330º	330º
298	"Hard by the fort are several wide cracks in the ground parallel to the river."	(referring to Dorchester Fort) The river here in 1903 (Johnson, 1905) trended 80º -85º.	082º
290	"At the 12-mile point.... The road-bed and cut were here crossed by cracks of unusual width coursing N. 40º E., developing into a series or network of cracks through a belt 150 feet wide and at least 700 feet long. The widest cracks were 21 inches in width."	(referring to the Northeast Railroad between Charleston and Holly Hill)	040º
306	"The craterlets also continued to be abundant and large. Fissures in the ground of considerable length and trending a little north of east and south of west also occurred. Opposite the 25-mile point and about a quarter of a mile from the track a fissure occurred more than 2,000 feet in length with a series of craterlets upon it."	(referring to the Charleston & Savannah railroad track at mile 222/3 near Ravenel's)	~085º
246-247 plate XIII	"Some of them measured a half inch in width and varied from six inches to many feet in length....In the fowl-yard (see diagram) there were two short cracks, about eight and ten feet long and three-quarters of an inch wide....These cracks...remained open; for each one lies along a well-defined ridge which slopes away three or four feet on either side....The direction of the fissures...is nearly northeast and southwest, with the exception of the two in the fowl-yard."	(referring to Mr. F. R. Fisher's description and map of cracks at his residence at 157 Wentworth Street, Charleston) On his map, the fowl-yard fractures trend 78º-88º and the others trend 35º-40º-45º.	083º 040º

Table 2. Comparison of orientation data (bold is dominant set)

FEATURES	DOMINANT (REGIONAL σ1) 065-245+/-15	ORTHOGONAL (REGIONAL σ3) 155-335+/-15	OTHER TRENDS	REFERENCE
SHMAX	063			Madabhushi and Talwani, 1993
IN SITU STRESS MEASUREMENTS	~**065**	~**340**	~040	Moos and Zoback, 1993; Zoback and others, 1978
JOINTS (FORT)	**080**+/-20	170+/-20		Bartholomew and others, 2000
JOINTS (REGIONAL) STOP 1		335+/-15	**315**+/-15 225+/-15	Bartholomew and others, 2000
STOP 2	**065**+/-15	~155		
STOP 3	**245**+/-15	~325		
STOP 4A	**065**+/-15	~325		
STOP 4B	**085**+/-15			
	055+/-15	345+/-15		
STOP 5				
JOINTS (REGIONAL)	**045**+/-20			Bartholomew and others, 1998
JOINTS (1886 GROUND)	~**080**	~**330**	~040	Dutton, 1889
MEAN FAULTS (FORT)	079, 54 249, 45	168 49 332, 34		Bartholomew and others, 2000; this study
FPS (1983 BLUFFTON EARTHQUAKE)	242, ~25			Talwani and Rajendran, 1991
MEAN FPS-SURFACE (SUMMERVILLE)		140, 46 148, 49		Madabhushi and Talwani, 1993
ORTHOGONAL SLIP PLANES	069, 74	159, 89		This study
LATE EOCENE ANALOGUE FAULT		144, 84, 91		Bartholomew and others, 2002a
PROPOSED SOURCE FAULT		~340, 85, 75		This study

a level interior surface. Erosion has exposed the footer along the exterior wall in the southwestern part of the fort and railroad ties have been placed between that corner and the river to help stabilize that part of the fort.

DESCRIPTION OF FRACTURES IN THE WALLS OF THE FORT

These nearly 1 meter-thick concrete walls have a unique internal property in being relatively homogeneous, except for a slight subhorizontal alignment of oyster shells, compared to other building materials in use at that time. Such material as the brick and mortar used in the nearby old bell tower, which was severely damaged in the 1886 earthquake (Dutton, 1889), impart strong anisotropy to such walls with little chance of preservation of relict strain features. Indeed, strong ground-motion typically produces nonsystematic cracks in material with strong anisotropy, such as asphalt pavement (e.g., Allen and others, 1998). Thus, these massive, relatively homogeneous, nearly orthogonal concrete walls of the fort, which are embedded in the ground, are ideal for recording strain from a nearby earthquake, as indeed they did in 1886. Furthermore, because the one set of these orthogonal walls trends within five degree of the principal horizontal stress, these walls are

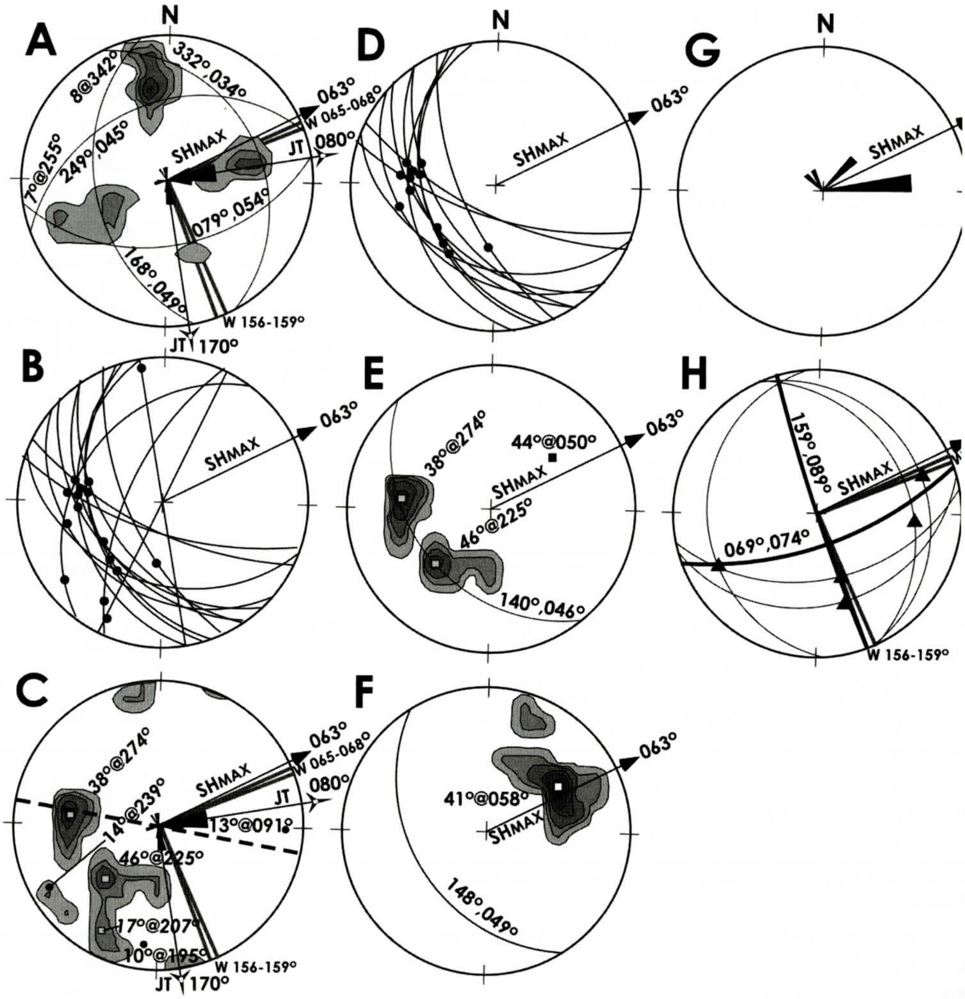

Figure 5. Rose diagrams and lower hemisphere equal-area stereographic projections of fractures in walls of 1757 Fort Dorchester and fault-plane solutions (FPS) from Madabhushi and Talwani (1993). A) 23 joints (circle = 50%) (from Bartholomew and others, 2000) and 1% area contour of poles to 24 fault surfaces (plot of surfaces shown in Bartholomew and others, 2000) in walls of fort with average fault planes derived from maximum pole orientations; trends of major walls (W) and SHMAX (from Madabhushi and Talwani, 1993) shown for comparison. B) 11 single FPS and 5 composite FPS (from Madabhushi and Talwani, 1993) with slip-vectors indicated. C) 1% area contour of slip-vectors for the 16 FPS from Madabhushi and Talwani (1993); squares are concentrations with plunges of 38° at 274°, 46° at 225°, 17° at 207°; dots are concentrations of 23 slip vectors on faults in walls of fort with plunges of 13° at 091°, 14° at 239°, and 10° at 195°, from Bartholomew and others (2000). D) 12 FPS, with slip-vectors, from Figure 4B that show unfavorably oriented steeply dipping, reverse faults. E) 1% area contour of slip-vectors from Figure 4D showing concentrations with plunges of 38° at 274° and 46° at 225° and with best fit plane through these concentrations oriented at 140°, 46° with pole plunge of 44° at 050°. F) 1% area contour of poles to 12 FPS from Figure 4D with maximum with plunge of 41° at 058° and plane define by maximum oriented at 148°, 49°. G) 8 crack-trends (circle = 80%) from Dutton (1889) for which accurate locations and orientations are known (Table 1) and Talwani (2000). H) 5 fault surfaces in walls of fort with restored slip-vectors used to defined orthogonal planes of slip (heavy lines) that could parallel subsurface reverse fault responsible for uplift and fracturing of fort during 1886 earthquake.

also ideally oriented for recording fractures specifically produced from earthquakes generated within the modern stress field.

No obvious vertical or steeply dipping planar features are present along any individual wall-section, each of which was poured along its entire length at one time, to influence orientations of developing fractures except for places where adjacent walls, which were poured independently, of the fort abut (Figures 3 and 4A, C). However, the lengths of individual sections of wall are 5 to 35 times the width. This anisotropy means that east-west-trending fractures more easily form in northwest-trending (156°-168°) walls and north-south-trending fractures form in northeast-trending (065°-078°) walls. Because of the embedded oyster shells (Figure 4B), both joint and fault surfaces (Figure 4A, C) that break the walls are rough (1-2 cm relief on surfaces) and lack ornamentation such as plumose structure or slickensides. Although joint and fault surfaces have somewhat irregular traces (Figure 4D, E), they still are easily defined and measured.

Dutton's (1889) reference to the fort is that "the earthquake broke it in many places and severely cracked it, especially at the northeast corner" (Figure 4C, D). Today these fractures in the northeast corner are not the most impressive. Wide, gaping fractures are most prevalent in the southwest corner where the slope to modern riverbank was reinforced with timbers to stabilize it. Likewise, wide fractures are present in both the northwest and southeast corners of the fort. The fact that fractures have increased in width since the time of Dutton's observation, *that the northeastern corner was the most severely damaged*, suggests that ongoing processes, such as gravity sliding toward the Ashley River, have altered fracture attributes since the earthquake. Our study addresses the question of how the 1886 fractures were subsequently affected and which fractures can still yield data pertinent to the 1886 earthquake and the source fault.

Unlike the modern seismicity at depth, the joints and normal faults in the walls of Fort Dorchester were documented by Dutton (1889) to have formed during the 1886 earthquake and thus are preserved surface strain-features of that event. The footing coupled the walls to the ground during the 1886 earthquake the same way that a concrete-slab couples a seismograph to the ground and the walls, albeit fortuitously, are orthogonally aligned with SH_{MAX} (Figure 5A). However, strain in the fort might still reflect local, rather than regional, stresses because most of each wall extends above ground (not continuously subjected to the regional stress field). But other strain features, which are below ground (Table 1), were also produced during the 1886 earthquake and exhibit the same orientations as fractures in the fort (Figure 5G; Table 2). Indeed, all of these features noted by Dutton (1889) and the fractures in the walls of the forts might be attributable to such things as liquefaction, lateral spreading or gravity sliding induced by strong ground motion during the 1886 earthquake.

That lateral spreading (gravity sliding) or hydraulic fracturing beneath the fort may have caused these fractures, has been a persistent, dismissal explanation since first suggested by Dutton (1889). Obermeier and Pond (1999), however, point out that clastic dikes (or fractures) associated with lateral spreads generally are approximately perpendicular to the direction that the slide is moving. Thus, gravity sliding toward the river during the earthquake would have produce classic fracture patterns more indicative of landslides rather than the orthogonal fracture sets observed here. Hydraulic fracturing, caused by high pore-water pressure typically produces either one dominant dike (or fracture) trend or a haphazard pattern (e.g., Obermeier and Pond, 1999), which likely reflect properties of the fractured, relatively unconsolidated material. If hydraulic pressure were sufficient to create a large upward bulge, then a classic radial joint pattern, similar to that found across many volcanic bulges, might even develop. Thus, neither lateral spreading nor hydraulic fracturing typically produce fracture patterns that are similar to those found in the walls of the fort. Moreover, systematic joint patterns are frequently found associated with active faults (e.g., Personius and Mahan, 2000) and may be used along with fault surfaces as tectonic indicators of the stress fields that caused them (e.g., Bartholomew and others, 2002b). Regardless of possible initiating factors, the orthogonal joints in the fort more likely reflect the regional stress field at the time of the 1886 earthquake rather than random effects of strong ground motion because, as discussed below, they did not develop perpendicular to free faces of the walls (Figure 5A) and are consistent with 1) the regional late Quaternary joint patterns, 2) SH_{MAX}, and 3) *in situ* stress measurements (Figures 1 and 2). Our premise does not preclude that strong ground motion may have affected individual fractures, but rather we emphasize that the consistent orientation of such fractures is not likely coincidental and, hence, reflect the regional stress field at the time of the 1886 earthquake.

FRACTURE DATA

Talwani (2000) interpreted two cracks (in the northwest and southwest corners) as having 10 cm of left-lateral strike-slip displacement and inferred that the other cracks lacked "...a systematic pattern of deformation." In contradistinction, Bartholomew and others (2000) measured 23 near-vertical joints and 24 normal faults with slip-vectors in the walls of Fort Dorchester (Figure 3). They defined a dominant set of joints trending 080° +/-20° in northwest-trending (156°, 159°, 165°, 168°) walls and a less numerous, orthogonal set trending 170° +/- 20° in northeast-trending (065°, 068°, 074°, 078°) walls (Figure 5A). Such consistent trends throughout the fort, regardless of variations in the trends of wall-segments (Figure 3), suggest that all of these joints formed at the same time during the 1886 earthquake. Two thirds of the fracture data occur in walls with trends of 065 °-068° and 156 °-159° and 17 percent are joints formed where adjacent walls abut. Furthermore, because the strikes of most of the fracture data are not simply perpendicular to the walls (Figure 5A), something other than the large free faces of the walls controlled fracture orientations.

We used the fault data from the fort (Bartholomew and others, 2000) and plotted poles to the 24 faults, from the two sets of conjugate faults, to define principal strikes and dips for each set (Figure 5A). The average strike and dip of the two sets of conjugate normal faults, that are consistent with the dominant and orthogonal joint-trends, are (079°, 54° and 249°, 45°) and (168°, 49° and 332°, 34°), respectively. Like the joint sets, these conjugate fault sets are orthogonal with their $\sigma 2$ axes defined by their respective intersections, with plunges of 7° at 255° and 8° at 342°, respectively. Because some joints utilized the existing crack between abutting walls (Figures 3 and 4A, C), the dominant joint-trends are skewed slightly (5°-8°) with respect to the fault intersections. Madabhushi and Talwani (1993) noted five events with normal FPS that they did not utilize in their composite solutions for reverse and strike-slip FPS. Several of these normal FPS are similar in orientation to the orthogonal sets of normal faults in the walls of the fort, suggesting that they are manifestations of similar processes.

Bartholomew and others (2000) showed that low-angle displacement-vectors (plunges of 10° at 195°; 13° at 091°; 14° at 239°) of offset features (e.g., molds and oyster shells; Figure 4F) on most of the faults are consistent with subsequent Mode I opening (i.e., "joint-reactivation" which is used herein to indicate subhorizontal opening of hanging wall and footwall rather than shearing along a fault surface, Figure 6) of these relict normal faults. The two fractures (Figure 4G), which Talwani (2000) suggested were indicative of left-lateral displacement during the 1886 earthquake, also have similar low-angle displacement vectors. Joint-reactivation is probably related to subhorizontal displacement (gravity sliding) along low-angle surfaces beneath the fort (Figure 6) that has produced the many large separations at the southwestern corner (Bartholomew and others, 2000). Bartholomew and others (2000) noted that all three slip-vectors had trends similar to those derived from FPS (Figure 5B) in the Summerville, South Carolina area (Madabhushi and Talwani, 1993; Marple, 1994) and suggested that opening of the fort's fractures (but not the formation of the original fractures) was due to slip during aftershocks and/or later small

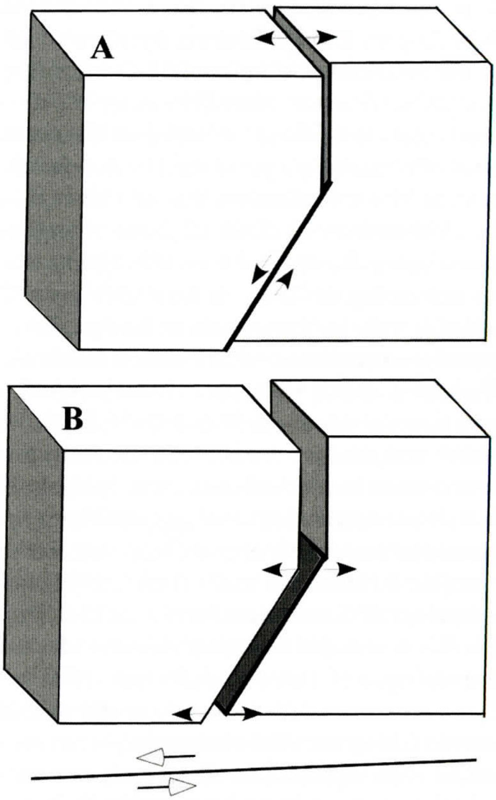

Figure 6. Diagram illustrating joint-reactivation of a normal fault. A: Minor dip-slip normal fault in wall terminates upward in near vertical mode I joint. B: Subhorizontal bedding-plane slip during minor seismic events causes lateral spreading beneath wall; both the joint walls and the hanging wall and footwall of the normal fault are separated along a subhorizontal vector not on the plane of the fault.

earthquakes. We plotted slip vectors from FPS of Madabhushi and Talwani (1993) and compared those to displacement-vectors for faults in the walls of the fort from Bartholomew and others (2000) (Figure 5C). Indeed, the similarity of the azimuths of their FPS slip-vectors (plunges of: 17° at 207°; 38° at 274°; 46° at 225°) to those of the displacement-vectors on joint-reactivated faults in the fort (noted above) is striking and suggests that most of the displacement-vector data at the fort reflect post-1886 slippage triggered by regional seismicity. The fort sits near the Ashley River on the fluvial-estuarine facies of the Middle Pleistocene Ten Mile Hill beds (Weems and Lemon, 1984; McCartan and others, 1984; Willoughby and others, 1999). Thus, during earthquakes on reverse faults, some low-angle surfaces, such as slightly tilted bedding, channel flanks, or paleosol surfaces in this unit beneath the fort, may act as low-angle extensional faults causing opening of pre-existing fractures in the walls of the fort.

SEISMIC AND STRUCTURAL FEATURES

Examination of the 11 single FPS and 5 composite FPS (Figure 5B) of Madabhushi and Talwani (1993) reveal some significant features. When the four strike-slip FPS are excluded (Figure 5D), the slip-vectors for the reverse faults concentrate in two groups (38° at 274°, 46° at 225°, Figure 5E) regardless of the strike of the fault planes (Figure 5D) which range over a 70° interval. Neither concentration is aligned with SH_{MAX} (063°). Moreover, fault planes through both concentrations exhibit similar large variations in orientation, suggesting that pre-existing surfaces are utilized as reverse faults during both east-west and northeast-southwest compression documented by Madabhushi and Talwani (1993). Sibson (1990) indicates that "...thrusts dipping at 22 to 32° in compressional regimes are *favorably* oriented for frictional reactivation." He notes that "...as the reactivation angle departs further from the optimal angle, by more than +/-15°, say, the stress ratio required for reshear increases by ~50 per cent and faults may be considered *unfavorably* oriented for reactivation". He also notes that, on reverse faults with dips greater than 50-55°, supralithostatic fluid pressures are required as a prefailure condition. Thus, these reverse faults documented by Madabhushi and Talwani (1993) are all *unfavorably* oriented for new reverse faults generated by horizontal compression, which suggests that they are reactivated pre-existing surfaces. Indeed the three steepest planes, which have oblique slip, are *se-*

verely misoriented (Sibson, 1990) with dips exceeding 75°.

The typical surface reactivated as a reverse fault can be approximated from the data of Madabhushi and Talwani (1993) by two methods. First, the plane through the two slip-vector concentrations (Figure 5E) is oriented at 140°, 46° with a pole plunging 44° at 050°. Second, poles to these fault-surfaces (Figure 5F) have a maximum plunging 41° at 058°, which is the pole to a plane oriented at 148°, 49°. These two planes and poles are quite similar but depart substantially in dip (i.e., *unfavorably* oriented) from the optimal orientation (~145°, ~27°) for thrusts generated by horizontal compression. These two planes are subparallel to one (168°, 49°) of the average normal fault-surfaces at the fort (Figure 5A). Indeed, the range of strikes and dips (Bartholomew and others, 2000) of this set of favorably oriented (Sibson, 1990) normal faults (southeast-striking, southwest-dipping) in the fort clearly overlaps the reverse FPS of Madabhushi and Talwani (1993) suggesting that their reverse FPS are utilizing pre-existing fault-surfaces at depth that mimic normal fault orientations.

Thus, understanding how the normal faults in the fort formed has important implications for interpreting the relationship of the modern microseismic activity on reactivated normal faults to the proposed source fault (discussed below) that caused the 1886 earthquake. Furthermore, although microseismicity on small, pre-existing fault-surfaces does provide useful constraints on both the principal stress directions and the orientation of the zone of current seismic activity, most of the microseismic activity is unlikely to provide FPS that consistently mimic the source fault that moved in the 1886 earthquake because strain was released on that fault more than a century ago. This would be analogous to the interpretations of Cox and others (2001) and Rydelek and Pollitz (1994) that high levels of modern seismicity on the southern arm of the New Madrid fault zone are related to aftershock activity of the 1811-1812 great earthquakes there, rather than to modern strain buildup which may actually be occurring on a different fault along the margin of the Reelfoot rift.

OTHER STRAIN FEATURES OF THE 1886 CHARLESTON EARTHQUAKE

Dutton (1889) noted joints, which he referred to as linear cracks, at numerous places, but we show (Figure 2) only those six locations of his where joint-orientations could be reasonably determined from his data (Table 1). We also show (Figure 2) the 315° trend of the crack across the marble plaque of the Drayton family tomb at Magnolia Gardens that is attributed to the 1886 earthquake (Talwani, 2000). Comparison (Figures 2 and 7) of these other joints that formed during the 1886 earthquake (Figures 2 and 5G) with 1) fracture sets in the fort, 2) regional joint patterns, and 3) borehole breakouts (Figures 1 and 2) shows consistency (+/-15°) with major trends at ~080° and ~045°. Thus, the orthogonal joint and normal fault sets at the fort have dominant trends (Figures 1 & 2; Table 2) that: 1) are subparallel to SH_{MAX} (063°) for focal mechanism solutions near Charleston, South Carolina (Madabhushi and Talwani, 1993) and indeed one FPS concentration (38° at 274°, Figure 5C) is actually favorably oriented (dashed line on Figure 5C) to produce the fort's joint set; 2) are consistent with the trends of other joints formed during the 1886 earthquake; 3) are consistent with regional Late Quaternary orthogonal joint sets; and 4) are consistent with *in situ* stress measurements (Zoback and others, 1978; Moos and Zoback, 1993).

SIGNIFICANCE OF THE ORTHOGONAL FRACTURE SETS IN THE FORT

Dunne and others (2003) summarized the three prevailing views of stress-switching mechanisms for development of orthogonal joint systems as caused by: 1) small fluctuations between two nearly equal regional horizontal principal stresses; 2) fluctuations at the scale of individual joints; and 3) regional 90° fluctuations of the horizontal principal stresses. They noted that the nearly isotropic stress of the first mechanism could easily result in columnar-cooling or random joints (e.g., Lachenbruch, 1962; Pollard and Aydin, 1988) rather than orthogonal orientations thus making it an unlikely mechanism; that the second mechanism, while plausible, was of limited applicability (e.g., Bai and others, 2002; Martel, 1994); and that the third mechanism could operate over time due to tectonic changes, uplift and/or erosion (e.g., Engelder, 1985; Hancock, 1985; Rives and others, 1994; Caputo, 1995) and that such orthogonal sets could actually form at different times due to different stress fields (e.g., Gross, 1993; Rawnsley and others, 1998). However, in the fort walls, the orthogonal sets formed within minutes of one another, thus precluding long-term factors or different stress fields as the cause.

Orthogonal joint sets, such as in the Appalachian fold and thrust belt and Plateau, are commonly referred to as strike joints and cross-strike joints (respectively parallel to and perpendicular to a fold axis) (e.g., Evans, 1994). These joints and associated normal faults develop perpendicular to effective tensile stresses due to three-dimensional bending of relatively rigid layers (e.g., Pollard and Aydin, 1988) during thrusting. Indeed, deformation in the arched area above blind thrusts, such as associated with the 1971 Sylmar, California, earthquake, includes both compressional and extensional structures (Cruikshank and others, 1996; Baldwin and others, 2000). The strike joints reflect the strike of both the fold axis and the underlying fault that produced the fold. The orthogonal cross-strike joints are perpendicular to the fold axis and their plane contains the slip-vector on the underlying fault. Anderson (1951) showed that joints typically form parallel to the strike of normal faults (perpendicular to the least principal stress) and Kattenhorn and others (1999) demonstrated how joints could develop orthogonal to normal faults.

Nickelsen and Hough (1967) first pointed out that, "unless there is proof of equal age of apparently conjugate joint sets…", their angular relationship can not be used as the basis for synchronous development. Hancock and Engelder (1989) argued that neotectonic joints in old rocks formed at shallow depths (<1 km) due to uplift and removal of overburden within the regional stress field with effective tensile stresses related to lateral relief. Bartholomew and others (2000) documented coeval Late Pleistocene-Holocene orthogonal joints in Late Pleistocene (~130 ka; Willoughby and others, 1999) strata that were never buried more than a few meters to tens of meters. They suggested that these orthogonal joints reflect extension over broad late Quaternary uplifts related to the regional stress field. Weems and Lewis (2002) presented evidence of broad uplift in the Charleston area through much of the Tertiary and Rhea (1989) documented Quaternary uplift in the epicentral area of the 1886 earthquake. Bartholomew and Rich (2001, 2002) suggest that such uplift in the Charleston area has continued through the Quaternary.

Bartholomew and others (2002a) documented an outcrop-scale example near Williston, South Carolina, (Figure 1) where orthogonal sets of conjugate strike and cross-strike normal faults developed near the ground surface in an arch above a syndepositional near-vertical, small reverse fault cutting upper Eocene strata within a stress field similarly oriented to that of today (Figure 7). We believe that this small-scale example is applicable to the Charleston region. Some of these normal faults subsequently were rotated and/or were reactivated as reverse faults during progressive displacement on the near-vertical main reverse fault and associated growth of the flanking folds. Such near-surface folding above an active fault has also been demonstrated elsewhere, such as at Anticline Ridge where it was associated with the 1983 Coalinga, California, earthquake (Stein and King, 1984) and at the Northridge Hills anticline where it was associated with the 1971 Sylmar and 1994 Northridge earthquakes (Baldwin and others, 2000). This is consistent with Weems and Obermeier (1990), who indicated that the Coastal Plain sediments in the region of the 1886 earthquake should be warped above the tectonically active fault at depth. Rhea (1989) in documenting uplift east of the Ashley River, drew attention to the deflections of the Ashley River/ Cypress Swamp and the Fourhole Swamp (a tributary of the Edisto River) along the northern flank of this uplift (Figures 1 and 2). We suggest that the Cooper River was deflected as well, but along the southeast-

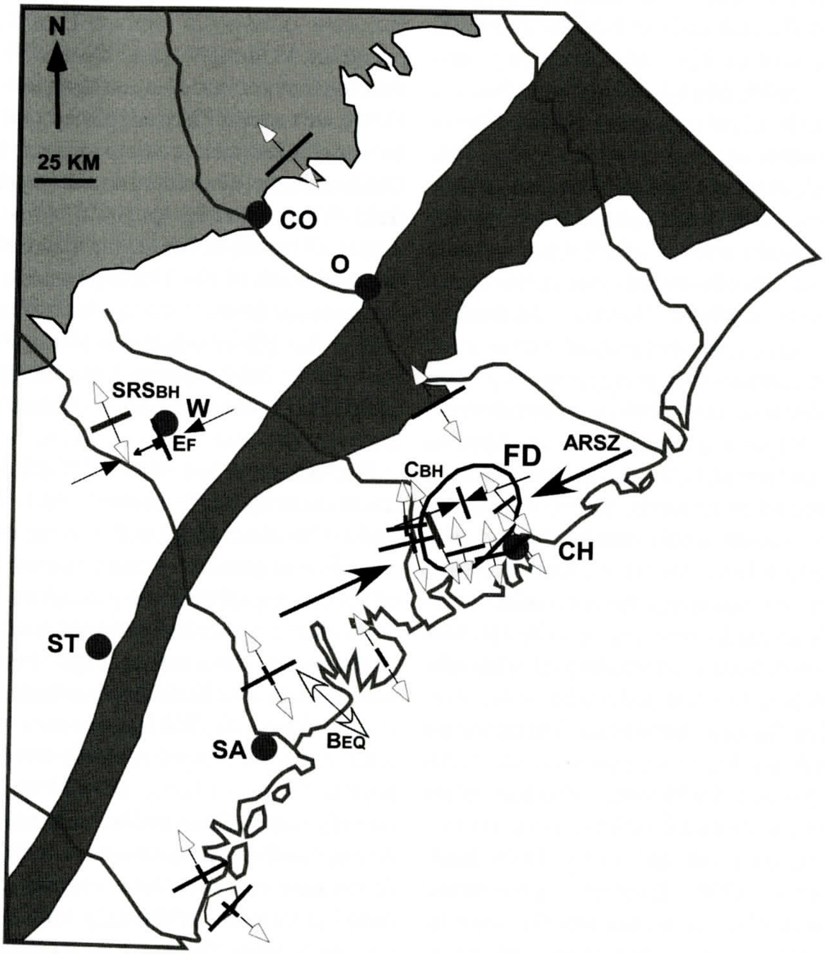

Figure 7. Simplified map of Figure 1 showing strain features of Atlantic Coastal Plain which are relevant to the 1886 Charleston earthquake. Large filled arrows- compression direction for modern seismicity within Ashley River zone of seismicity (ARSZ) in the epicentral area (Madabhushi and Talwani, 1993); small open arrow- extension direction for the January 4, 1989, Bluffton (B_{EQ}) earthquake (Talwani and Rajendran, 1991); gray bars- in situ stress measurements (borehole breakouts) in the Clubhouse Crossroads well (C_{BH}) (Zoback and others, 1978) and at the US DOE Savannah River Site (SRS_{BH}) (Moos and Zoback, 1993); Smaller filled arrows- compression direction for fracture data at Fort Dorchester (FD) (this study) and for syndepositional Late Eocene fault (E_F) (Batholomew and others, 2002a); heavy bars with open arrows- extension directions for Late Quaternary (younger than ~130-33 ka) joint trends (Bartholomew and others, 1998, 2000); CH- Charleston; CO- Columbia; O- Orangeburg; SA- Savannah; ST- Statesboro; W- Williston.

ern flank of this uplift, thus its profile did not exhibit the characteristics of those streams that were incised across the uplift (Rhea, 1989). The uplift defined by the deflected Ashley River/ Cypress Swamp and Cooper River mimics the eastern half of Bollinger's (1977) isoseismal line of X. Marple and Talwani (1993, 2000) inferred that the topographic high above the Summerville scarp, which is the erosional demarcation of the ancient barrier island complex (Colquhoun, 1965, 1969), represented the uplift. Indeed the migration of the Summerville escarpment, but not the next older (Plio-Pleistocene) escarpment (e.g., Colquhoun, 1969; Marple and Talwani, 2000) as well as the migration and westward termination of younger Middle to Late Pleistocene strata, suggest that deflection of the Ashley River/Cypress Swamp and the Fourhole Swamp was initiated as the Middle Pleistocene shoreline of the Atlantic Ocean migrated across an active fault, with up-to-the-east relative offset, that trended normal to the shoreline (Figure 2) (Bartholomew and Rich, 2001, 2002). The lack of deflection of the youngest late Pleistocene barrier island complex indicates the time that the migrating shoreline passed beyond this fault. The progressive northwestward (landward) deflection of these escarpments in the vicinity and west of the Ashley River is consistent with relative uplift east of the river and hence southeastward (seaward) migration of the shoreline and preservation of older deposits farther to the southeast. Relative subsidence west of the river resulted in destruction or burial of older deposits with the youngest coastal deposits (older Late Pleistocene) preserved at the southwestern margin of the subsidence area. Marple and Talwani (2000) suggest 2-3 m of uplift of the Summerville escarpment to the east of the Ashley River, however, this is a minimal displacement estimate across the fault due to continued shoreline development on the downdropped western side of the Ashley River. Poley and Talwani (1986) used a releveling line to demonstrate uplift in the vicinity of Ravenel (Figure 2), but boundaries of this uplift are not shown because they are not confined beyond a single releveling line.

CONSTRAINTS ON SOURCE FAULT FOR THE 1886 CHARLESTON EARTHQUAKE

The fault that caused the 1886 Charleston earthquake must be consistent with the following observations (Figures 2 and 7):

1. Formation of orthogonal sets of joints and normal faults at ~070° and ~170° at the fort and in the surrounding region (Bartholomew and others, 2000).
2. Borehole breakouts in the nearby Clubhouse Crossroads corehole at ~340° and 040° (Zoback and others, 1978).
3. Right-lateral flexures of railroad tracks (Dutton, 1889; Bodin and Johnston, 1999, 2000) and joint trends.
4. Uplift of the area of maximum MMI (X) east of the Ashley River (Rhea, 1989) with at least 2-3 m of uplift since the Middle Pleistocene (Marple and Talwani, 2000) and earlier uplift during the Tertiary (Weems and Lewis, 2002).
5. Northwestward deflection of Middle Pleistocene (including the Summerville) escarpments across the Ashley River and westward termination of the younger one in the vicinity of the Ashley River (e.g., Colquhoun, 1965, 1969; Marple and Talwani, 2000), which is consistent with uplift east of the river (and hence preservation of these sediments) relative to the area west of the river.
6. Deflection and eastward termination of the older Late Pleistocene coastal deposits (e.g., Colquhoun, 1969; Marple and Talwani, 2000) is consistent with development only on the downdropped western side of the epicentral area.
7. Westward deflection of the Edisto River/ Fourhole Swamp and the Ashley River/ Cypress Swamp along the northern flank of the uplift (Rhea, 1989; Marple, 1994; Marple and Talwani, 1993, 2000) and eastward deflection of the Cooper River along the southeastern flank of the uplift.
8. The maximum horizontal stress (SH_{MAX}) is at 063° for focal mechanism solutions near Charleston, South Carolina (Madabhushi and Talwani, 1993).
9. A southeast-trending, southwest-dipping zone of modern seismicity between 4 and 8 km depth beneath the Ashley River that is characterized by reverse faulting (Madabhushi and Talwani, 1993) and is consistent with reactivation of pre-existing normal fault surfaces.
10. More diffuse modern seismicity at depths of 9-13 km that is consistent with right-lateral strike-slip faulting attributed to the Woodstock zone of seismicity (Madabhushi and Talwani, 1993).

11. A moment magnitude of **M** 7.3 and a 30-80 km rupture length at a depth of 16-25 km (Johnston, 1996).

THE FAULT THAT CAUSED THE 1886 CHARLESTON EARTHQUAKE

We used the normal fault data from Fort Dorchester to derive the main planes of slip characterizing the orthogonal extensional faults and joints formed in its walls at the time of the 1886 earthquake. We selected five faults with minimal displacement and with displacement-vectors whose plunges fall on or very near their respective fault surfaces. This minimizes effects of large subhorizontal displacements due to later joint-reactivation of faults in the fort. These five have plunges that are nearly dip slip (Figures 4D, H and 5H). We removed the post-1886 extension across these surfaces by increasing the plunge on each of these five so as to place it on the associated fault plane. Three of the five are part of the north-northwest–south-southeast–striking fault set and these three define a plane of slip of 069°, 74° with a pole plunging 14° at ~339° (Figure 5H). This pole and the two displacement vectors of the east-northeast–west-northwest–striking set define the orthogonal plane of slip (Figure 5H) of ~159°, ~89° (Figure 5H). Inasmuch as these fractures developed as strike-parallel and cross-strike fractures, these two orthogonal planes of slip, derived from the extensional faults in the fort, mimic possible reverse faults beneath the fort that caused the uplift that produced them during the 1886 earthquake. Our analogue (Figure 7) is the small reverse fault (~144°, 84°, 91°), which is exposed near Williston, South Carolina, and was active during the Late Eocene when the nearby, larger Pen Branch fault, which bounds the northern flank of the Dunbarton Triassic rift basin, was reactivated (Aadland and others, 1995) (Figure 1). This small fault produced strike-parallel and cross-strike fractures in the arch above it (Bartholomew and others, 2002a). The 1.5m of cumulative reverse displacement on that fault is associated with folds and orthogonal sets of normal faults in zones that are more than 30 times and 10 times, respectively, the displacement in width.

Either of these orthogonal orientations (069°, 74° and 159°, 89°) is consistent with concomitant development of both sets of faults and joints over an arched uplift at the time of the 1886 Charleston earthquake. However, consideration of both the uplifted area that lies east of the Ashley River and the relatively shallow, southeast-striking, southwest-dipping zone of modern reverse faulting across the center of the area of maximum MMI (X), suggests that the 1886 Charleston earthquake was along a near vertical to steeply northeast-dipping reverse fault oriented ~340° (Figure 8, top). The slip vector was probably 075° +/-15°, thus the 1886 displacement was reverse with a small component of right-lateral slip which is consistent with both bends observed in the railroad tracks and with the right-lateral sense of shear in joint trends (Figure 2). Not only is this orientation similar to the southeast-striking Late Eocene fault analogue, but it is consistent with Tarr and Rhea's (1983) interpretation that the 1886 earthquake was along a northwest-trending near-vertical fault that strikes subparallel to the Ashley River seismic zone of Talwani (1982). It is also consistent with the relative sense of uplift and subsidence inferred both from subsurface Tertiary strata (Weems and Lewis, 2002) and from deflections of Pleistocene coastal deposits and river deflections in the epicentral area (Bartholomew and Rich, 2001, 2002).

CONCLUSIONS

We suggest that the source fault is actually below the Ashley River zone of seismicity, which represents strain accommodation in the upper crust (4-8 km depth) following strain release on the source fault in 1886 (Figure 8, bottom). Thus modern seismicity near the Ashley River is more like the diffuse, shallow, post-1994 seismicity above the intersection of the Northridge and Sylmar aftershock zones of seismicity (Tsutsumu and Yeats, 1999) and is not a direct reflection of the fault that caused the Charleston earthquake. Like our Williston analogue, numerous smaller normal faults were progressively developed during major events

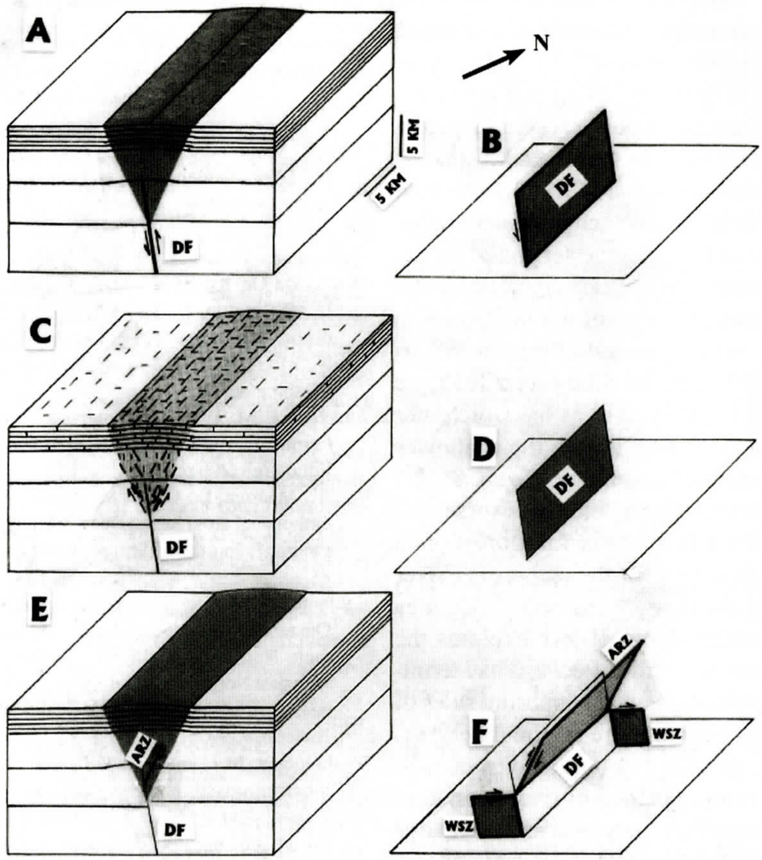

Figure 8. Diagrams showing relationships of arching of Coastal Plain sediments (closely spaced lines at top), development of joints and normal faults, the Ashley River and Woodstock zones of seismicity, and the proposed Dorchester fault. A) 1886 Charleston earthquake caused by movement on Dorchester fault contributes to arch (shaded area) developed above upward tip of the fault over time. B) Sketch showing inferred Dorchester fault as a northwest-trending, steeply northeast-dipping discrete fault at a depth from ~8 km to ~13-25 km. C) Strike-parallel, near-vertical joints and small normal faults (~60° dips) developed across arch during events like the 1886 Charleston earthquake on the Dorchester fault (D). E) strain accommodation after the 1886 earthquake reactivates numerous earlier formed, small normal faults above tip of Dorchester Fault as dispersed reverse faults characterizing the Ashley River zone of seismicity (4-8 km depth; F), and dispersed strike-slip faulting at 8-13 km depth (Woodstock Fault) perhaps near the lateral tips of the now dormant Dorchester Fault.

and upward growth of the source fault. These smaller normal faults were then rotated and/or reactivated as reverse faults to accommodate strain during subsequent minor events. Moreover, the deeper (8-13 km) regional strain accommodations (e.g., Woodstock zone of seismicity of Talwani, 1982, 2000) may indicate both the depth to which the main fault broke in 1886 and the orientation of the strike-slip tips (Figure 8F) accommodating movement on the main oblique (right-lateral) reverse fault in 1886. Thus we infer that the minimal portion of the main fault that ruptured in 1886 extended from 8 to13+ km throughout the length of the Ashley River zone of seismicity. But more likely, the rupture length extended roughly across the uplifted area, and thus the source fault length would be about 43 km (dark shaded zone on Figure 2), which falls within the 30-50 km range of the representative models determined by Johnston, (1996) for an **M** 7.3 earthquake on a source fault at depths of 25km and 16km, respectively. If the maximum reverse displacement on the near vertical source fault was near the center of the area with a MMI of X, then the high level of modern seismicity on small faults in the vicinity of Fort Dorchester would be expected to accommodate strain induced by the 1886 earthquake. Because of the difference in dip direction and the amount of dip, as well as the greater depth of the inferred source fault, we suggest that it be referred to as the Dorchester fault to avoid confusing it with the shallower Ashley River zone of seismicity (Figure 8).

Finally, oblique (right-lateral) reverse displacement on the Dorchester fault provides a consistent explanation for the contrasting river deflections on the margins of the uplifted area east of the Ashley River. It also explains the landward versus seaward deflections and terminations of coastal deposits on opposing sides of the fault. Thus from a more regional perspective, perhaps detailed fracture studies coordinated with a re-examination of river anomalies and ancient shorelines may provide alternative explanations for better assessment of seismic hazards in the Coastal Plain of the southeastern United States.

ACKNOWLEDGEMENTS

Reviews by Randel T. Cox, Diane I. Doser, Arleen A. Hill, John Stamatakos, Charles H. Trupe, Roy B. Van Arsdale and Robert E. Weems significantly improved the manuscript. Discussions with Ralph H. Willoughby on Cenozoic stratigraphy in South Carolina, with Donald U. Wise and Kevin G. Stewart on fractures and seismites, with Pradeep Talwani and Richard Cannon concerning aspects of seismicity in the Charleston area, and with Arch Johnston and Paul Bodin regarding deformation of the railroad tracks are gratefully acknowledged. We used R. W. Allmendinger's STERONET v.4.9.6 program for rose diagrams and stereonet plots.

REFERENCES CITED

Aadland, R. K., Gellici, J. A., and Thayer, P. A., 1995, Hydrogeologic framework of west-central South Carolina: South Carolina Department of Natural Resources, Water Resources Division, Report 5, 200 p.

Allen, C. R., Brune, J. N., Cluff, L. S., and Barrows, A. G., Jr., 1998, Evidence for unusually strong near-field ground motion on the hanging wall of the San Fernando fault during the 1971 earthquake: Seismological Research Letters, v. 69, p. 524-531.

Amick, D., Gelinas, R., Maurath, G., Cannon, R., Moore, D., Billington, E., and Kemppinen H., 1990, Paleoliquefaction features along the Atlantic seaboard: NUREG/CR-5613, Nuclear Regulatory Commission, Washington, DC.

Anderson, E. M., 1951, The Dynamics of Faulting and Dyke Formation with Applications to Britain: Oliver & Boyd, Edinburgh, 206 p.

Bai, T., Maerten, L., Gross, M. R., and Aydin, A., 2002, Orthogonal cross joints: Do they imply a regional stress rotation?: Journal of Structural Geology, v. 24, p. 77-88.

Baldwin, J. N., Kelson K. I., and Randolph, C. E., 2000, Late Quaternary fold deformation along the Northridge Hills fault, Northridge, California: Deformation coincident with past Northridge blind-thrust earthquakes and other nearby structures?: Seismological Society of America Bulletin, v. 90, p. 629-642.

Bartholomew, M.J., and Rich, F. J., 2001, A new method for locating possible active faults beneath the Lower Coastal Atlantic Plain, southeastern USA: Geological Society of America, Abstracts with Program, v. 33, no. 6, p. A-393.

Bartholomew, M.J., and Rich, F. J., 2002, Pleistocene shorelines and coastal rivers: sensitive indicators of Quaternary faults, Atlantic Coastal Plain, USA: EOS, Transactions, American Geophysical Union, v. 83, no.19, p. S353.

Bartholomew, M. J., Whitaker, A. E., and Barker, C. A., 1998, Preliminary Mesozoic-Cenozoic brittle-deformation history of Eocambrian rocks (Ridgeway gold mine, South Carolina), Carolina Terrane, *in* Secor, D. T., Jr., ed., Special Issue Devoted to the 1998 Field Trip of the Carolina Geological Society: South Carolina Geology, v. 40, p. 19-27.

Bartholomew, M. J., Rich, F. J., Whitaker, A. E., Lewis, S. E., Brodie, B. M., and Hill, A. A., 2000, Preliminary interpretation of fracture sets in Late Pleistocene and Tertiary strata of the lower Coastal Plain in Georgia and South Carolina, *in* Abate, C., ed., A Compendium of Field Trips of South Carolina Geology with Emphasis on the Charleston, South Carolina Area: South Carolina Geological Survey, p. 19-27.

Bartholomew, M. J., Brodie, B. M., Willoughby, R. H., Lewis, S. E., and Syms, F. H., 2002a. Mid-Tertiary paleoseismites: Syndepositional features and section restoration used to indicate paleoseismicity, Atlantic Coastal Plain, South Carolina and Georgia, *in* Ettensohn, F. R., Rast, N., and Brett, C. E., eds., Ancient Seismites: Geological Society of America, Special Paper 359, p. 63-74.

Bartholomew, M. J., Stickney, M. C., Wilde, E. M., and Dundas, R. G., 2002b, Late Quaternary paleoseismites: Syndepositional features and section restoration used to indicate paleoseismicity and stress-field orientations during faulting along the main Lima Reservoir fault, southwestern Montana, *in* Ettensohn, F. R., Rast, N., and Brett, C. E., eds., Ancient Seismites: Geological Society of America, Special Paper 359, p. 29-47.

Bodin, P., and Johnston, A. C, 1999, "Tracking" Historical Earthquakes: Railroads as Deformation Meters and the Source Characteristics of the 1886 Charleston Earthquake: Annual Meeting of the Eastern Section of the Seismological Society of America, Memphis, October 1999.

Bodin, P., and Johnston, A. C, 2000, "Tracking" Historical Earthquakes: Railroads as Deformation Meters and the Source Characteristics of the 1886 Charleston Earthquake: Seimological Research Letters, v. 71, p. 123.

Bollinger, G. A., 1977, Reinterpretation of the intensity data for the 1886 Charleston, South Carolina, earthquake, *in* Rankin, D. W., ed., Studies related to the Charleston, South Carolina, earthquake of 1886 – A preliminary report: U. S. Geological Survey, Professional Paper 1028-B, p. 17-32.

Caputo, R., 1995, Evolution of orthogonal sets of extensional joints: Terra Nova, v.7, p. 479-490.

Colquhoun, D. J., 1965, Terrace sediment complexes in central South Carolina, in Atlantic Coastal Plain: Geological Association Field Conference 1965 Guidebook, Columbia, South Carolina, Department of Geological Sciences, University of South Carolina, 62 p.

Colquhoun, D. J., 1969, Geomorphology of the lower Coastal Plain of South Carolina: South Carolina Geological Survey, MS-15, 36 p.

Cox, R. T., Van Arsdale, R. B., Harris, J. B., and Larsen, D., 2001, Neotectonics of the southeastern Reelfoot rift zone margin, central United States, and implications for regional strain accommodation: Geology, v. 29, p. 419-422.

Cruikshank, K. M., Johnston, A. M., Fleming, R. W., and Jones, R., 1996, Winnetka deformation zone: surface expression of coactive slip on a blind fault during the Northridge earthquake sequence, California: U. S. Geological Survey, Open-File Report 96-698, 73 p.

Dewey, J. W., 1983, Relocation of instrumentally recorded pre-1974 earthquakes in the South Carolina region, *in* Gohn, G. S., eds., Studies related to the Charleston, South Carolina, earthquake of 1886 – Tectonics and seismicity: U. S. Geological Survey, Professional Paper 1313, p. Q1-Q9.

Dewey, J. W., 1985, A review of recent research on the seismotectonics of the southeastern seaboard and an evaluation of hypotheses on the source of the 1886 Charleston, South Carolina, earthquake: NUREG/CR-4339, Nuclear Regulatory Commission, Washington, DC.

Dunne, W. M., Ferrill, D. A., Crider, J. G., Hill, B. E., Waiting, D. J., La Femina, P. C., Morris, A. P., and Fedors, R. W., 2003, Orthogonal jointing during coeval igneous degassing and normal faulting, Yucca Mountain, Nevada: Geological Society of America Bulletin, v. 115, p. 1492-1509.

Dutton, C. E., 1889, The Charleston earthquake of August 31, 1886: U. S. Geological Survey, Ninth Annual Report, p. 203-528.

Engelder, T., 1985, Loading path to joint propagation during loading cycle: An example from the Appalachian Plateau, USA: Journal of Structural Geology, v. 7, p. 459-476.

Evans, M. A., 1994, Joints and décollement zones in Middle Devonian shales: Evidence for multiple deformation events in the central Appalachian Plateau: Geological Society of America Bulletin, v. 106, p. 447-460.

Gohn, G. S., (ed.), 1984, Studies related to the Charleston, South Carolina, earthquake of 1886 – Tectonics and seismicity: U. S. Geological Survey, Professional Paper 1313.

Gross, M. R., 1993, The origin and spacing of cross joints: Examples from the Monterey Formation, Santa Barbara coastline, California: Journal of Structural Geology, v. 15, p. 737-751.

Hancock, P. L., 1985, Brittle microtectonics: Principles and practice: Journal of Structural Geology, v. 7, p.437-457.

Hancock, P. L., and Engelder, T., 1989, Neotectonic joints: Geological Society of America Bulletin, v. 101, p. 1197-1208.

Hoyt, J. H., and Hails, J. R., 1974, Pleistocene stratigraphy of southeastern Georgia, *in* Oaks, R. Q., Jr., and DuBar, J. R., eds., Post-Miocene stratigraphy central and southern Atlantic Coastal Plain: Logan, Utah, Utah State University Press, p. 191-201.

Johnson, J., 1905, The old fort at Dorchester, S.C.: South Carolina Historical and Genealogical Magazine, v. 6, p. 127-129.

Johnston, A. C., 1996, Seismic moment assessment of earthquakes in stable continental regions – III. New Madrid 1811-1812, Charleston 1886 and Lisbon 1755: Geophysical Journal International, v. 126, p. 314-344.

Kattenhorn, S. A., Aydin, A., and Pollard, D. D., 1999, Joints at high angles to normal fault strike: an explanation using 3-D numerical models of fault-perturbed stress fields: Journal of Structural Geology, v. 22, p. 1-23.

Lachenbruch, A. H., 1962, Mechanics of thermal contraction cracks and ice-wedge polygons in permafrost: Geological Society of America Special Paper 70, 65p.

Madabhushi, S., and Talwani, P., 1993, Fault plane solutions and relocations of recent earthquakes in Middleton Place Summerville seismic zone near Charleston, South Carolina: Seismological Society of America Bulletin, v. 83, p. 1442-1466.

Marple, R. T., 1994, Discovery of a possible seismogenic fault system beneath the Coastal Plain of South and

North Carolina from an integration of river morphology and geological and geophysical data (Ph.D. dissertation): Columbia, South Carolina, University of South Carolina, 354 p.

Marple, R. T., and Talwani, P., 1993, Evidence of a possible tectonic upwarping along the South Carolina Coastal Plain from an examination of river morphology and elevation data: Geology, v. 21, p. 651-654.

Marple, R. T., and Talwani, P., 2000, Evidence for a buried fault system in the Coastal Plain of the Carolinas and Virginia: Implications for neotectonics in the southeastern United States: Geological Society of America Bulletin, v. 112, p. 200-220.

Martel, S., 1994, On the paradox of systematic, contemporaneous, orthogonal opening-mode fractures, in Nelson, R., and Laubach, S., eds., Rock Mechanics: Balkema, Rotterdam, The Netherlands, p. 801-808.

McCartan, L., Lemon, E. M., and Weems, R. E., 1984, Geologic map of the area between Charleston and Orangeburg, South Carolina: U. S. Geological Survey, Miscellaneous Investigations, Map I-1472, 1:250,000 scale.

Moos, D., and Zoback, M. D., 1993, Near-surface, "thin skin" reverse faulting stresses in the southeastern United States, in 34th U.S. Symposium on Rock Mechanics: International Journal of Rock Mechanics, Min. Sci. and Geomech. Abstract, v. 30, p. 965-971

Nickelsen, R. P., and Hough, V. D. N., 1967, Jointing in the Appalachian Plateau of Pennsylvania: Geological Society of America Bulletin, v. 78, p. 609-629.

Obermeier, S. F., and Pond, E. C., 1999, Issues in using liquefaction features for paleoseismic analysis: Seismological Research Letters, v. 70, p. 34-58.

Personius, S. F., and Mahan, S. A., 2000, Paleoearthquake recurrence on the East Paradise fault zone, metropolitan Albuquerque, New Mexico: Seismological Society of America Bulletin, v. 90, p. 357-369.

Poley, C. M., and Talwani, P., 1986, Recent vertical crustal movements near Charleston, South Carolina: Journal Geophysics Research, v. 91, p. 9056-9066.

Pollard, D. D., and Aydin, A., 1988, Progress in understanding jointing over the past century: Geological Society of America Bulletin, v. 100, p. 1181-1204.

Rankin, D. W., ed., 1977, Studies related to the Charleston, South Carolina, earthquake of 1886 – A preliminary report: U. S. Geological Survey Professional Paper 1028.

Rawnsley, K. D., Peacock, D. C. P., Rivies, T., and Petit, J. –P., 1998, Joints in the Mesozoic sediments around the Bristol Channel Basin: Journal of Structural Geology, v. 20, p. 1641-1661.

Rhea, S., 1989, Evidence of uplift near Charleston, South Carolina: Geology, v. 17, p. 311-315.

Rives, T., Rawnsley, K. D., and Petit, J. P., 1994, Analogue simulation of natural orthogonal joint set formation in brittle varnish: Journal of Structural Geology, v. 16, p. 419-429.

Rydelek, P. A., and Pollitz, F. F., 1994, Fossil strain from the 1811-1812 New Madrid earthquakes: Geophysical Research Letters, v. 21, p. 2302-2306.

Sibson, R. H., 1990, Rupture nucleation on unfavorably oriented faults: Seismological Society of America Bulletin, v. 80, p. 1580-1604.

Smith, H. A. M., 1905, The town of Dorchester, in South Carolina – A sketch of its history: South Carolina Historical and Genealogical Magazine 6, p. 62-95 and p. 130.

Stein, R. S., and King, G. C. P., 1984, Seismic potential revealed by surface folding: 1983 Coalinga, California, earthquake: Science, v. 224, p. 869-872.

Stihler, S. D., 1985, Seismic refraction anisotrophy and seismicity in South Carolina (M.S. thesis): Columbia, South Carolina, University of South Carolina, 102 p.

Talwani, P., 1977, A preliminary shallow crustal model between Columbia and Charleston, South Carolina, determined from quarry blast monitoring and other geophysical data *in* Rankin, D. W., ed., Studies related to the Charleston, South Carolina, earthquake of 1886 – A preliminary report: U. S. Geological Survey, Professional Paper 1028, p. 177-187.

Talwani, P., 1982, internally consistent pattern of seismicity near Charleston, South Carolina: Geology, v. 10, p. 654-658.

Talwani, P., 1989, Seismotectonics in the southeastern United States *in* Gregersen, S., and Basham, P. W., eds., Earthquakes at North-Atlantic passive margins: Neotectonics and Postglacial Rebound: Kluwer Academic Publishers, Dordrecht, The Netherlands, NATO ASI Series C: Mathematical and Physical Sciences, v. 266, p. 371-392.

Talwani, P., 2000, Macroscopic effects of the 1886 Charleston earthquake, *in* Abate, C., ed., A Compendium of Field Trips of South Carolina Geology with Emphasis on the Charleston, South Carolina Area: South Carolina Geological Survey, p. 1-6.

Talwani, P., and Rajendran, K., 1991, The January 4, 1989, earthquake in Bluffton, South Carolina, and the tectonic implications: Seismological Research Letters, v. 62, p. 139-142.

Tarr, A. C., 1977, Recent seismicity near Charleston, South Carolina, and its relationship to the August 31, 1886, earthquake, *in* Rankin, D. W., ed., Studies related to the Charleston, South Carolina, earthquake of 1886 – A preliminary report: U. S. Geological Survey, Professional Paper 1028-D, p. 43-57.

Tarr, A. C., and Rhea, S., 1983, Seismicity near Charleston, South Carolina, March 1973 to December 1979, *in* Gohn, G. S., ed., Studies related to the Charleston, South Carolina, earthquake of 1886 – tectonics and seismicity: U. S. Geological Survey, Professional Paper 1313, p. R1-R17.

Tsutsumi, H., and Yeats, R. S., 1999, Tectonic setting of the 1971 Sylmar and 1994 Northridge earthquakes in the San Fernando Valley, California: Seismological Society of America Bulletin, v. 89, p. 1232-1249.

Weems, R. E., and Lemon, E. M., Jr., 1984, Geologic map of the Stallsville quadrangle, Dorchester and Charleston counties, South Carolina: U. S. Geological Survey, MAP GQ-1581, 1:24,000 scale.

Weems, R. E., and Lewis, W. C., 2002, Structural and tectonic setting of the Charleston, South Carolina, region: Evidence from the Tertiary stratigraphic record: Geological Society of America Bulletin, v. 114, p. 24-42.

Weems, R. E., and Obermeier, S. F., 1990, The 1886 Charleston earthquake – An overview of geologic studies, *in* Proceedings, Water Reactor Safety Information Meeting: 17th U.S. Nuclear Regulatory Commission Report NUREG/CP-0105, p. 289-313.

Willoughby, R. H., Nystrom, P. G., Jr., Campbell, L. D., and Katuna, M. P., 1999, Cenozoic stratigraphic column of the Coastal Plain of South Carolina: South Carolina Geological Survey, General Geologic Chart 1.

Zoback, M. D., Healy, J. H., Roller, J. C., Gohn, G. S., and Higgins, B. B., 1978, Normal faulting and in situ stress in the South Carolina coastal plain near Charleston: Geology, v. 6, p. 147-152.

SOUTHEASTERN GEOLOGY
V. 44, No. 4, February 2007, p. 171-189

CRADLE-OF-FORESTRY-IN-AMERICA FAULT, AN ACADIAN AND ALLEGHANIAN DEXTRAL STRIKE-SLIP FAULT WITHIN THE EASTERN BLUE RIDGE, TRANSYLVANIA COUNTY, NORTH CAROLINA

JAMES A. DOCKAL

Department of Geography and Geology
University of North Carolina Wilmington
Wilmington, North Carolina 28403

ABSTRACT

Cradle-of-Forestry-in-America fault, a strike-slip fault that cuts amphibolite grade gneiss and schist of the Neoproterozoic Ashe-Tallulah Falls Formation and Paleozoic granitoid gneiss of the Looking Glass and Pink Beds plutons, is situated within the Tugaloo terrane, eastern Blue Ridge, northwest of the Brevard fault zone. The fault is a zone several hundred meters wide that contains block-in-matrix tectonic mélange that consists of blocks of a wide variety of lithologies both indigenous and exotic, and a matrix dominated by white mica with lesser amounts of biotite and chlorite. The fault zone is oriented northeast-southwest and dips steeply northwest. Kinematic indicators suggest a dextral shear sense. Crosscutting relationships of fault-related features indicate two major episodes of strike-slip movement. The earliest was a ductile event under amphibolite facies conditions, the second a ductile-brittle event. A third event was very weak, brittle and dip-slip in nature. A modest retrograde greenschist overprint of the earliest features suggest one or both of the latter two events occurred under greenschist facies conditions. The earliest movement could have been no earlier than ~380 Ma or Neoacadian. The latter movements were probably a result of Alleghanian events.

INTRODUCTION

The Cradle-of-Forestry-in-America fault is a newly discovered dextral strike-slip fault within the Tugaloo terrane of the eastern Blue Ridge belt of the southern Appalachians. The mapped portion of the fault extends northeast-southwest for 21 km from an area approximately 12 km west of Brevard, North Carolina, to an area 15 km north of Brevard (Figure 1). It passes through the southeastern portion of the Cradle of Forestry in America National Historic Site in the Davidson River Ranger District in Pisgah National Forest. The Cradle-of-Forestry-in-America fault nearly parallels the Brevard fault zone, which lies 10 km to its southeast.

The Cradle-of-Forestry-in-America fault cuts Neoproterozoic amphibolite grade gneiss and schist of the Ashe-Tallulah Falls Formation and Paleozoic weakly metamorphosed granitoid gneiss of the Looking Glass and Pink Beds plutons. Rocks of the Ashe-Tallulah Falls in the area had experienced at least three episodes of ductile deformation prior to formation of the fault, and at least one episode of brittle deformation afterwards.

The fault is actually a zone, 300 to 600 m wide of intensely sheared rock that is in part a block-in-matrix structure or mélange in the sense of Raymond (1984). Blocks represent lithologies adjacent to the fault and lithologies exotic to the area. The matrix is mica schist. Rock laterally adjacent to the mélange zone exhibits a fault-parallel mineral elongation lineation and/or a fault associated spaced cleavage.

The area cut by the fault was previously mapped by Keith (1907) at the 1:125,000 scale. Keith did not recognize the existence of the fault nor does his map indicate the Brevard fault, however the general trend of each roughly corresponds to mapping unit boundaries on the map. Keith's map is useful in that it delineates soapstone and other ultramafic bodies that are no longer exposed, which are probably blocks within the mélange zone of the fault. The area

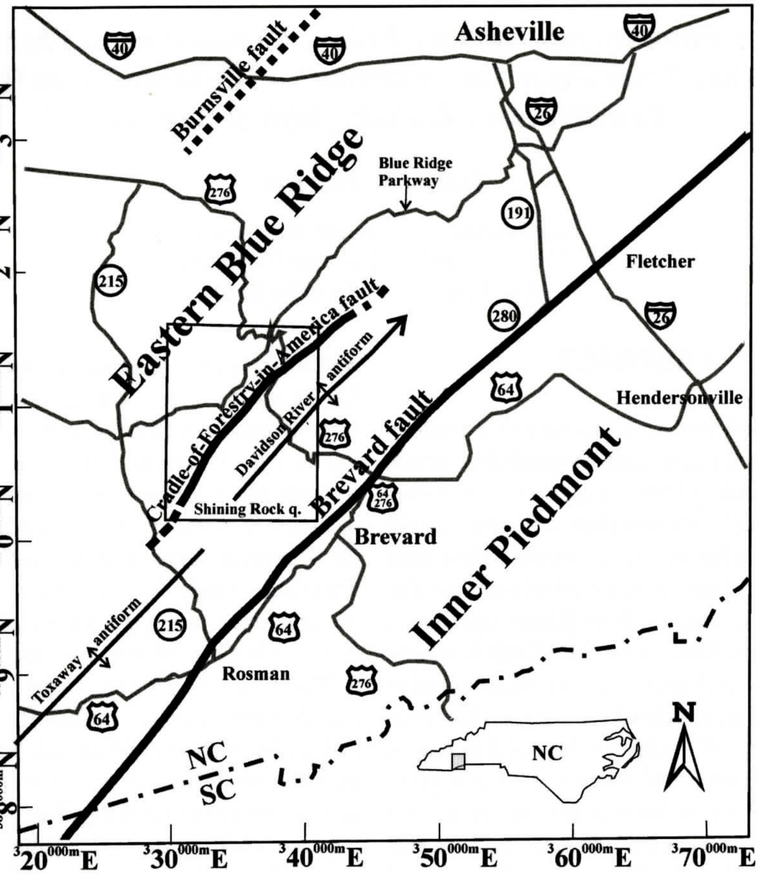

Figure 1. Location map of the Cradle-of-Forestry-in-America fault and other major structural features. Rectangular area corresponds to the study area or Figure 2.

was also mapped at the 1:250,000 by Hadley and Nelson (1971), but again without recognition of the fault.

The mapped area of the fault lies principally within the Shining Rock 7 ½ minute quadrangle (Figure 2). The fault extends southwestward into the northwest corner of the Rosman quadrangle. Northeast of the Shining Rock quadrangle it has been mapped cutting the northwest corner of the Pisgah Forest quadrangle and seems to continue on into the Dunsmore Mountain quadrangle. Louis Acker, in the mid-1970's, mapped at the 1:24,000 scale the principal area of the fault in the Shinning Rock quadrangle (Acker, 1982). Acker did not recognize the fault, although some of his unit boundaries correspond to the approximate position of the mélange zone. Acker's study is particularly useful for its description of the character of the country rock and the accompanying map delineates fault related features exposed by then active logging operations, features now obscured by vegetation. The Rosman quadrangle was studied by Livingston (1966) and Horton (1974) and mapped at the 1:24,000 scale by Horton (1982). Horton did not recognize the fault, but features that appear on his map indicate the possible extension of the fault across the northwest corner of the Rosman quadrangle. Livingston (1966) also mapped at the 1:24,000 scale portions of the Rosman and portions of the adjoining Lake Toxaway, Reid, and Eastatoe Gap quadrangles. The western portion of the Pisgah Forest quadrangle was mapped at the 1:24,000 scale by Worley (2000). The northern limit of his mapping includes the area adjacent to the mélange.

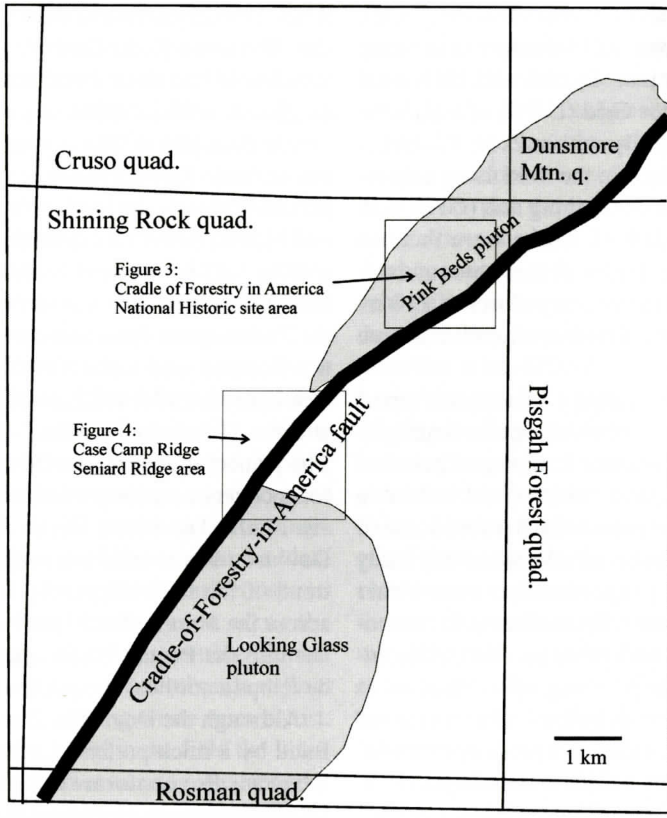

Figure 2. Study area location map of the Shining Rock quadrangle and portions of adjacent quadrangles. The two delineated rectangular areas refer to more detailed geologic maps, Figures 3 and 4. Shaded areas are the outcrop belts of the granitoid gneiss plutons.

The Dunsmore Mountain quadrangle was mapped at the 1:24,000 scale by Dabbagh (1975) who did not recognize the fault zone although structural futures typical of the fault are indicted on the map.

The existence of the Cradle-of-Forestry-in-America fault came to light during a study of the architecture and boundary relationships of the Looking Glass pluton (Dockal, 2001). That study noted the abrupt termination of the northwest flank of the Looking Glass pluton and a similar termination of the southeastern flank of the Pink Beds pluton and speculated on the possibility of a fault offsetting the two possibly once-joined plutons (Figure 2). The objective of this paper is to formally name the Cradle-of-Forestry-in-America fault, document the evidence for the fault, and discuss its chronological relationships to the geology of the area. The significance of the Cradle-of-Forestry-in-America fault is that since it cuts weakly foliated and chronologically studied plutonic rock, whose intrusion and foliation development postdate the Taconic orogeny, an analysis of structural fabric elements associated with the fault and fabric elements, which it cross-cuts or is cross-cut by it, can be used to further elucidate and differentiate features of the Taconic from features that were formed during the Acadian and Alleghanian orogenies thus providing a clearer view of the geologic history of the eastern Blue Ridge portion of the southern Appalachians.

The study is based upon field observations made principally in the Shining Rock and Pisgah Forest quadrangles between 1994 and 2004. This is supported by a modest amount of oriented and un-oriented thin section studies, some of which were stained for feldspar identification.

Specific locations will be referred to using 1927 North American Datum and Universal Transverse Mercator Grid (UTM) of which the study area lies entirely within Zone 17. Locations were determined in the field using a hand-held satellite global positioning unit (GPS) with an accuracy of ± 100 m. These were then re-checked using the digital orthophotoquads of the area, resulting in accuracy closer to ±10 m. All azimuths reported here are relative to true north.

Rock related terminology used in this report follows that of the North American Geologic-Map Data Model Science Language Technical Team (2004). The term 'white mica' is used in this report in lieu of muscovite because some of the 'white mica' observed relative to this study displayed optical properties that were either outside of those generally attributed to muscovite or overlapped with other possible white micas. The term 'mineral elongation lineation' is used here to refer to an outcrop observable rod like shape or appearance of a particular monocrystalline or polycrystalline mineral species irrespective of its mode of formation.

DESCRIPTION

Lithologic Units Involved in Faulting

A significant problem in recognizing the Cradle-of-Forestry-in-America fault is that the lithologies exposed on either side of the fault bear a fair amount of resemblance to one another. This together with the lack of good exposures of the fault zone apparently led some previous workers in the area to draw some map unit boundaries across the fault. At the outcrop level the dominant rocks on either side of the fault are well-foliated biotite-plagioclase-quartz gneiss, mica schist and weakly foliated 'granitoid' gneiss. However, upon closer examination the rocks or either side are only superficially similar.

The strata to the southeast of the fault consist of several thousand meters of schist and gneiss that have been intruded by a sequence of weakly foliated seemingly concordant granitoid sills. Acker (1982) referred to the schist and gneiss as the 'Davidson River Group', which he further subdivided into three lithodems: feldspathic mica gneiss, sulfidic mica schist, and porphyroclastic mica gneiss. These strata together form a broad, very flat, northeast-southwest trending antiform that is defined by mica (white mica and biotite) preferred orientation foliation. This feature will be referred to in this study as the Davidson River antiform to distinguish it from the Toxaway antiform found to the southwest in the Rosman and Lake Toxaway quadrangles (see Horton, 1974, 1982, and Livingston, 1966) and the 'Toxaway anticline' of Acker (1982). The principal area of the Davidson River antiform covers a major portion of the drainage basin of the Davidson River. The axis of the Davidson River antiform roughly parallels the trend of the fault (Figure 1). It cuts diagonally across the Shining Rock quadrangle and continues into the Pisgah Forest quadrangle where it develops a northeastern plunge (Worley, 2000).

Although the Davidson River antiform is defined by a mica-preferred orientation foliation the strata also conforms to a uniform and predicable structural-stratigraphic configuration. The structurally lowest part of the strata of the Davidson River antiform in the Shining Rock and Pisgah Forest quadrangles is feldspathic biotite-white mica gneiss. This is structurally overlain by sulfidic mica schist, which is in turn is overlain by porphyroclastic gneiss. The feldspathic biotite-white mica gneiss (bmg-lithodem) is characterized and recognized in the field by its very well formed and pervasive mica-preferred orientation. It easily parts parallel to this foliation, even in fresh outcroppings thus giving it a characteristic slabby appearance. The gneiss has a weak compositional banding foliation that is sub-parallel to the mica-preferred orientation. Upon parting parallel to the mica-preferred orientation the compositional banding foliation forms a conspicuous foliation intersection lineation that can easily be confused with the mineral elongation lineation associated with the fault. The rock as a whole is predominately feldspar and quartz with lesser amounts of biotite, white mica, and chlorite. Biotite is the dominant phyllosilicate and frequently occurs as layers of biotite schist. White mica occurs with the biotite or as thin white mica exclusive lamellae interspaced within the gneiss. Chlorite is volumetrically insignificant and generally occurs as a replacement of biotite. Excellent exposures of the bmg-lithodem can be examined in Moore Cove in the Shining Rock quadrangle (338280E, 3908480N).

Sulfidic mica schist (sms-lithodem) structurally overlies the bmg-lithodem and is gradational with it. Where exposed the unit has a conspicuous red buff to red brown coloration though usually it is expressed as reddish soil or saprolite. The mica is predominately a white mica with lesser amounts of biotite and chlorite. The rock is rich in garnet and may carry kyanite and/or staurolite. At the fresher outcroppings, on warm humid days, the lithodem can be identified solely by its characteristic and conspicuous sulfurous odor. In weathered areas the lithodem is recognized by the combination of reddish soil, gentle slopes, and abundant float of cobbles of garnet-bearing white mica schist. When it can be recognized in the field the lithodem forms a good marker horizon. Representative exposures of nearly fresh sulfidic mica schist occur at the base of Looking Glass Falls (339210E, 3907160N) and nearby along Forest Service road FS 475 (338600E, 3906660N), both in the Shining Rock quadrangle. Typical weathered exposures occur at the head of Coontree Creek (339690E, 3908440N) and along the ridge crest near Saddle Gap (339550E, 3909220N), also in the Shining Rock quadrangle.

The porphyroclastic gneiss (pcg-lithodem) is the structurally highest unit in the area southeast of the Cradle-of-Forestry-in-America fault. When observed in contact with the sms-lithodem the contact is very sharp almost fault-like. The pcg-lithodem typically forms cliffs of massive-looking grayish rock. In areas of good outcrop or fresh exposure, it is readily differentiated from the bmg-lithodem by its lack of significant parting, which is related to a much weaker mica-preferred orientation foliation. Compositional banding is much more evident as well as is the presence of rootless folds. The most conspicuous feature is the presence of porphyroclasts that are identifiable in hand sample. In saprolitic outcroppings of the lithodem, where the feldspar component is rendered to clay, the mica component exerts a strong control on the mechanical strength of the rock resulting in formation of a modest platy parting that can render the lithodem difficult to differentiate from the bmg-lithodem. In areas that are deeply weathered, where the sulfidic mica schist also cannot be recognized, the pcg-lithodem can only be differentiated from the bmg-lithodem with difficulty. Acker (1982) considered the top of his porphyroclastic gneiss in the Shining Rock quadrangle to be at the base of the lowest garnet-rich schist layer. That, which he considered to lay above this point, was assigned to his 'Shining Rock group.' In the adjacent Pisgah Forest quadrangle, where better and more continuous exposures exist, there are at least three garnet-rich schist horizons that occur within typical porphyroclastic gneiss with the structurally lowest one correlating with Acker's boundary garnet schist. What Acker is calling 'Shining Rock group' in the area describe here to the southeast of the Cradle-of-Forestry-in-America fault is actually pcg-lithodem and rock belonging to 'Shining Rock group' occurs only northwest of the fault. Rock of Acker's Shining Rock group is visually similar to rock of the pcg-lithodem, but is otherwise quite different. The three most significant and field observable differences between the two are: 1) the nature of the compositional banding foliation; 2) the character of mesoscopic folding; and 3) the character of the mica-preferred orientation foliation. In the pcg-lithodem compositional banding results from the transposition of preexisting rock fabric elements into planar composition planes. What few mesoscopic folds that are found are rootless. The mica-preferred orientation foliation consistently reflects the structure of the large-scale or area-wide Davidson River antiform, and is axial-planar to the rootless folds. The compositional banding in the Shining Rock group results from migmatization and the mica-preferred orientation foliation remains parallel to the compositional banding even at the hinges of the ubiquitous isoclinal similar folds. Hereafter the Shining Rock group will be referred to as migmatitic gneiss (mmg-lithodem). Excellent exposures of typical pcg-lithodem occur along a logging road on the south face of Black Mountain near Maxwell Cove in the Pisgah Forest quadrangle (342040E, 3909650N). Excellent exposures of the mmg-lithodem can be found in the area of Black Balsam Knob (329625E, 3910800N) whereas typical exposures closer to the fault can be found on Pilot Mountain (330140E, 3904760N), both within the Shining Rock quadrangle. The mmg-lithodem as used here also encompasses the 'banded gneiss' and 'migmatite' of Acker (1982). Further subdivision of this lithodem along the lines of work by Acker (1982) or Lesure and Dunn (1982) is possible.

To the northwest of the fault and at what appears to be a structural position below the mmg-lithodem is hornblende-plagioclase-clinozoisite gneiss (hpg-lithodem). Acker (1982) referred to this as 'amphibolite.' Good exposures can be found in a series of cascades above the Pink Beds near to and northeast of US 276 (338740E, 3915600N).

At most localities, where both the hpg-lithodem and the mmg-lithodem can be observed in an objective sequence, garnet-white mica schist separates them. This sequence, which is found in the study area only northwest of the Cradle-of-Forestry-in-America fault, closely resembles the sequence of strata typically reported for Ashe-Tallulah Falls Formation (see Hatcher, 1971). The sequence that lies southeast of the fault appears quite different from the typical Ashe-Tallulah Falls sequence but this may be due to a combination of differing structural overprint and lateral litho-facies changes.

Crosscutting the bmg-lithodem is a light-colored medium- to coarsely crystalline granitoid gneiss, the Looking Glass gneiss of Acker (1982) or gglg-lithodem as used in this study. The gglg-lithodem occurs as a series of lit-par-lit sill-like bodies, which for the most part appears concordant to the mica-preferred orientation foliation of the bmg-lithodem though the actual boundary is clearly discordant (Dockal, 2001). Some portions of one or more sills swell forming significantly thick lenses of granitoid gneiss. Looking Glass Rock, located near the center of the Shining Rock quadrangle, provides the best example of this. The gglg-lithodem has a very weak sub-horizontal biotite preferred orientation. The interlayering of the gglg-lithodem and the bmg-lithodem can be readily observed in Looking Glass Creek valley along US 276 in the area that lies upstream from Looking Glass Falls (339270E, 3907300N) and extending to an area just above the Sliding Rock Recreation Area (337500E, 3908900N).

Northwest of the Cradle-of-Forestry-in-America fault is another granitoid gneiss, the Pink Beds pluton of Acker (1982) or the ggpb-lithodem of this study. It is generally more coarsely crystalline than that of the gglg-lithodem though portions of the gglg-lithodem are coarsely crystalline or even coarser. The ggpb-lithodem has a barely discernable biotite-preferred orientation. A good exposure of the fresh ggpb-lithodem is present in a small quarry adjacent to Forest Service road FS 1206 in the southwest corner of the Cusco quadrangle (340400E, 3916350N).

For a more detailed description of the rocks of the area refer to Acker (1982) and Worley (2000). Additional descriptive information can be found in Dabbagh (1975, 1981), Horton (1974, 1982), Livingston (1966), McKniff (1967), and Morrow (1977). Additional detailed petrography and the geochemistry of the granitoid gneisses can be found in Miller and others (1997, 2000).

Reference Areas

The Cradle-of-Forestry-in-America fault is so named because some of the best exposures of typical features of this fault can be observed along the eastern side of the Cradle of Forestry in America National Historic Site (Figure 3). Most prominent of these is where the Mountains-to-the-Sea Trail passes from the Pink Beds (339970E, 3914340N) to the top of Soapstone Ridge (340530E, 3913620N). The trail traverses the entire width of the fault zone from relatively slightly deformed granitoid gneiss of the ggpb-lithodem on the northwest side of the

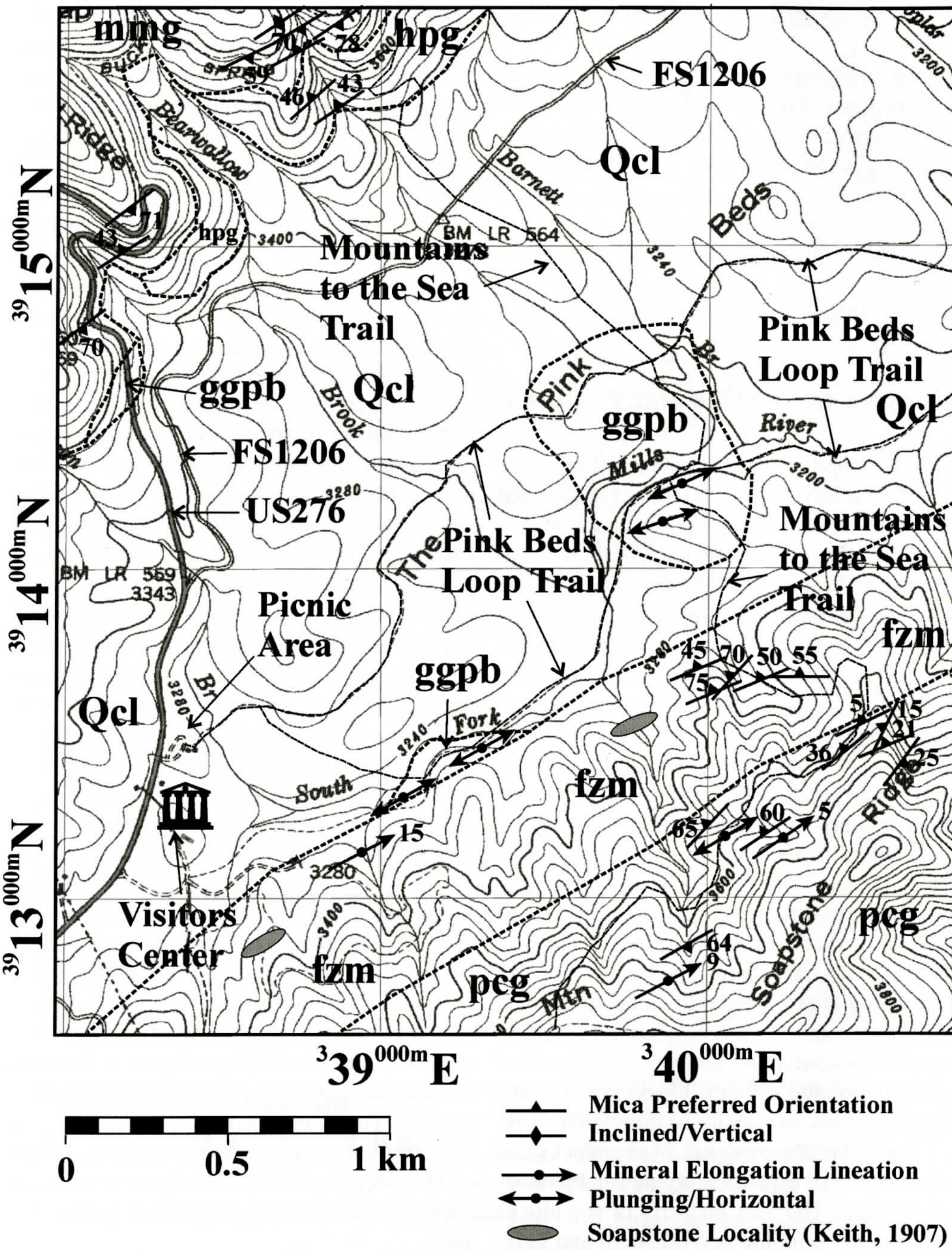

Figure 3. Cradle of Forestry in America Historic Site geologic map. (Qcl)-Quaternary colluvium and alluvium, (fzm)-fault zone mélange of the Cradle-of-Forestry-in-America fault, (pcg)-porphyroclastic gneiss or pcg-lithodem, (mmg)-migmatitic gneiss or mmg-lithodem, (hpg)-hornblende-plagioclase-clinozoisite gneiss or hpg-lithodem, and (ggpb)-granitoid gneiss of the Pink Beds pluton. Dashed contacts are approximate, dotted are concealed. Base map from the Shining Rock 7 ½ minute quadrangle, 40 ft. contour interval.

fault to slightly deformed pcg-lithodem on the southeast.

Good exposures of the fault can also be easily reached from Forest Service road FS 475B in an area extending from Case Camp Ridge Gap to Bennett Knob (Figure 4). The saddle in the ridge where FS 475B passes over Case Camp Ridge is a geomorphic expression of the fault zone. Additionally, good exposures of fault zone features can be observed on Lanning Ridge (333950E, 3907530N) and at Gloucester Gap (331810E, 3903900N).

Synopsis of Fault Related Features

The Cradle-of-Forestry-in-America fault is a laterally continuous zone of intensely deformed rocks that trends northeast-southwest across principally the Shining Rock quadrangle for at least 19 km. Features on the geologic map of the Rosman quadrangle (Horton 1982) indicate that it continues to the southwest an additional kilometer before it passes into unmapped portions of the Lake Toxaway quadrangle near the community of Balsam Grove, North Carolina. To the northeast it passes from the northwest corner of the Pisgah Forest quadrangle into the lightly mapped Dunsmore Mountain quadrangle. The fault zone is vertical to steeply northwest-dipping. The width of the zone ranges from 300 to 600 meters. The central portion of the zone is a tectonic mélange consisting of a block-in-matrix structure. The blocks range in maximum dimension from a few centimeters to nearly 100 meters. Their long axes are generally oriented horizontal and parallel to the trend of the fault. Lithologically the blocks are all of the mylonite-series, especially ultramylonite (Figures 5 and 6). The protolith of the blocks can only be inferred by evaluating their mineralogical makeup. The vast majority of the blocks were derived from the pcg-lithodem and gglg-lithodem situated on the southeast side of the fault zone and the hpg-lithodem and ggpb-lithodem situated on the northwest side. In addition to these there are a few blocks that must have been derived from a source exotic to the area; in particular blocks of chlorite-talc schist or 'soapstone' as they were referred to by Keith (1907).

All the blocks except the 'soapstone' display some sort mineral elongation lineation. Those that probably originated from the hpg-lithodem have blade shaped crystals of hornblende that are oriented with the long axis, which corresponds to the crystallographic c-axis, roughly parallel to the trend of the fault zone (Figure 5). Single crystals of clinozoisite also display an elongation tendency in the same direction but no preferred crystallographic orientation could be ascertained. Plagioclase either forms porphyroclasts or polycrystalline ribbons that are elongate parallel to the fault. Blocks that probably originated from the pcg-lithodem have polycrystalline quartz ribbons oriented parallel to the trend of the fault zone. Groups of ribbons will display a modest quartz lattice preferred orientation, c-axis parallel to the trend of the fault zone. Plagioclase porphyroclast are not easily evaluated suggesting some shape inheritance from previous deformations. Blocks, which were probably derived from one of the granitoid gneiss lithodems, in hand sample appear to have a well-formed mineral elongation, however microscopically such is not easily observed. The apparent elongation seems to be due largely to the smearing out of biotite in streaks parallel to the fault. Quartz and k-feldspar crystals are equant and without any preferred crystallographic orientation. The plagioclase is also equant but oddly it appears almost like a porphyroblast and many crystals have a myremekite mantle (Figure 6). The orientation of these lineations does not always parallel the trend of the fault. Few but significant numbers of blocks display a lineation that is off trend either vertically and/or horizontally (Figure 7A). This is interpreted here to indicate that the lineations originated prior to the formation of the blocks and that blocks have experienced some rotation during translation in the fault zone.

Typical fault zone matrix is quartz-white mica schist. Biotite and chlorite are also present and chlorite can locally be the dominant phyllosilicate. Porphyroclasts of garnet, staurolite, and kyanite may present but their distribution is not uniform. Staurolite and kyanite generally have a post-tectonic sericite alteration while the

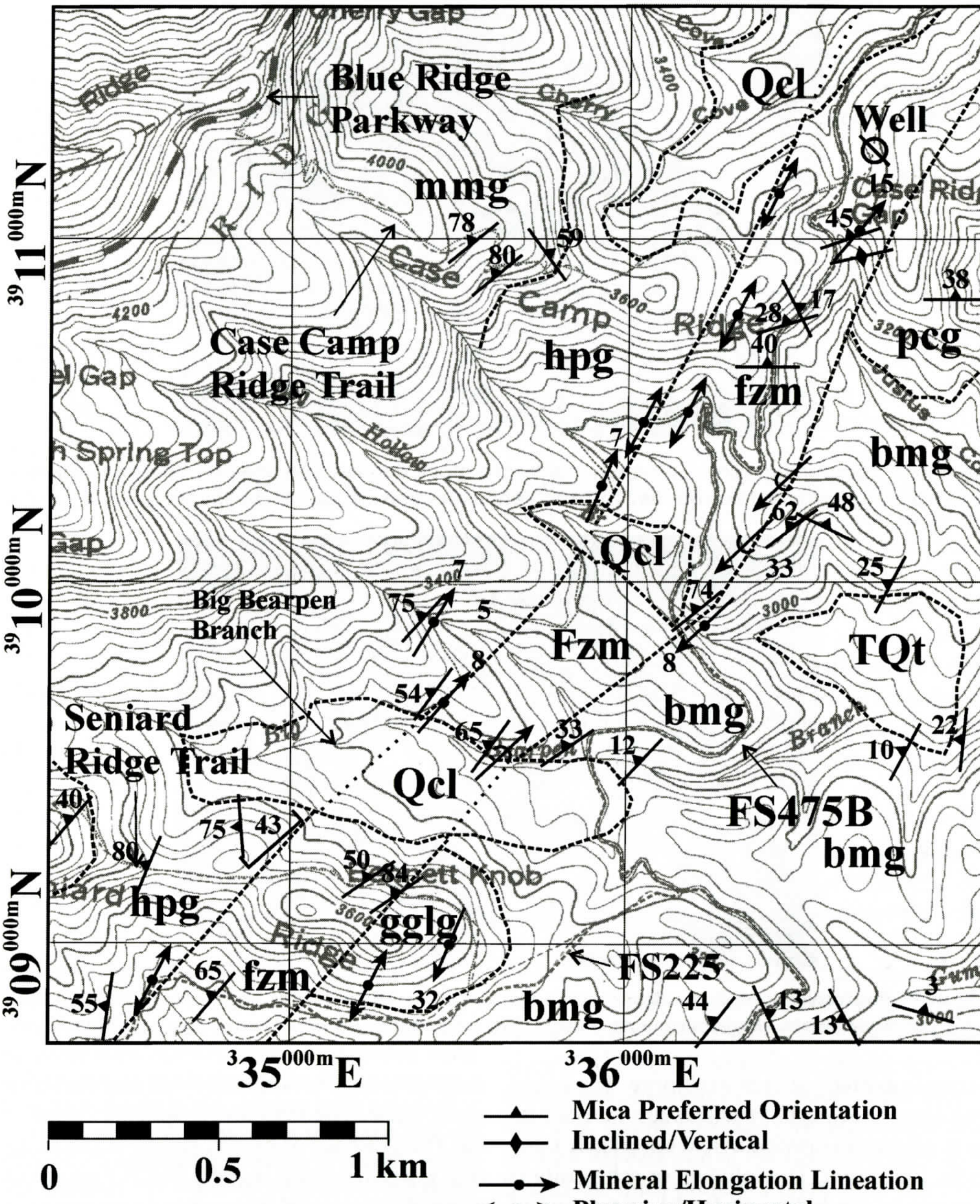

Figure 4. Case Camp Ridge-Seniard Ridge area geologic map. (Qcl)-Quaternary colluvium and alluvium, (TQt)-saprolitic talus, (fzm)-fault zone mélange of the Cradle-of-Forestry-in-America fault, (pcg)-porphyroclastic gneiss or pcg-lithodem, (mmg)-migmatitic gneiss or mmg-lithodem, (hpg)-hornblende-plagioclase-clinozoisite gneiss or hpg-lithodem, (bmg)-biotite white mica gneiss or bmg-lithodem, and (gglg)-granitoid gneiss of the Looking Glass pluton, mappable sized bodies only. Dashed contacts are approximate, dotted are concealed. Base map from the Shining Rock 7 ½ minute quadrangle, 40 ft. contour interval.

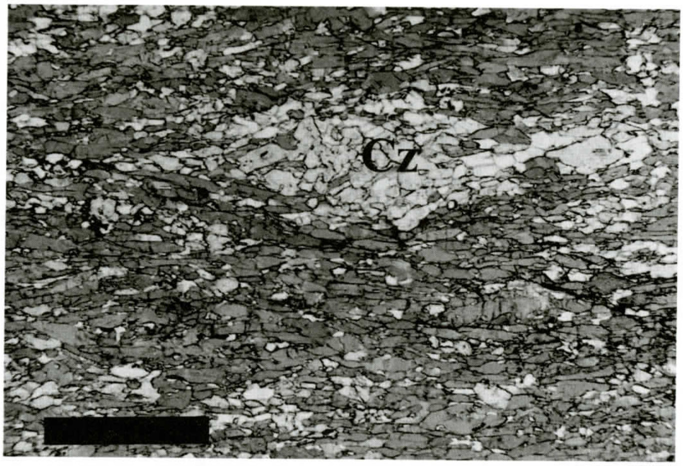

Figure 5. Photomicrograph of ultramylonite from a block derived from the hpg-lithodem. (Cz)-clinozoisite porphyroclast surrounded by hornblende. Section cut parallel to lineation. Bar = 1.0 mm

Figure 6. Photomicrograph of ultramylonite from a block derived from granitoid gneiss. (F)-feldspar porphyroclasts, (My)-myrmekite mantle. Bar = 0.2 mm.

garnet is partially altered to chlorite. The garnet and staurolite porphyroclasts are sometimes large enough to provide a field observable kinematic indication. The foliation or schistosity is defined by the lattice-preferred orientation of the white mica and parallel oriented platy quartz crystals. This foliation parallels the trend of the fault zone (Figure 7B). Chlorite generally adheres to this trend but also occurs without preferred orientation, especially in close proximity to garnet porphyroclasts. The orientation of the foliation is frequently deflected somewhat close to the surface of the blocks. If a large enough area were to be excavated, these deflections probably would supply an indication of shear sense. The matrix is frequently crenulated. The presence of garnet, staurolite, and kyanite porphyroclasts suggest that the origin of some of the material that makes up the matrix is highly deformed (smeared) sections of the bmg-lithodem, sms-lithodem, and garnet-mica schist from the mmg-lithodem and pcg-lithodem.

The ratio of matrix to blocks varies considerably. Some portions of the mélange are nearly entirely matrix whereas others are a mass of blocks each separated by a mere few centimeters of matrix. The matrix is generally more abundant in the central portion of the fault zone

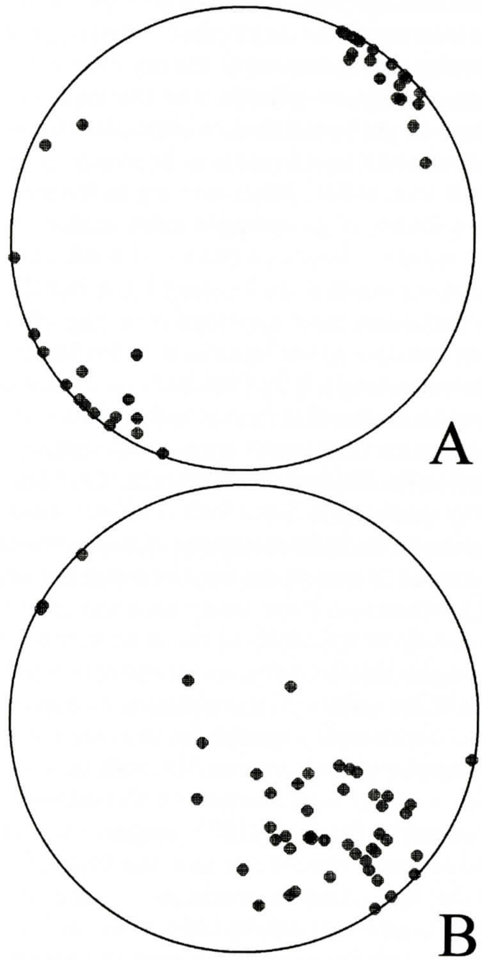

Figure 7. Lower hemisphere, equal area plot of microfabric data. (A) Mineral elongation lineation associated with the Cradle-of-Forestry-in-America fault (N= 43). Data set includes lineation observed in blocks within the mélange and those observed in the country rock adjacent to the fault zone mélange. Note the ones that are off trend suggesting rotation of blocks within the mélange. (B) Poles to mica preferred orientation foliation from the fault zone mélange of the Cradle-of-Forestry-in-America fault (N=40).

and areas where the adjacent country rock was probably of the bmg-lithodem.

The contact of the mélange to country rock seems abrupt though it is rarely observable. Poor exposure makes it difficult to ascertain if one is observing the true contact of the mélange or merely the matrix contact with another block. At one really good exposure near where FS 475B crosses Log Hollow Branch (336230E, 3909900N) the boundary between the mélange and granitoid gneiss of the country rock was abrupt.

The country rock that is generally within 100 m of the contact is of the mylonite-series and displays a field observable mineral elongation lineation that may be pervasive producing an L-tectonite. However the degree of mylonitization as well as the mineral elongations diminishes latterly away from the contact. This lineation trends parallel to trend of the fault and it exhibits a sub-horizontal plunge (Figure 7A). The character of the mineral elongation lineations is nearly identical to that which is found in the blocks of the mélange. However, the lineation within granitoid gneiss at some distance from the mélange becomes principally due to stretching of quartz into polycrystalline ribbons with some reorientation of the quartz lattice to give a c-axis preferred orientation parallel to the fault. K-feldspar also forms ribbons but to a lesser degree; while biotite and white mica form bladed anhedral crystals with their long axis crudely parallel to the fault trend.

The country rock that surrounds the mélange also may contain a spaced cleavage. The general width of the lithons between cleavages increases with increasing lateral distance from the mélange. These can at times be recognized well beyond the range of the field observable lineation. The strike of these is parallel to somewhat oblique to the trend of the fault. The dip is moderately to steeply northwest. White mica is sometimes observed in the plane of the cleavage. This spaced cleavage is readily recognized on the southeast side of the fault where it steeply cuts the mica-preferred orientation foliation and compositional banding foliation in the country rock. To the northwest of the fault this cleavage can be recognized only with difficulty, as it is generally slightly oblique to the trend of the pre-faulting foliations. The cleavage is also observed within the mélange, especially where it cuts blocks or is exposed in a stream bank or road cut.

Shear Sense

Determination of the sense of shear along the Cradle-of-Forestry-in-America fault is complicated by: 1) correlative rocks units on either side of the mapped extent of the fault have not as yet been identified and 2) the surrounding rock, which is multiply deformed, contains microscopic and mesoscopic shear-derived features that predate the fault but may be retained within the fault-disturbed rocks. The general picture that is emerging is that this is a ductile strike-slip fault with a dextral shear sense with a small brittle dip-slip reactivation component.

Examining Figure 2 one may be tempted to jump to the conclusion that this is a dextral fault with 12 km of lateral displacement based upon the apparent offset of the Looking Glass and Pink Beds plutons. These two plutons seem to differ; they have different radiometric ages (Miller and others, 2000), differ in texture and mineralogy (Acker, 1982; Miller and others, 1997; Dockal, 2004), and differ in amount of metamorphic overprint (Acker, 1982; Miller and others, 1997). Furthermore, the Looking Glass intruded the bmg-lithodem in lit-par-lit fashion whereas the Pink Beds seems to have intruded as a single mass into the hpg-lithodem. However, the two plutons may be different parts of the same pluton in differing styles of intrusion (Hatcher, personal communication). The radiometric ages are close enough to not rule this out nor does the mineralogical makeup rule such out since it is still poorly understood in terms of lateral variations. The differences in metamorphic overprint could easily be explained as the result of deformation associated with the fault. The problem is with the rock that was intruded by the plutons and trying to match that and the plutons together at the same time. Simply sliding the two mapped extents back so that they are juxtaposed with the northeast side of the Looking Glass corresponding to the northeast edge of the Pink Beds does not work, as the stratigraphy and structural fabric of the adjoining country rock are different. However, if the offset was greater such that the Pink Beds pluton was juxtaposed to portions of the apparent Looking Glass pluton now position in the Lake Toxaway quadrangle a possible match could be argued for. Livingston (1966) mapped portions of this area but he did not make a distinction between what is now known as the Toxaway gneiss and the Looking Glass pluton, both of which he referred to as Whiteside Granite. Horton (1974, 1982) working in the adjacent Rosman quadrangle does make the distinction. These two bodies of work combined suggest that the Looking Glass intrudes progressively more amphibolite or hpg-lithodem like rock to the southwest of the Shining Rock quadrangle. If the Pink Beds are so related then this implies that: 1) the Cradle-of-Forestry-in-America fault passes west of the northwest flank of the Toxaway antiform in the Lake Toxaway quadrangle; 2) the fault is dextral strike-slip in nature; 3) the magnitude of displacement is around 25 km; 4) the bmg-lithodem and the hpg-lithodem of the study area are lateral metasedimentary facies of the same portion of the Ashe-Tallulah Falls; and 5) the cut off portion of the Looking Glass pluton in the Shining Rock quadrangle might be found in the northeast corner of the Dunsmore Mountain quadrangle or northwest corner of the Skyland quadrangle. Dabbagh (1975) mapped 'layered biotite gneiss (lgn) in this area. His description of the 'layered biotite gneiss' bears some similarity to how the Looking Glass 'sills' are intermixed with the bmg-lithodem in the Shining Rock quadrangle. He does note that the southeastern side of the (lgn) is a 'fault contact' with 'signs of intense shearing and cataclasis.' The extension of the Cradle-of-Forestry-in-America fault to this area or the Lake Toxaway area is plausible but will require more detailed mapping and structural analysis to demonstrate such.

Mesoscopic features including, S-C fabric, garnet and staurolite porphyroclasts in the mélange matrix, and block trains give the best indication of shear sense. S-C fabric occurrences along the known extent of the fault yield a dextral shear sense. The occasional pockets of larger garnet or staurolite porphyroclasts, when found in saprolite matrix, can be excavated to reveal a shear sense. These consistently indicate a dextral shear sense. Trains of blocks become incorporated in the mélange and lag behind the source area as the fault moves. The occurrence of blocks of granitoid gneiss within the mélange near Case Camp Ridge Gap suggests dextral shear. This area lies between the Pink Beds pluton to the northeast and Looking Glass pluton to the southwest. If the sense of shear were sinistral then such blocks at this locality would not be expected.

Microscopic shear sense indicators within the blocks of the mélange are unreliable because: 1) rotation of the block during translation could render a dextral shear sense sinistral and 2) the indicator may have been inherited from an earlier deformation. This later problem also plagues the use of kinematic indicators in the country rock adjacent to the mélange zone, except within the fault deformed granitoid gneiss. The single reliable microscopic shear sense indicator is staurolite porphyroclasts within the matrix of the mélange. Staurolite in the study area formed only in the metamorphic contact aureoles surrounding the Looking Glass and Pink Beds plutons. Such porphyroclast would therefore not have formed during the earlier deformations that proceeded fault development and their kinematic indication should therefore reflect fault shear sense. The two samples observed thus far both give a dextral shear sense whereas the majority of the other microscopic kinematic indicators observed in thin sections from the blocks and country rock also give a dextral shear sense but there are enough with a sinistral sense to exert caution in their application.

DISCUSSION: CHRONOLOGICAL RELATIONSHIPS

Prior to development of the Cradle-of Forestry-in-America fault the area had experienced three recognizable deformations. All the exposed rock bodies in the study area are assumed to have formed after the ~1100 Ma Grenville orogeny. Grenville basement rocks are exposed to the southwest of the study area where they form the core of the Toxaway antiform. They may also occur at depth within the study area. The rocks of the Ashe-Tallulah Falls in the study area are probably metasedimentary. However, there is no evidence for mesoscale or microscale sedimentary layering (S_0). The first really represented deformation in the study area (D_1) resulted in the formation of a strong compositional banding foliation (S_1) that characterizes the rock to the northwest of the fault. It is associated with syntectonic garnet, kyanite, and sillimanite. This foliation is largely obscured by later events southeast of the Cradle-of-Forestry-in-America fault, but it can be recognized in boudins, mesoscale lithons, and inclusions within garnet. This foliation is the S_c foliation of Horton (1975), the S_0 of Dabbagh (1975) and Morrow (1977), and the S_1 foliation of Worley (2000). It also probably corresponds to the S_1 of the Inner Piedmont (Merschat and others, 2005) and S_1 and/or dominant compositional layering foliation referred to in Hatcher and Merschat (2005).

The second deformation (D_2) formed the pervasive, gently dipping mica preferred orientation foliation (S_2) in the region to the southeast of the fault. This foliation is the S_1 foliation of Acker (1982), Dabbagh (1975), Horton (1974) and the S_2 foliation of Worley (2000). Northwest of the fault this deformation produced macroscopic and mesoscopic isoclinal similar folds (F_2). These folds correspond to the F_1 folds of Dabbagh (1975), Horton (1974), and Morrow (1977); the F_2 folds of Acker (1982) and the 'third order folds' of Livingston (1966). The axial surfaces of these folds parallel the S_2 foliation of Morrow (1977). The variation of style of features attributed to this deformation from one side of the fault to the other may in the future prove useful in further defining shear sense and magnitude of displacement of the fault.

The third deformation (D_3) corresponds to a complex intrusive sequence that was initiated first by formation of mafic dikes that are discordant to the earlier foliations. These are rather fancifully illustrated on Keith's (1907) map. This is followed by the emplacement of the two granitoid masses the Looking Glass (gglg-lithodem) and the Pink Beds plutons (ggpb-lithodem). Both intruded cooler rock and formed weak but recognizable contact aureoles, which are best characterized by the appearance of staurolite, second-generation kyanite, and secondary garnet overgrowths (Dockal, 2001; 2004). The Looking Glass intruded in lit-par-lit fashion utilizing the weakness formed by the mica-preferred orientation foliation, S_2, of the country rock formed during the D_2. Intrusions of the masses of the granitoid gneiss created, at the macroscopic level, the Davidson River antiform and, at the mesoscopic level, drape-like folding of the overlying biotite-white mica gneiss due to variations in sill thickness. This is especially evident at the terminus of each sill. One of these is illustrated in Horton (1974, his Figure 14) as an example of a F_2 fold. This is followed by the intrusion of aplitic dikes that crosscut the rock on both sides of the fault, including the granitoid gneiss bodies, but have not been observed within or crosscutting the fault zone. These dikes presumably correspond to the 'trondhjemite dikes' of Acker (1982), Dabbagh (1975), and Morrow (1977).

The next deformation (D_4) resulted in the formation of the Cradle-of-Forestry-in-America fault and possibly some other features in the area including the Kings Creek fault describe by Acker (1982) and the S_3 foliation of Worley (2000). Crosscutting relationships suggest that there were two stages to the deformation. The first (D_{4A}) produced the pronounced mineral elongations (L_{4A}) that are observable in outcrop. The second (D_{4B}) resulted in the mélange formation, its matrix with a mica-preferred orientation (S_{4B}) and its attendant blocks with rotated mineral elongations. There may also be some mesoscale folding associated with this deformation in the rock adjacent to the mélange. The two stages are lumped together in a single deformation mainly because of their close field associations, however they probably represent two different activations of the fault zone each occurring under differing P-T conditions. The preferred growth orientation of hornblende and the myremekite mantled plagioclase porphyroclasts associated with mylonite-series rocks of the fault indicate earliest stage of fault movement was under amphibolite facies conditions. The white mica-chlorite mélange zone matrix suggests that the second stage was under greenschist facies conditions.

A fifth deformation (D_5) characterized by a spaced cleavage (S_5) post dates the fault but is spatially associated with the fault. This is a brittle event with mesoscale faulting crosscutting the mica-preferred orientation foliation (S_{4B}) of the mélange (Figure 8). The shear sense indicated is dip-slip, tops up indicating a final reactivation of the Cradle-of-Forestry-in-America fault as a reverse fault. Similar features were described by Worley (2000), his S_4 foliation, from a construction site within the Brevard fault zone located on the north side of Brevard, North Carolina. Acker (1982) reported similar 'cataclastic' features associated with the Kings Creek fault. The 'cataclastic' features noted by Dabbagh (1975) might also be related to this deformation. The formation of these structural elements may be coeval with the formation of the Rosman fault described by Horton (1980, 1982), Horton and Butler (1986), Liu (1991), and Hatcher (2001), which is located 10 km southeastward in the Rosman quadrangle along the northwest margin of the Brevard fault zone.

A second brittle deformation (D_6) follows. This produced a sparse set of fractures that is dominated by east-west striking, vertical fractures that have observable displacement and associated folding. An east-west fracture exposed in the small quarry at Gloucester Gap (331810E, 3903900N) clearly crosscuts features attributed to the Cradle-of-Forestry-in-America fault. These fractures also exert a greater influence on the development of the geomorphology of the area than does the Cradle-of-Forestry-in-America fault. Acker (1982) noted that one of these fractures located in the small quarry along US 276 (337930E, 3908300N) had slickensides that plunged 10° east. Dabbagh (1975) and Morrow (1977) considered these fractures to be their S_4 foliation. Similar east-west oriented fractures or lineaments have been reported else where in the Blue Ridge and Piedmont (Hack, 1982; Merschat and Wiener, 1988; Alcott, 1997; Lowe, 1997; Crenshaw and others, 2000; Gay, 2000; Dennison and Stewart, 2001; and Hatcher and others, 2005), but their age is uncertain beyond being post orogenic.

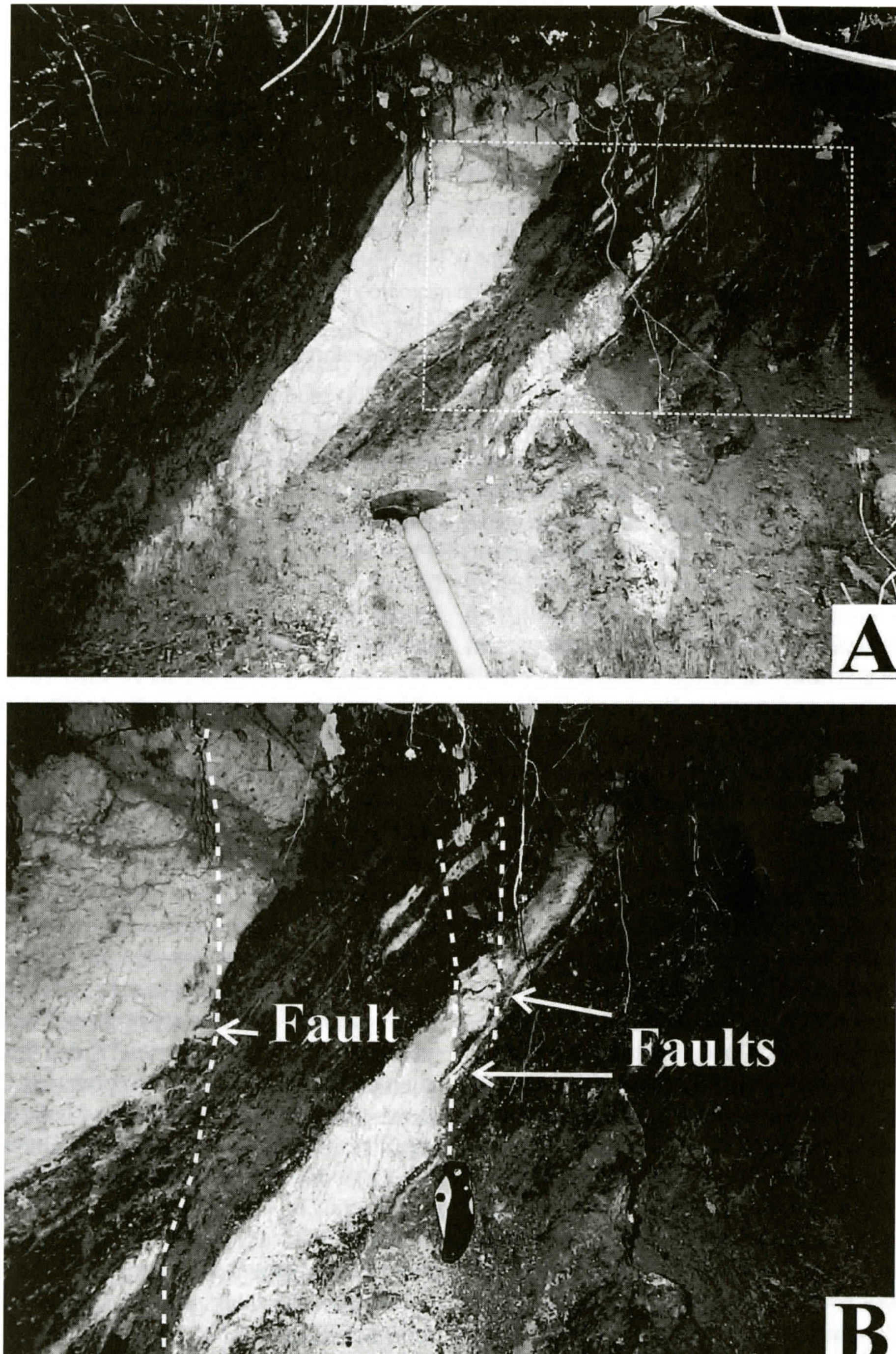

Figure 8. Saprolitic mélange of the Cradle-of-Forestry-in-America fault located near Big Bearpen Branch, see Figure 4. (A) General view, light-colored portions are blocks of mylonite derived from granitoid gneiss; darker areas are reddish brown saprolitic mica schist or mélange matrix. Hammer for scale. (B) Close-up view of the dashed rectangle area of view (A). White dashed lines denote spaced cleavages (faults) that cut both blocks and matrix and indicate tops (right side) up shear sense. Pocketknife for scale.

Table 1. Radiometric dates from the Looking Glass and Pink Beds plutons.

Pluton	Age	Method	Reference
Looking Glass	414-420 Ma	Rb-Sr whole-rock analysis cooling age	Personal communication, 1976 of S. Kish reported in Acker (1982)
	415 Ma	Rb-Sr whole-rock analysis	Kish (1983) as reported in Miller and others (1997)
	380±3 Ma	High-resolution ion microprobe analysis of zircon rims ($^{206}Pb/^{238}U$)	Miller and others (2000)
	377±4 Ma	High-resolution ion microprobe analysis of zircon rims ($^{207}Pb/^{235}U$)	Miller and others (2000)
Pink Beds	310-330 Ma	Rb-Sr mineral and whole-rock analysis	Miller and others (1997)
	443-480 Ma	zircon ($^{206}Pb/^{238}U$)	Miller and others (1997)
	499-844 Ma	zircon ($^{207}Pb/^{206}Pb$)	Miller and others (1997)
	388±5 Ma	High-resolution ion microprobe analysis of zircon rims ($^{206}Pb/^{238}U$)	Miller and others (2000)
	374±6 Ma	High-resolution ion microprobe analysis of zircon rims ($^{207}Pb/^{235}U$)	Miller and others (2000)

Looking Glass and Pink Beds plutons are the only rock within the mapped area of the fault that has been radiometrically dated (Table 1). Ion-microprobe analysis of the rims of zircons from the Looking Glass, Pink Beds and Rabun plutons by Miller and others (2000), indicate formation to have occurred 370-395 Ma, mid-Devonian or during the Acadian orogeny. This presents a problem in that the intrusion of the Looking Glass exploited the S_2 foliation. The S_2 foliation most probably corresponds to the S_2 foliations of Hatcher (2001) and Merschat and others (2005), which they consider Neoacadian 360-345 Ma. Since an intruding body can not be older that what it intrudes either the age of the Looking Glass pluton or the age of the S_2 foliation is in error.

Miller and others (2006) considered the ion-microprobe ages too "imprecise to provide tight constraints on rates and time spans of tectonic and metamorphic processes." They report an ID-TIMS U-Pb zircon age of 335.1±2.8 Ma for the Rabun but do not report ages for the Looking Glass and Pink Beds plutons. The 335 Ma age for the Rabun was confirmed by Stahr and others (2006) whose description of the Rabun closely parallels that of the Looking Glass. If the results of Miller and others (2006) and Stahr and others (2006) can be extended to the Looking Glass and Pink Beds then they also may have crystallized ~335 Ma. In this study area peak metamorphism was concurrent with the D_1 deformation and formation of the S_1 compositional banding with the area reaching amphibolite facies sillimanite zone. Moecher and others (2005) considered regional peak metamorphism in the Blue Ridge to be Taconian. They further noted "Ashe metapelites and particularly the amphibolites exhibit evidence of Acadian-age mineral growth, and resetting or disturbance of Taconian isotopic systematics." The S_2 foliation of this study probably corresponds to this 'mineral growth' and is thus Acadian or Neoacadian. The interpretation of this study is that the 370-395 Ma age for the Looking Glass and Pink Beds plutons is incorrect, that they are probably related to the Mississippian plutons of ~335 Ma, and that the development of the Cradle-of-Forestry-in-America fault is Alleghanian.

The Looking Glass and Pink Beds plutons both have a well formed contact aureole characterized by the formation of kyanite and staurolite in the metapelites that are within one kilometer of the plutons and new garnet and secondary overgrowths on older garnets out to several kilometers from the plutons (Dockal, 2001; 2004). Thus most of the area traversed by the fault was under amphibolite facies conditions as a consequence of the plutonism. The mineral elongation lineation, specifically dynamically recrystallized hornblende, found in the hpg-lithodem immediately adjacent to the fault zone and blocks within the fault zone mélange are indicative of temperatures of ~600°C (Hacker and Christie, 1990). Myrmekite associated with feldspar porphyroclasts like that observed in blocks of granitoid gneiss in the mélange suggest temperatures above 500°C (Passchier and Trouw, 1998). This may indicate that the initial strike-slip movement (D_{4A}) occurred shortly after intrusion of the plutons while the area was still hot. Chronologically this would correspond to the D_3 deformation in the Inner Piedmont of Merschat and others (2005) or early Alleghanian 330-325 Ma.

The presence of well-foliated chlorite and white mica and the frequent absence of biotite in the matrix of the mélange suggest somewhat cooler conditions of greenschist facies prevailed during the D_{4B} mélange stage of strike-slip movement on the fault. Similar conditions prevailed in the Inner Piedmont during the D_4 deformation of Merschat and others (2005) or Alleghanian ~300 Ma.

The spaced cleavage and brittle faults of the D_5 that are spatially related to the Cradle-of-Forestry-in-America fault indicate final reactivation as a reverse dip-slip event. This is similar to and probably corresponds chronologically with the development of the Rosman fault which is late Alleghanian ~260 Ma (Hatcher, 2001; Merschat and others, 2005). The Rosman fault lies only a few kilometers to the southeast of the Cradle-of-Forestry-in-America fault along the northwest side of the Brevard fault zone (Figure 1).

CONCLUSIONS

The Cradle-of-Forestry-in-America fault occurs in the Shining Rock quadrangle as a zone, 300 to 600 meters wide that contains a block-in-matrix tectonic mélange consisting of blocks that were derived from the adjacent country rock plus some exotic to the area in a quartz-white mica matrix. Mesoscopic and to a lesser extent microscopic kinematic indicators from the mapped extent of the Cradle-of-Forestry-in-America fault support a dextral shear sense.

The dissimilarity of the rock units on either side of the Cradle-of-Forestry-in-America fault, including apparent stratigraphic succession and textural fabric, support a substantial degree of offset, probably in excess of 15 km and possibly as much as 25 km, however detailed field mapping in the areas adjacent to this study, specifically Lake Toxaway and Dunsmore Mountain quadrangles, will be required to demonstrate this.

Initial ductile strike-slip movement on the Cradle-of-Forestry-in-America fault probably occurred during the early Alleghanian 330-325 Ma; however the conflicting ages of the Looking Glass pluton and the rock fabric that it intruded will have to be resolved in order to more definitely establish this. Reactivation of the fault under cooler conditions of greenschist facies resulted in additional strike-slip movement probably during the Alleghanian ~300 Ma while a final reactivation as a brittle dip-slip reverse fault occurred during the late Alleghanian ~260 Ma.

ACKNOWLEDGMENTS

This paper benefited considerably from the thorough review by Robert D. Hatcher, Jr. I wish to express my appreciation to those members of the Transylvania County Sheriff's Department who spent a cold and snowy night looking for the author thinking him lost or injured somewhere in the mountain laurel of the Cradle of Forestry in America.

REFERENCES CITED

Acker, L.L., 1982, Geology of the Shining Rock Quadrangle, North Carolina (M.S. thesis): Chapel Hill, University of North Carolina, 110 p.

Alcott, A.E., 1997, A study of lineaments in the Knoxville, Johnson City, Winston-Salem, and Charlotte quadrangles (B.S. thesis): Chapel Hill, University of North Carolina, 22 p.

Crenshaw, B.A., Garihan, J.M., Ranson, W.A., and Carroll, A.D., 2000, Geology of part of the Table Rock 7.5-minute quadrangle and outlying pavement exposures, western inner Piedmont, Pickens and Greenville counties, South Carolina: Geological Society of America Abstracts with Programs, v. 32, no. 2, p. 13.

Dabbagh, A.E., 1975, Geology of the Skyland and Dunsmore Mountain quadrangles, western North Carolina (Ph.D. dissertation): Chapel Hill, University of North Carolina, 228 p.

Dabbagh, A.E., 1981, Geologic map and minerals resources summary of the Skyland Quadrangle, North Carolina: North Carolina Geological Survey Geologic Map GM 193-NE, scale 1:24,000.

Dennison, J.M., and Stewart, K.G., 2001, Regional structural and stratigraphic evidence for dating Cenozoic uplift of southern Appalachian highlands: Geological Society of America Abstracts with Programs, v. 33, no. 2, p. 6.

Dockal, J. A., 2001, Boundary relationships of the Looking Glass Pluton, Shining Rock Quadrangle, Transylvania County, North Carolina: Geological Society of America Abstracts with Programs, v. 33, no. 2, p. 50.

Dockal, J.A., 2004, 'Cradle-of-Forestry-in-America Fault', a newly discovered Northeast-southwest trending dextral fault in the Eastern Blue Ridge, Transylvania County, North Carolina: Geological Society of America Abstracts with Programs, v. 36, no. 2, p. 74.

Gay, S. P., Jr., 2000, Unmapped topographic alignments visible on 3D stereo terrain map of a 2 degrees X 2 degrees segment of the Southern Appalachians: Geological Society of America Abstracts with Programs, v. 32, no. 2, p. 19.

Hack, J.T., 1982, Physiographic divisions and differential uplift in the Piedmont and Blue Ridge: U.S. Geological Survey Professional Paper 1265, 49 p.

Hacker, B.R. and Christie, J.M., 1990, Brittle/ductile and plastic/cataclastic transitions in experimentally deformed and metamorphosed amphibolite, *in* Duba, A.G., Durham, W.B., Handin, J.W., and Wang, H. F., (eds.), The Brittle-ductile transition in rocks, American Geophysical Union, Geophysical Monograph 56, p. 127-147.

Hadley, J.B. and Nelson, A.E., 1971, Geologic map of the Knoxville Quadrangle, North Carolina, Tennessee, and South Carolina: U.S. Geological Survey Geologic Investigations Map I-654, scale 1:250,000.

Hatcher, R.D., Jr., 1971, Stratigraphic, petrologic, and structural evidence favoring a thrust solution to the Brevard problem: American Journal of Science, v. 270, p. 177-202.

Hatcher, R.D., Jr., 2001, Rheological partitioning during multiple reactivation of the Paleozoic Brevard Fault Zone, southern Appalachians, USA *in* Holdsworth, R.E., Strachan, R.A., Magloughlin, J.F., and Knipe, R.J., (eds.), The Nature and Tectonic Significance of Fault Zone Weakening. Geological Society, London, Special Publications, 186, p. 257-271.

Hatcher, R.D., Jr., Merschat, A.J., and Thigpen, J.R., 2005, Blue Ridge Primer *in* Hatcher, R.D., Jr. and Merschat, A.J. (eds.), Blue Ridge Geology Geotraverse East of the Great Smokey Mountains National Park, Western North Carolina: North Carolina Geological Survey, Carolina Geological Society Annual Field Trip Guidebook, p. 1-24.

Horton, J.W., Jr., 1974, Geology of the Rosman area, Transylvania County, North Carolina (M.S. thesis): Chapel Hill, University of North Carolina, 63 p.

Horton, J.W., Jr. 1980, Post-mylonitic brittle deformation in the Brevard fault zone, North Carolina [abstract], *in* Wones, D.R., (ed.), Proceedings, the Caledonides in the USA, IGCP Project 27-Caledonide Orogen, 1979 Meeting: Blacksburg, Virginia Polytechnic Institute and State University, Department of Geological Sciences Memoir 2, p. A17.

Horton, J.W., Jr., 1982, Geologic map and mineral resources summary of the Rosman quadrangle, North Carolina: North Carolina Geological Survey, Geologic Map GM 185-NE, scale 1:24,000.

Horton, J.W., Jr., and Butler, J.R., 1986, The Brevard fault zone at Rosman, Transylvania County, North Carolina, *in* Neathery, T.L., (ed.), Centennial Field Guide Volume 6, Southeastern Section: Boulder, CO, Geological Society of America, p. 251-256.

Keith, A., 1907, Description of the Pisgah quadrangle, North Carolina-Tennessee: U.S. Geological Survey Geologic Atlas, Folio 147, 8 p.

Kish, S.A., 1983, A geochronological study of deformation and metamorphism in the Blue Ridge and Piedmont of the Carolinas (Ph.D. dissertation): Chapel Hill, University of North Carolina, 220 p.

Lesure, F.G. and Dunn, M.L., Jr., 1982, Mineral resource potential map of the Shining Rock Wilderness, Haywood County, North Carolina: U.S. Geological Survey Miscellaneous Field Studies Map MF-1290-C, scale 1:48,000.

Liu, A., 1991, Structural geology and deformation history of the Brevard fault zone, Chauga Belt, and Inner Piedmont, Northwestern South Carolina and adjacent areas (Ph.D. dissertation): Knoxville, The University of Tennessee, 167 p.

Livingston, J.L., 1966, Geology of the Brevard zone and Blue Ridge in southwestern Transylvania County, North Carolina (Ph.D. dissertation): Houston, TX, Rice University, 100 p.

Lowe, A.L., 1997, A topographic analysis of a post-orogenic lineament set in the Blue Ridge Mountains of North Carolina (B.S. thesis): Chapel Hill, University of North Carolina, 59 p.

McKniff, J., 1967, Geology of the Highlands-Cashiers area, North Carolina-South Carolina (Ph.D. dissertation): Houston, TX, Rice University, 99 p.

Merschat, A.J., Hatcher, R.D., Jr., and Davis, T.L., 2005, The northern Inner Piedmont, southern Appalachians, USA: kinematics of transpression and SW-directed mid-crustal flow: Journal of Structural Geology, v. 27, p. 1252-1281.

Merschat, C.E., and Wiener, L.S., 1988, Geology of the Sandymush and Canton quadrangles, North Carolina: North Carolina Geological Survey Bulletin, no. 90, 55 p.

Miller, B.V., and Stewart, K.G., 2002, Pluton ages in the eastern Blue Ridge Province, North Carolina; constraints on timing of tectonics and metamorphism in deep levels of an Ordovician accretionary wedge complex: Geological Society of America Abstracts with Programs, v. 34, no. 6, p. 41.

Miller, B.V., Fetter, A.H., and Stewart, K.G., 2006, Plutonism in three orogenic pulses, Eastern Blue Ridge Province, southern Appalachians: Geological Society of America Bulletin, v. 118, p. 171-184.

Miller, C.F., Fullagar, P.D., Sando, T.W., Kish, S.A., Solomon, G.C., Russell, G.S., and Steltenpohn, L.F.W., 1997, Low-potassium, trondhjemitic to granodioritic plutonism in the eastern Blue Ridge, southwestern North Carolina-northeastern Georgia, *in* Sinha, A.K, Whalen, J.B., and Hogan, J.P., (eds.), The nature of magmatism in the Appalachian orogen: Boulder, CO, Geological Society of America Memoir 191, p. 235-254.

Miller, C.F., Hatcher, R.D., Jr., Ayers, J.C., Coath, C.D., and Harrison, T.M., 2000, Age and zircon inheritance of eastern Blue Ridge plutons, southwestern North Carolina and northeastern Georgia, with implications for magma history and evolution of the Southern Appalachian orogen: American Journal of Science, v. 300, no. 2, p. 142-172.

Moecher, D.P., Massey, M.A., and Tracy, R.J., 2005, Timing and pattern of metamorphism in the western and central Blue Ridge, TN and NC: Status and outstanding problems, *in* Hatcher, R.D., Jr. and Merschat, A.J. (eds.), Blue Ridge Geology Geotraverse East of the Great Smokey Mountains National Park, Western North Carolina: North Carolina Geological Survey, Carolina Geological Society Annual Field Trip Guidebook, p. 57-66.

Morrow, H.B., 1977, Structural geology of the southern half of Cruso quadrangle, North Carolina, (M.S. thesis): Chapel Hill, University of North Carolina, 67 p.

North American Geological-Map Data Model Science Language Technical Team, 2004, Report on progress to develop a North American science-language standard for digital geologic-map databases; Appendix B-Classification of metamorphic and other composite-genesis rocks, including hydrothermally altered, impact-metamorphic, mylonitic, and cataclastic rocks, Version 1.0 (12/18/2004), *in* Soller, D.R., (ed.), Digital Mapping Techniques'04-Workshop Proceedings: U.S. Geological Survey Open-File Report 2004-1415, 56 p.

Passchier, C.W. and Trouw, R.A.J, 1998, Microtectonics: Berlin, Springer-Verlag, 289 p.

Raymond, L.A., 1984, Classification of mélanges, *in* Raymond, L.A., (ed.), Mélanges: Their nature, origin, and significance: Geological Society of America Special Paper 198, p. 7-20.

Stahr, D.W., Hatcher, R.D., Jr., Miller, C.F., and Wooden, J.L., 2006, Alleghanian deformation in the Georgia and North Carolina eastern Blue Ridge: Insights from pluton ages and fabrics: Geological Society of America Abstracts with Programs, v. 38, no. 3, p. 20.

Worley, B.D., 2000, Geology across the western boundary of the Brevard Fault Zone, Transylvania County, North Carolina, (M.S. thesis): Wilmington, NC, University of North Carolina at Wilmington, 120 p.

SOUTHEASTERN GEOLOGY
V. 44, No.4, February 2007, p. 191-201

THE STRATIGRAPHIC UTILITY OF THE TRACE FOSSIL *PTERIDICHNITES BISERIATUS* IN THE UPPER DEVONIAN OF EASTERN WEST VIRGINIA AND WESTERN VIRGINIA, USA

RONALD R. MCDOWELL[1]

KATHARINE L. AVARY

West Virginia Geological and Economic Survey, Morgantown, WV 26508

DAVID L. MATCHEN

Department of Geology and Physical Sciences, Concord University, Athens, WV 24712

JAMES Q. BRITTON

West Virginia Geological and Economic Survey, Morgantown, WV 26508

1. mcdowell@geosrv.wvnet.edu

ABSTRACT

Similar lithologies and lithofacies are present in two Upper Devonian siliciclastic units, the Brallier and Foreknobs formations, in eastern West Virginia and western Virginia, USA. Specimens of an unusual trace fossil, *Pteridichnites biseriatus*, occur in variable numbers throughout both stratigraphic units. *P. biseriatus* is present in abundance in the lowermost Brallier and this abundance-zone serves as a local stratigraphic marker for the Brallier. The trace fossil, originally suggested as an indication of polychaete or arthropod locomotion, is herein proposed as the locomotion trace of an unidentified ophiuroid.

INTRODUCTION

Traditionally, ichnofossils are used in paleoecology and sedimentology to aid in the interpretation of paleoenvironmental conditions. They have become important in the fields of sequence and event stratigraphy (Pemberton and others, 1992; Pemberton and others, 2004) particularly with regard to detecting and delineating discontinuities and omission surfaces. However, because ichnofossils are, for the most part, *facies* fossils, i. e., restricted to a particular set of environmental and sedimentological conditions, they are not typically useful for stratigraphic correlation or identifying stratigraphic units. In fact, the *Treatise on Invertebrate Paleontology, Part W* states, "Lebensspuren usually have little importance in stratigraphy." (Hantzschel, 1979, p. 9).

Exceptions do occur. The *Treatise* cites the ichnogenus *Oldhamia* as being restricted to the Cambrian and the ichnospecies *Phycodes cincinnatum* as being restricted to the Ordovician. Crimes (1968; 1969; 1970) and Seilacher (1960; 1970) give stratigraphic examples in which ichnofossils have utility in either determining the age of a group of sedimentary strata or in correlation.

This paper discusses the use of the ichnofossil *Pteridichnites biseriatus* in differentiating Upper Devonian formations for the purposes of geologic mapping and briefly speculates on the origin and interpretation of *P. biseriatus* in light of the examination of numerous new specimens.

GEOLOGIC SETTING

The authors have been engaged in bedrock geologic mapping in eastern West Virginia (Figure 1) since 1997 under the auspices of the STATEMAP program jointly funded by the United States Geological Survey (USGS) and the West Virginia Geological and Economic

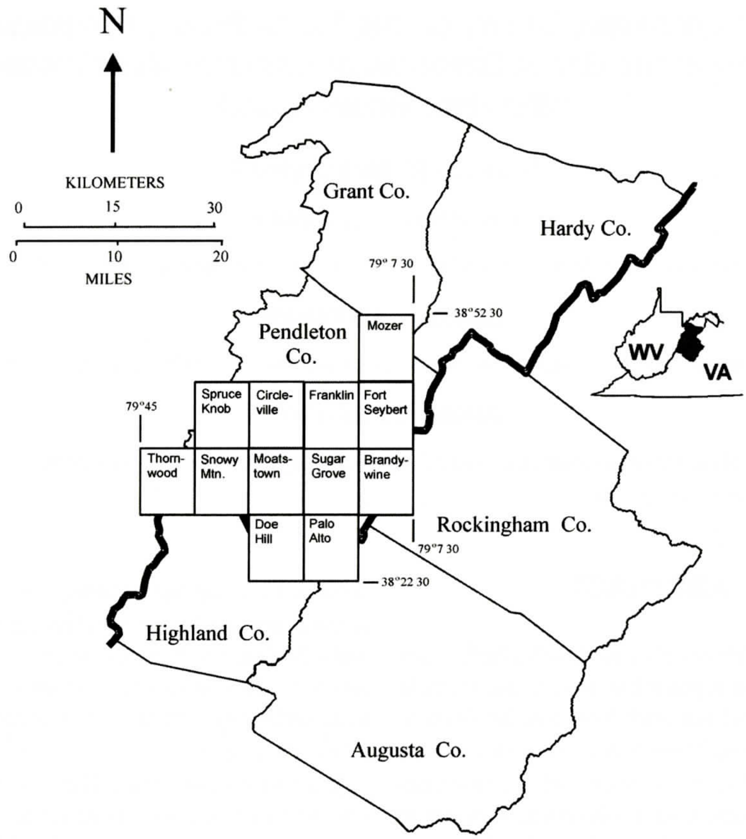

FIGURE 1. Map of eastern West Virginia (Grant, Hardy, and Pendleton counties) and western Virginia (Augusta, Highland, and Rockingham counties) showing the 7 ½ minute quadrangles mapped by the authors at 1:24,000 scale under various STATEMAP projects from 1997 through 2005.

Survey (WVGES). Strata in the area under investigation range in age from Ordovician through Pennsylvanian. A smattering of Jurassic and Eocene igneous intrusives are also present. The current discussion deals specifically with the Upper Devonian strata of the region (Figure 2).

The study area lies east of or on the eastern margin of the Allegheny Plateau (Figure 3) and, as such, has been deformed by a variety of tectonic events. Typical of the eastern United States, outcrop exposures within the study area are limited by vegetation, thick soil cover, or human activities. New construction is prized for fresh exposures of rock (McDowell and others, 2004). However, once a mapping traverse leaves areas immediately adjacent to primary and secondary roads, exposures become scarce and frequently difficult to place into proper stratigraphic context.

Limited or sparse outcrop exposure is not the only factor that may hamper the geologist's ability to assign an outcrop to the correct geological formation. The Upper Devonian siliciclastic strata of the region, specifically, the Brallier, Foreknobs (formerly Chemung), and Hampshire formations represent a complex mix of lithofacies deposited during a major, Late Devonian, regressive episode (Dennison, 1970; Avary, 1978; Avary and Dennison, 1980). The majority of the strata comprising the Hampshire Formation are red mudstones and red or greenish-grey, fine-grained quartz sandstones. Color alone is usually diagnostic in the identification

Series	Stage	Stratigraphic Units			General Lithology	Occurrence of *P. biseriatus*
Devonian	Famennian	Hampshire Formation			Nonmarine, red sandstones, shales, and mudstones with occasional plant fossils.	
Devonian	Famennian	Greenland Gap Group	Foreknobs Formation	Red Lick Member	Fossiliferous marine siltstones and sandstones grading into nonmarine siltstones and sandstones.	? ?
Devonian	Frasnian	Greenland Gap Group	Foreknobs Formation	Pound Member	Conglomeratic medium to coarse-grained sandstone.	
Devonian	Frasnian	Greenland Gap Group	Foreknobs Formation	Blizzard Member	Very fossiliferous, marine siltstones, sandstones, and minor shale. Several thick sand beds in the middle of the unit.	
Devonian	Frasnian	Greenland Gap Group	Foreknobs Formation	Briery Gap Member	Conglomeratic fine to coarse-grained sandstone.	
Devonian	Frasnian	Greenland Gap Group	Foreknobs Formation	Mallow Member	Fossiliferous marine sandstones and siltstones. Base is marked by first occurrence of medium to coarse sandstone.	
Devonian	Frasnian	Greenland Gap Group	Scherr Formation		Scherr is recognized as siltstone with shale and fine sandstones, all of which weather a light olive grey.	
Devonian	Frasnian	Brallier Formation			Marine, turbiditic, dark grey to light olive grey shales with interbedded siltstones. Rare invertebrate fossils.	Acme Zone
Devonian	Frasnian	Millboro Shale			Marine, anoxic waters, black, carbonaceous, silty shale with calcareous lenses and nodules. Contains a depauperate invertebrate fauna.	

FIGURE 2. Upper Devonian stratigraphic terminology for the study area. Lithologic descriptions from field observations and Rossbach and Hall, 1998. Greenland Gap Group lithologies and stratigraphic subdivisions from Dennison, 1970; 1988; and 1996. Occurrence of *Pteridichnites biseriatus* from field observations and Rossbach and Hall, 1998.

of the Hampshire. On the other hand, the Brallier and the middle, fine-grained portion of the Foreknobs (Blizzard Member) have similar lithologies, namely interbedded brown and greenish-grey shales and siltstones that may be indistinguishable when observed in an isolated exposure, i. e., out of stratigraphic context.

STRATIGRAPHIC UNCERTAINTY

After struggling with differentiating the Brallier and Foreknobs for the 1997 mapping season, the authors began to note the presence of a distinctive trace fossil (Figures 4 and 5) in siltstones and shales exposed within the field area. Examination of the more continuous exposures of Upper Devonian strata seemed to indicate that this unique ichnofossil was restricted to the Brallier. However, Rossbach and Hall (1998) and Rossbach (personal communication, 2002) reported the presence of the trace within the overlying Scherr and Foreknobs formations. Repeated visits to spectacular new exposures of Foreknobs near Elkins, WV (Rutledge and others, 2002; Cole and McDowell, 2003), eventually yielded a limited number of specimens identifiable as *Pteridichnites biseriatus*. In addition, in our map area to the east, we have also confirmed the presence of *P. biseriatus* in the Foreknobs, albeit in similarly small numbers. For our study area, we believe that the stratigraphic range and abundance of *P. biseriatus* is as shown in Figure 2. One of the paper's reviewers (John Dennison, personal communica-

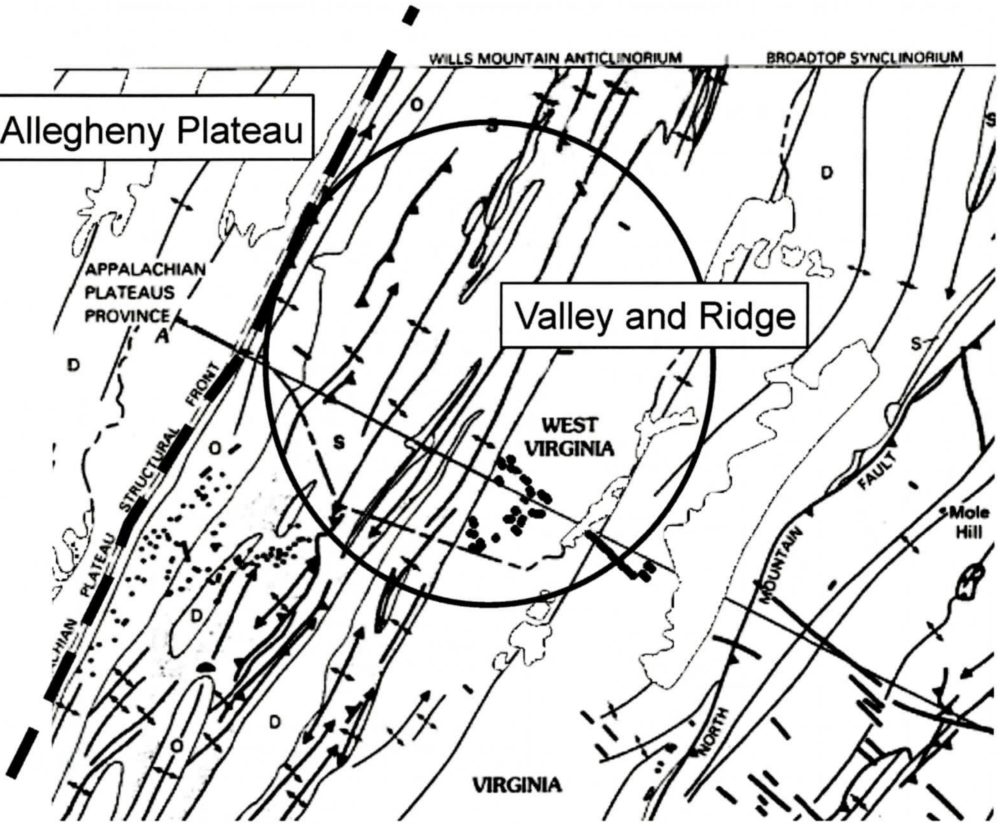

FIGURE 3. Generalized geologic map of eastern Western Virginia and western Virginia showing the approximate boundary (dashed line) between the Allegheny Plateau and Valley and Ridge structural provinces. The intensity of structural deformation increases to the east. Study area enclosed with an ellipse. Modified from Southworth and others, 1993, p. 3.

tion, 2006) cautions that the abundance of *P. biseriatus* within the Foreknobs is strongly linked to the geographic variation of the unit's lithologies and suggests that we expand our investigations to cover a larger area, perhaps into Pennsylvania or even into equivalent strata in New York.

The trace in question was identified as *Pteridichnites biseriatus*, Clarke and Swartz, 1913 by examination of Butts' (1941) paleontological work on the Paleozoic rocks of the central Appalachians. A literature search yielded a limited number of additional references to *Pteridichnites*, e. g., Woodward's (1943) monograph on the Devonian of West Virginia which mentioned *P. biseriatus* in the Chemung Formation and Yang's (1984) description of another species, *P. sintanensis* from the Silurian of China.

The ichnofossil *Pteridichnites biseriatus* was first described from the Woodmont shale member of the Upper Devonian Jennings Formation of Maryland (Clarke and Swartz, 1913a). "The Jennings formation consists of interbedded shales and sandstones. . . in Maryland, the study of which presents great difficulties. This is due in part to the great variability in the composition of the sediments. Sandstones and shales succeed each other at frequent intervals in vertical sequence, while beds of sandstones that appear very massive at one locality may pass into a series of sandstones and shales, or *vice versa*, rendering it very difficult to discover persistent horizons in them." (Swartz, 1913, p. 410).

The stratigraphic uncertainties noted by Swartz still cause confusion in the outcrop belt in eastern West Virginia and northwestern Virginia. In Maryland, the name "Jennings Formation" has been abandoned and its members, the Brallier, Chemung, and Hampshire, have been elevated to the status of formations (Patchen, and others, 1984). In addition, the name "Chemung Formation" has been abandoned and replaced, in part, by the Greenland Gap Group in which the Foreknobs Formation is the uppermost member (Dennison, 1970). It is clear from previous work (Dennison, 1970; 1988; 1996), that the Brallier, Greenland Gap Group, and Hampshire succeed each other in vertical sequence as a result of a seaward progradation of terrestrial deposits. All observed formation contacts are either gradational or interfingering. But, as noted previously by Swartz (1913), extensive lateral and vertical variation of lithologies within individual formations is pervasive. As a result, it is difficult to be certain of formation boundaries where good exposures are infrequent and the nature of contacts may be obscured by later structural deformation.

Although the Foreknobs Formation is considerably sandier, the Brallier and Foreknobs contain similar lithologies, i. e., brown to greenish-grey siltstones and shales that weather to a light tan color. Whether fresh or weathered, these fine-grained strata in isolated outcrops are nearly indistinguishable and not readily assignable to formation. Unique sedimentological features or laterally persistent marker beds would greatly facilitate correct and confident identification of isolated outcrops of the two formations. Indeed, Clarke and Swartz (1913a) and others (Eugene Rader, Virginia Division of Mineral Resources, personal communication, 1999) observed fossiliferous lag deposits within the Foreknobs dominated by crinoid fragments. Unfortunately, these fossiliferous zones are poorly exposed or absent within much of our study area and only become common and of stratigraphic utility on the eastern and southern margins.

AN ICHNOFOSSIL AS A STRATIGRAPHIC MARKER?

We have noted, as did Clarke and Swartz (1913a) in Maryland and Rossbach and Hall (1998) in West Virginia, that the ichnofossil *Pteridichnites biseriatus* is extremely abundant in the siltstones and shales of the lower Brallier Formation. Although similar lithologies occur in the overlying Foreknobs Formation, we have found few specimens of *P. biseriatus* within that unit. Based on this fact, we have been able to assign isolated exposures to the Brallier Formation when *P. biseriatus* is present in large numbers. While the idea of using an ichnofossil for stratigraphic rather than paleonenvironmental purposes may seem dubious, we suggest, that for field mapping purposes, *P. biseriatus* can serve as a guide fossil when found in abundance because this abundance- or acme-zone corresponds consistently to the lower Brallier Formation (see Figure 2). Although *P. biseriatus* is restricted to a particular set of lithofacies, its acme-zone also appears to be limited in stratigraphic range and can serve as a local stratigraphic indicator and correlative.

ICHNOFOSSIL *PTERIDICHNITES BISERIATUS*

Description

Clarke and Swartz (1913a, p. 545-546) (see Figure 4a) described *P. biseriatus* as "Imprints consisting of two parallel grooves with raised borders, divided by narrow transverse ridges into shallow, nearly square or slightly rounded pits, which commonly alternate in position. The median ridge dividing the two grooves is not straight but is crenulated by slight inflections directed toward the transverse ridges. Length and width of pits subequal. The impressions usually become faint toward their ends and are often curved.

Width of track about 4 mm., diameter of pits about 2 mm. Tracks are several centimeters long. Similar tracks are abundant in the beds containing the Naples fauna in New York."

We add the following observations. Impressions may be preserved as either epireliefs or hyporeliefs on bedding surfaces. Impressions tend to decrease in preserved detail with increasing grain size. Indeed, in siltier material, the pits noted for the type specimen may disap-

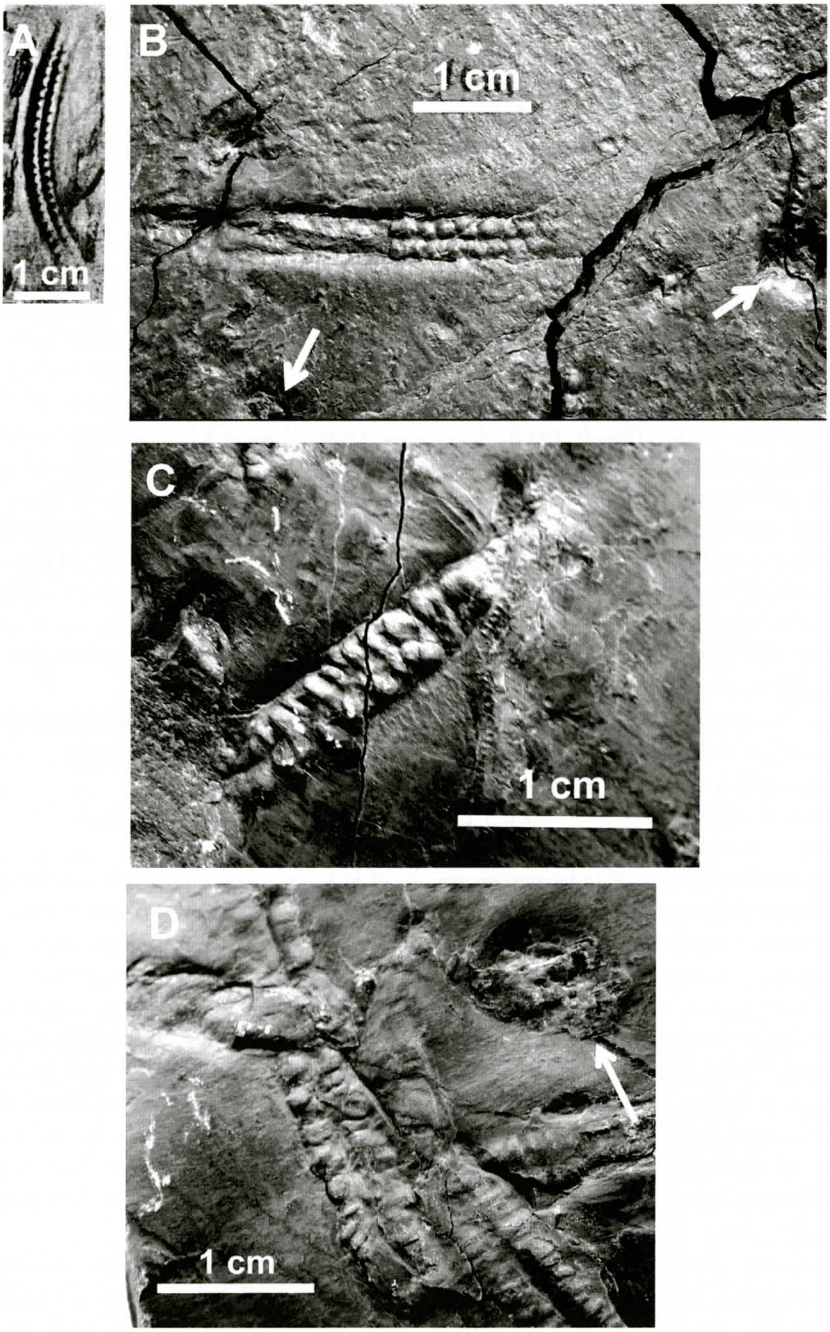

FIGURE 4 – a-d. Examples of *Pteridichnites biseriatus*. A. Scanned image of the type specimen of *P. biseriatus* from Clarke and Swartz (1913b, Plate XLVI – 6). Specimen is from the Woodmont Member of the Jennings Formation from Tonoloway, Maryland. 4b,c,d from the Brallier Formation north of Elkins, West Virginia. B. Hypichnial cast of *P. biseriatus*. Possible impressions of the oral area of the tracemaker are indicated with arrows; C. Hypichnial cast of *P. biseriatus*. Trace appears to have been superimposed on the crawling trace of a small arthropod; D. Hypichnial casts of *P. biseriatus*. Two separate traces are present in close proximity. Possible impression of the oral area of the tracemaker is indicated with an arrow.

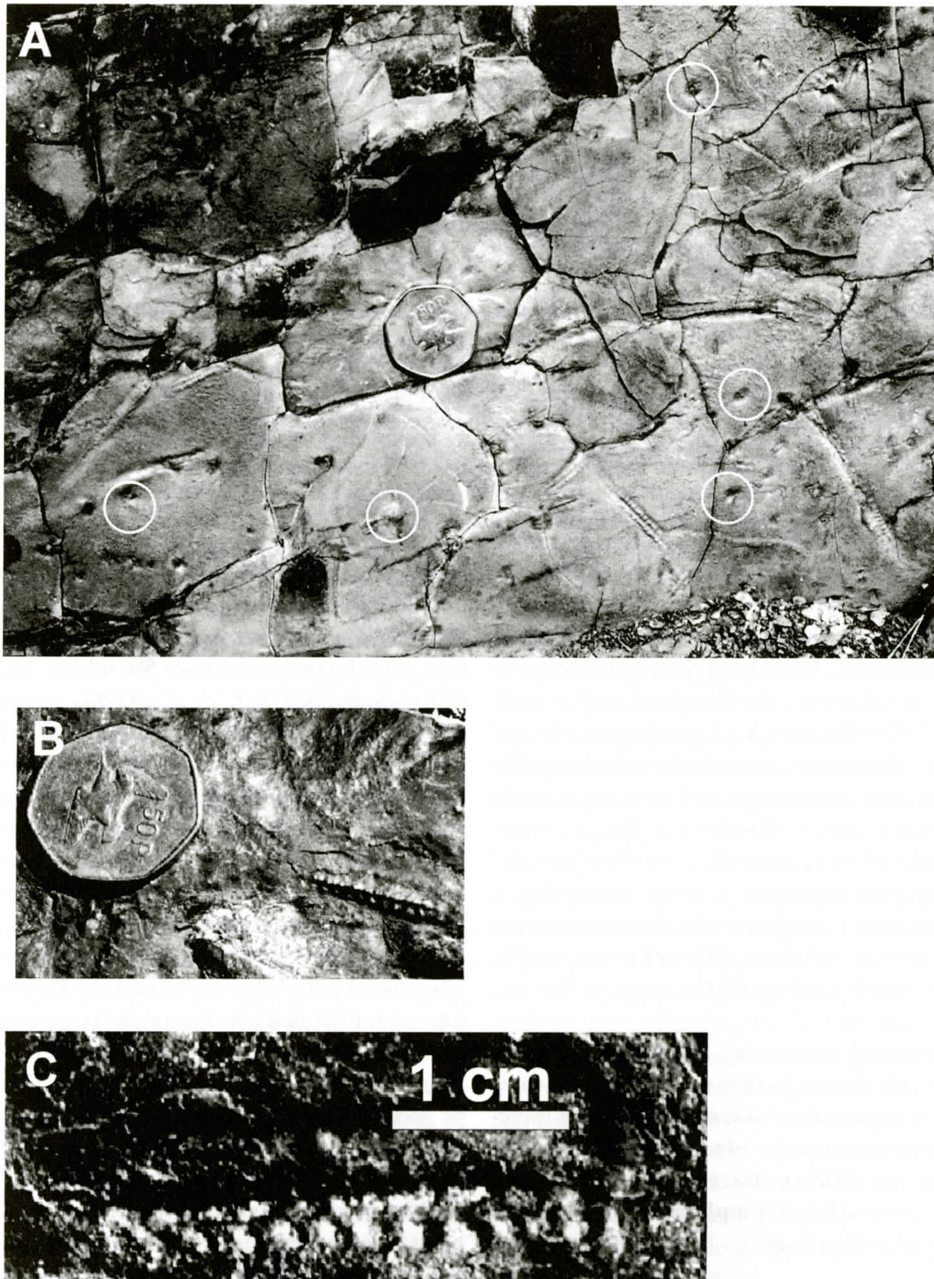

FIGURE 5 – a-c. Additional examples of *P. biseriatus*. 5a from the Brallier Formation south of Circleville, West Virginia. A. Underside of bedding surface with numerous examples of *P. biseriatus* and possible impressions of the oral area (white circles) of the tracemaker. Coin is 3 cm in diameter. 5b, c from the Brallier Formation north of Elkins, West Virginia. B. Cast of the ambulacral surface and side of one arm of an unidentified echinoderm. Because the arm has a distinct taper, the maker of the impression is thought to have been an asterozoan. This impression is probably best classified as a *sitzmark* (the product of unintentional contact between the organism and the bottom sediment) rather than an ichnofossil. Coin is 3 cm in diameter; C. Enlargement of 5b showing more detail.

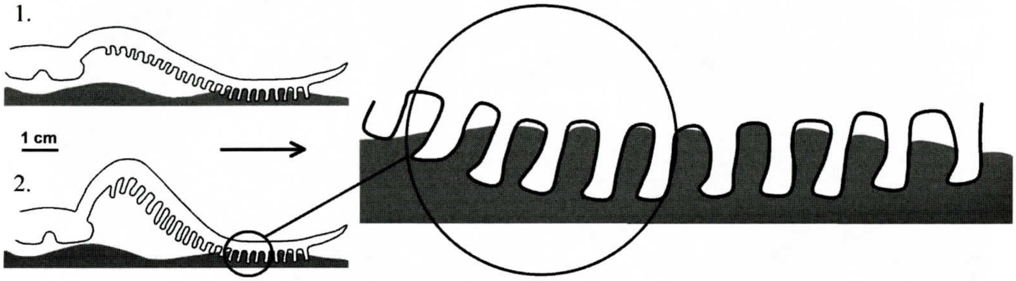

FIGURE 6. Proposed formation of *Pteridichnites biseriatus* by the action of ophiuroid tube feet during locomotion: 1) Ophiuroid anchors tube feet at the distal end of one arm in the bottom sediment; 2) ophiuroid arches the arm and at the same time pulls its body forward. Enlargement of the anchored tube feet shows that the bottom of each foot distorts as the foot attempts to maintain its position within the sediment. This produces a small *bulge* in the sediment adjacent to each foot. Original illustration by McDowell.

pear altogether leaving only the parallel grooves and the medial ridge. Furthermore, there appears to be a significant variation in the shape of pits from specimen to specimen. In some specimens, the pits are perfectly circular (see Figure 4a – Clarke and Swartz's type specimen); in others, pits are elongated, with a small mound of sediment at one end (Figures 4b and 4c); in still others, pits disappear altogether leaving only the mounded sediment observed in the second variant. However, in this last form, mounds of sediment may be compressed against each other into a shape resembling a stack of coins (see Figure 4d). The discussion as to whether or not these different forms qualify as new species is beyond the scope of this paper.

Individual traces may be straight, slightly curved, or arcuate but are never observed to be sinuous or to curve back in the opposite direction. Traces are never observed to bifurcate or branch but different traces may intersect and cross each other. Complete traces range in length from 2 to 6 cm.

Origin and Interpretation

Clarke and Swartz (1913a, p. 545) suggested that *Pteridichnites biseriatus* was "probably the tracks of crustaceans or possibly of annelids." However, along with the illustration of the type specimen of *P. biseriatus*, Clarke and Swartz (1913b, Plate XLVI) also figured a new species of asterozoan, *Paleaster clarki*, Clarke and Swartz, 1913a. The arms of this starfish are similar in dimensions to *P. biseriatus.* Based on our examination of specimens of *P. biseriatus* and an isolated impression of what appears to be a starfish arm (see Figures 5b and 5c), we initially speculated that *P. biseriatus* was produced by an asterozoan similar to *P. clarki.* The medial ridge of *P. biseriatus* might correspond to the ambulacral groove and the pits on each side of the medial ridge might correspond to the impressions of individual tube feet. *P. biseriatus* would then become the imprint of undersurface of an asterozoan arm and its tube feet.

It should be noted that *P. biseriatus* is a true ichnofossil rather than a *sitzmark* (an incidental impression created when an organism comes into accidental contact with bottom sediment). Many specimens of *P. biseriatus* (see Figures 4c and 4d) show an intentional modification of the substrate. Tube feet appear to have been pushed downward into the sediment and then pushed *backward* against the enclosing sediment (Figure 6) perhaps in an attempt to propel the tracemaker forward or hold its position against current. The three distinct variants of *P. biseriatus* (Figures 4 and 7) appear to be related to how extensively the individual tube feet have modified the sediment surface.

Subsequently, upon examination of several specimens of the *P. biseriatus* supplied by the authors, Thomas Kammer of West Virginia University noted (personal communication,

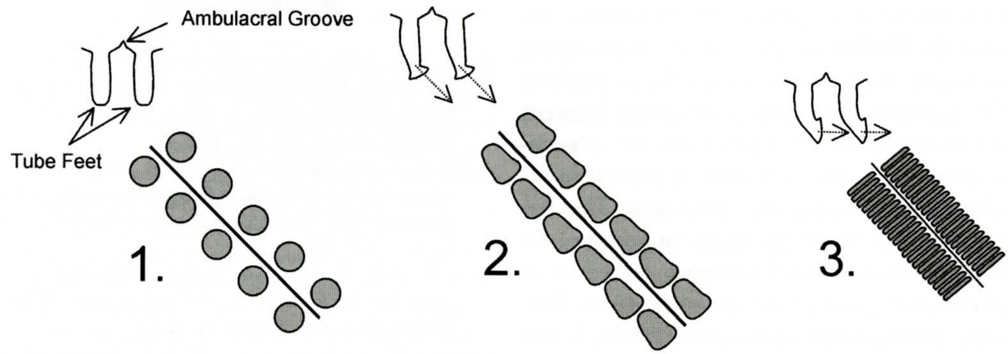

FIGURE 7. Action of tube feet and the resulting variations in *Pteridichnites biseriatus*: 1) Tube feet simply inserted into the bottom sediment and then removed - no distortion in the outline of the imprint of individual feet (see the type specimen, Figure 4a); 2) tube feet inserted, pushed against the sediment, and then removed - imprints of individual feet are elongated and a small mound of sediment forms at the rear of each imprint (see Figures 4b and 4c); 3) tube feet inserted, ends of feet rotated ~90° and pushed against the sediment, tube feet removed, entire process is repeated several times - sediment is forced into a configuration resembling a stack of coins lying on edge (see Figure 4d). Original illustration by McDowell.

2001) the presence of possible imprints of the mouth area of the tracemaker (Figures 4b and 4d) in association with *P. biseriatus* and suggested that the tracemaker was an ophiuroid rather than an asterozoan. Closer examination of existing specimens and recovery of new material led us to concur and speculate that this is the reason that impressions of the rows of tube feet in specimens of *P. biseriatus* do not typically converge or taper at one end (as opposed to those of an asterozoan as seen in Figures 5b and 5c). It should be noted that we have never recovered echinoderm body fossils from the Brallier formation. Indeed, body fossils of any kind are rare in the Brallier (Avary, 1978; Avary and Dennison, 1980) and the chances of finding preserved ophiuroid remains are probably even more unlikely than for an asterozoan.

Multiple specimens of *P. biseriatus* have been observed on bedding surfaces (see Figure 5a). Contrary to what might be expected if the tracemakers were responding to a strong, unidirectional bottom current, there does not appear to be a consistent orientation of *P. biseriatus* along the bedding horizon. This forces us to conclude that *P. biseriatus* is more likely to be a locomotion trace rather than an *anchoring* or resting trace.

As pointed out by one of the paper's reviewers (Philip Novack-Gottshall, personal communication, 2006), if *P. biseriatus* is the product of an ophiuroid or an asterozoan, the lack of pentameral symmetry in the impressions of arms, especially in association with possible feeding marks, seems contradictory. We would offer the observation that intact bedding surfaces containing multiple *P. biseriatus* are commonly marked by very small (less than 1 cm. in height), broad ripples. The irregular topography of this sediment surface may have precluded the preservation of the imprints of all five arms. Alternatively, as illustrated and discussed by Schäfer (1972, Figure 117, p. 210), the typical mode of ophiuroid movement is by *single-arm locomotion* where one arm propels the organism (see Figure 6) and the remaining arms trail behind. This may help explain the predominance of single *P. biseriatus* even in conjunction with mouth impressions, especially if the tracemaker was feeding opportunistically as it moved across the bottom.

CONCLUSIONS

Pteridichnites biseriatus is restricted both sedimentologically and stratigraphically within the Upper Devonian strata of the central Appalachian region. It is notably abundant in the lower Brallier Formation. Where outcrop exposure of this unit is limited and discontinuous and where there is a possibility of confusion between the Brallier and portions of the overlying Foreknobs strata, the presence of large numbers of *P. biseriatus* may help discriminate between the two formations. It appears that a *P. biseriatus* abundance- or acme-zone is present in the lower Brallier within the study area. This has been found to be of particular importance for the purposes of bedrock mapping. However, as pointed out by one of the reviewers (John Dennison, personal communication, 2006), Upper Devonian siliciclastic strata are extremely variable geographically, so the occurrence of *P. biseriatus* needs to be investigated over a wider area before it can be given more than local stratigraphic utility.

Although originally proposed as the crawling traces of arthropods or polychaetes, examination of numerous, well-preserved specimens of the ichnofossil *P. biseriatus* suggests that it is the result of the activities of an echinoderm, specifically, an unidentified ophiuroid. The ichnofossil represents the attempt of such an organism to move across or hold its position on a substrate of soft consistency, perhaps while feeding. *P. biseriatus* is in large part a locomotion trace and, to a lesser extent, a resting trace.

ACKNOWLEDGEMENTS

Our geological investigations were performed under STATEMAP contracts 97HQAG01713, 98HQAG2069, 99HQA60050, 00HQAG0050, 01HQAG0040, 02HQAG0046, 03HQAG0051, 04HQAG0078, and 05HQAG0055. Funding from the USGS is gratefully acknowledged. The authors wish to thank Tom Kammer, for his suggestions as to the identity of the tracemaker for *Pteridichnites biseriatus*. The authors also acknowledge critical and thorough reviews of initial versions of this paper by Mitch Blake, Michael Hohn, Andy Rindsburg, John Harper, and Tom Rossbach. Finally, we wish to thank John Dennison and Philip Novack-Gottshall for thought-provoking reviews of the final version of this paper which significantly improved its content and clarity.

REFERENCES

Avary, K. L., 1978, Stratigraphy and sedimentology of the Back Creek Siltstone (Devonian) in Virginia and West Virginia: unpublished M. S. Thesis, University of North Carolina, Chapel Hill, NC, 89 p.

Avary, K. L. and Dennison, J. M., 1980, Back Creek Siltstone member of Devonian Brallier Formation in Virginia and West Virginia: Southeastern Geology, v. 21, no. 2., p. 121-153.

Butts, C., 1941, Geology of the Appalachian Valley in Virginia, Part II - Fossil plates and explanations: Virginia Geological Survey Bulletin 52, 271 p.

Clarke, J. M. and Swartz, C. K., 1913a, Systematic paleontology of the Upper Devonian deposits of Maryland: *in* Maryland Geological Survey, Middle and Upper Devonian Volume, p. 535-701.

Clarke, J. M. and Swartz, C. K., 1913b, Systematic paleontology of the Upper Devonian deposits of Maryland: *in* Maryland Geological Survey, Devonian Plates, 156 p.

Cole, S. L., and McDowell, R. R., 2003, Implications of *Bifungites* from the Upper Devonian of West Virginia, USA: Geological Society of America Abstracts with Programs, v. 35, no. 3, p. 91, abstract.

Crimes, T. P., 1968, *Cruziana*: a stratigraphically useful trace fossil: Geology Magazine, v. 105, p. 360-364.

Crimes, T. P., 1969, Trace fossils from the Cambro-Ordovician rock of North Wales and their stratigraphic significance: Geological Journal, v. 6, p. 333-338.

Crimes, T. P., 1970, The significance of trace fossils in sedimentology, stratigraphy, and paleoecology with examples from lower Paleozoic strata: *in* Trace Fossils, Crimes, T. P. and Harper, J. C., eds., Geological Journal Special Issue, no. 3, Seel House Press, Liverpool, p. 101-126.

Dennison, J. M., 1970, Stratigraphic divisions of the Upper Devonian Greenland Gap Group ("Chemung Formation") along Allegheny Front in West Virginia, Maryland, and Highland County, Virginia: Southeastern Geology, v. 12, p. 53-82.

Dennison, J. M., ed., 1988, Geologic Field Guide: Devonian Delta, East-Central West Virginia and Adjacent Virginia: Appalachian Geological Society, Charleston, WV, 169 p.

Dennison, J. M., ed., 1996, Geologic Field Guide: Devonian Hydrocarbon Stratigraphy of Southeastern West Virginia and Adjacent Virginia: Appalachian Geological Society, Charleston, WV, 160 p.

Hantzschel, W., 1975, Treatise on Invertebrate Paleontology, Part W - Miscellanea, Supplement 1, Trace Fossils and Problematica, 2nd Edition, Geological Society of America, Boulder, CO, 269 p.

McDowell, R. R., Matchen, D. M., and Avary, K. L., 2004, Opportunistic geology - staying one step ahead of the hydroseeder: Geological Society of America Abstracts with Programs, v. 36, no. 2, p. 115, abstract.

Patchen, D. G., Avary, K. L., and Erwin, R. B., 1984, Correlation of Stratigraphic Units of North America (COSUNA) – North Appalachian Region Correlation

Chart, American Association of Petroleum Geologists Correlation Chart Series, 1 sheet.
Pemberton, S. G., Frey, R. W., Ranger, M. J., and MacEachern, J. A., 1992, The conceptual framework of ichnology, *in* Pemberton, S. G., ed., Applications of Ichnology to Petroleum Exploration: A Core Workshop, Society of Economic Paleontologists and Mineralogists Core Workshop no. 17, Tulsa, OK, 429 p.
Pemberton, S. G., MacEachern, J. A., and Saunders, T., 2004, Stratigraphic applications of substrate-specific ichnofacies: delineating discontinuities in the rock record, *in* McIlroy, D., ed., The Application of Ichnology to Palaeoenvironmental and Stratigraphic Analysis: Geological Society of London, Special Publication no. 228, 490 p.
Rossbach, T. J. and Hall, J. C., 1998, The Late Devonian (Frasnian-Famennian) Extinction Event in the Catskill delta of Virginia and West Virginia: Field Trip Guidebook, Southeastern Section, Geological Society of America, 35 p.
Rutledge, F., McCoy, H, Avary, K., Matchen, D., and McDowell, R., 2002, Preliminary investigation of new exposures of Upper Devonian strata, Elkins, West Virginia: Geological Society of America Abstracts with Programs, v. 34, no. 2, p. 86, abstract.
Schäfer, W., 1972, Ecology and Paleoecology of Marine Environments: University of Chicago Press, Chicago, 568 p.
Seilacher, A., 1960, *Lebensspurren als Leitfossilien*: Geologische Rundschau, v. 49, p. 41-50. (in German)
Seilacher, A., 1970, *Cruziana* stratigraphy of "nonfossiliferous" Paleozoic sandstones: *in* Crimes, T. P. and Harper, J. C., eds., Trace Fossils, Geological Journal Special Issue, no. 3, p. 447-476.
Southworth, C., Gray, K., and Sutter, J., 1993, Middle Eocene intrusive rocks of the central Appalachian Valley and Ridge province - setting, chemistry, and implications for crustal structure: United States Geological Survey, Bulletin 1839-J, p. 1-24.
Swartz, C. K., 1913, Correlation of the Upper Devonian, *in* Middle and Upper Devonian Volume, Maryland Geological Survey, p. 410-439.
Woodward, H. P., 1943, The Devonian System of West Virginia: West Virginia Geological Survey Reports, v. 5, 655 p.
Yang, S., 1984, Silurian trace fossils from the Yangzi Gorges and their significance to depositional environment study: Acta Palaeontologica Sinica, v. 23, no. 6, p. 705-715. (in Chinese)

SOUTHEASTERN GEOLOGY
V. 44, No. 4, February 2007, p. 203-210

QUATERNARY COASTAL DEVELOPMENT IN NW FLORIDA: MISCONCEPTIONS RELATED TO EOLIAN PROCESSES:

DISCUSSION OF A PAPER BY CARL R. FROEDE, JR., BRIAN R. RUCKER AND RICHARD L. GILLAM

ERVIN G. OTVOS

Department of Coastal Sciences, USM,
PO Box 7000
Ocean Springs, MS 39566-7000
ervin.otvos@usm.edu

INTRODUCTION

A recent note by Froede et al. (2006) on the geological evolution of "Santa Rosa Peninsula" between Pensacola Bay and Santa Rosa Sound, NW Florida, regrettably represents a major backward step in the understanding of the Quaternary coastal evolution and stratigraphy of the NW Florida coast. Unfortunately, almost all the conclusions in this confusingly argued paper lack consistency, solid supporting evidence, and appropriate explanations. The paper displays a number of obsolete, irrelevant, and/or incorrectly applied references, among them several of my own publications. At the same time, the paper shuns critical recent material, some of which Froede et al. cite without discussing content. The present communication is intended to shed light on several important topics involved, correcting severely flawed, unsupported conclusions and assumptions in the process. It provides the interested reader with guidance, essential facts and refutes several statements made by Froede and his coauthors.

LATE QUATERNARY GEOLOGICAL DEVELOPMENT AND STRATIGRAPHIC UNITS

LATE PLEISTOCENE

While none of the Pleistocene stratigraphic units, defined and described by name and specific age in my earlier publications (Otvos, 1997, 2004) are reproduced in the Froede paper, they have been routinely and consistently utilized in the coastal literature during the last thirty years.

The oldest late Pleistocene units, the transgressive fossiliferous nearshore-to-estuarine Biloxi Formation and the Gulfport Formation of the Sangamon Interglacial sea-level highstand at ca. +7 m, and composed of regressive barrier strandplain ridges do not outcrop in the Santa Rosa Peninsula proper but are buried in the shallow subsurface under younger units. Following the Sangamon, in the Wisconsin a major sea-level decline took place. During the Wisconsin arid climate phases the Gulfport ridges and other exposed surface units were partially reworked into eolian dunes. Throughout this glacial stage the shoreline was located well south of its current position. The dunes could not have been impacted by shore erosion. In addition, early Holocene dune dates (Otvos, 2004) indicate limited dune formation and/or reworking from Wisconsin eolian deposits during arid phases between 9-6 ka B.P. The Gulfport Formation was buried under an almost continuous blanket of Wisconsin eolian sandsheets, parabolic, and other types of sand dunes, as also observed in SE Alabama and the eastern Florida Panhandle {Otvos, 2004).

A Sangamon interglacial luminescence age of 116,000 yr B. P. was obtained from the cross-stratified lower part of the northern dune scarp exposure at "Butcherpen Cove" on Pensacola Bay in the Naval Like Oaks Reservation. The unconformity between the Sangamon and Wisconsin intervals has been masked by slump and rainwash deposits that, except after storm-scarping of the bottom interval, usually cover most of the bluff face (Otvos, 1997, 2004, 2005). Several luminescence dates were obtained from Wisconsin dunes in the northwestern and east-central coastal areas of the Florida Panhandle.

Mixing various facts that pertain to Sangamon interglacial and Wisconsin deposits and glacial geological conditions, without their appropriate analysis, Froede et al. assume that the large isolated (Wisconsin age) "sand dunes and ridges" along portions of the peninsula were likely initiated along shoreline associated with elevated sea-levels. Because of the distance from the mainland seashore at the time of lowered Wisconsin-early Holocene sea-levels, it would be absurd to assume with Froede et al. (pp. 87, 90) that storm washovers could have contributed to the degradation of Wisconsin dunes. Neither could landform-impacting human activity be implicated ca. 40-21 thousand years ago (Otvos, 2004, p. 106) when no humans yet lived anywhere in the Americas. Significant native activity resulting in such an influence was nonexistent until the late Holocene, at the earliest. Equally unfounded and unreasonable is Froede's curious speculation that an eolian process could have *combined* linear (Sangamon Interglacial) barrier strandplain ridges into "larger coastal (Wisconsin!) dune ridges." While at one point Froede et al. maintain that in its present configuration Santa Rosa Peninsula reflects a relatively *stable* high former sea-level; elsewhere in their paper the authors emphasize *sea-level changes* in the development of the Peninsula.

This overall stratigraphic ambiguity goes back to the refusal to acknowledge previous publications on the "Butcherpen Cove" dune bluff exposure and adjacent Quaternary eolian deposits on the mainland coastal plain (Otvos, 1997, 2004, 2005). Most curiously, no mention is made about the recently published Sangamon, Wisconsin, and early Holocene luminescence dates, even if the paper where they were published has been cited in their note. Quite to the contrary, Froede states that in the absence of paleontologically-based age designations "remained unchanged even with recent geological mapping." Considering the verbiage, this concealed, **silent** rejection of, even refusal to debate the use of numerical dates may not be related to scientific considerations but to an ideological stance against the use of geochronologically derived absolute dates. The silty sands and sands of the alluvial Sangamon-Wisconsin Prairie Formation that underlies a gently seaward-sloping flat surface occur in the surface landward of the buried Gulfport strandplain in the Pensacola city and Pensacola Bay area.

PRESENT COASTAL CLIMATE: WIND EROSION AS CAUSE FOR DUNE MIGRATION AND SCARP DEVELOPMENT?

It is uniformly accepted that as on coasts worldwide, the Pensacola area valley system evolved by processes of fluvial erosion in incised coastal valley systems at a low eustatic sea-level stand. During later Holocene sea-level rise coastal marine processes, associated with wave erosion took over. This resulted in still continuing shore recession. The highest coastal scarps formed along valleys cut in the most elevated sectors of the Citronelle Upland surface. High bluffs on Santa Rosa Peninsula's north (bay) and south (Santa Rosa Sound) shore (see: Fig. 1, in Froede et al.) and elsewhere also formed where the receding shoreline truncated high Wisconsin dune ridges. The terms *cliff ("cliff scarp")* and *escarpment* are misused by Froede et al.: cliffs are cut into rocks *not* in soft sediments. Escarpments are *long*, steep-to-vertical faces, cut into in rocks, possibly also in well-consolidated sediments (Neuendorf et al., 2005).

In Froede's novel assumption, proferred without adequate reasoning, shore recession and southward-directed dune migration is the result of eolian erosion by northerly surface winds. This was claimed as the dominant wind direction in the area. Wind channeled through valleys in this theory was powerful enough to move sand grains from the bare sandy bluff face over the razor-narrow top of the 15 m high dune crest, avoiding lower dune surfaces where sand could more easily settle. Strong north winds of this magnitude occur briefly and very rarely during the passage of the most intensive Arctic weather fronts that exist only during the late fall-to-late winter season. In the rest of the year, occasionally even between the passage of winter fronts, S, SE winds are not uncommon. The generally weaker N, NW winds that blow across the lagoons form the low, narrow dunes on barrier island north shores. The more frequent and effective south-southeast winds are responsible for creating the wider and higher island foredunes on the south shores. However, early Holocene north winds occasionally may also be credited with the creation or partial reworking of tall white north-shore sand dunes. This occurred at Gulf Breeze, just west of Naval Live Oaks *Reserve* (not "*Area*").

This is not the case at all in the discussed high north dune. Ripples observed on the bluff face indicate lateral sand transport after windy periods. Sand transfer by slumping and slopewash is downward. An unlikely, nearly vertical upward sand movement by exceptional heavy winds would be stopped, at any rate, by the overhanging root zone and arrested by the heavy forest-shrub vegetation at the upper rim (see Froede's Fig. 5, p. 90). *The oxidized orange-gray and yellowish-gray colors of the Naval Reserve dune lithosome provide the clue to its Pleistocene age.* In contrast, late Holocene dune sands, unoxidized due to limited age, are white. There are no indications for Holocene, let alone Recent dune aggradation and migration.

Where did the Froede claim originate for a recently doubled dune elevation as a result of sand buildup? The bluff truncates the high, relatively long SW arm of a large Wisconsin parabolic dune that originally opened toward the NW. The NE arm became degraded; lowered, and segmented by heavy surface erosion during late Wisconsin and Holocene times. A narrow, steep crest area of this relict SW dune arm rises from +7.5 to +15 m elevation along the bluff (see arrow in Froede et al. Fig. 1) This Pleistocene dune interval was misinterpreted as a still aggrading Recent dune lithosome.

GEOLOGICAL MAPPING AND TERRAIN DESIGNATIONS

In comparison with modern stratigraphy (Otvos, 2004, Table 1), Froede's stratigraphic units are non-specific, incorrect, and outdated in several respects. *First,* the "Quaternary undifferentiated" area (*Qu*) represents the Pleistocene Prairie alluvial surface and sedimentary units. *Second, Qu* and *Qbd* ("Quaternary beach ridge and dune") include various types of eolian deposits underlain in the shallow subsurface by Gulfport strandplain sands. Third, *Qal* ("Pleistocene Quaternary alluvium") again represents Prairie; in narrow adjacent valleys, also Holocene alluvium.

Finally, the topographic delineation between Pleistocene coastal plain deposits and the Citronelle surface is well defined in the area. The + 15 m elevation as the recommended cutoff value between the two surface units is untenable. The tallest Wisconsin dunes rise above 15 m. More significantly, north of Gulfport, MS and of Gulf Shores, AL and at many other Gulf coastal locations where the Formation directly underlies the land surface, the toe of the Citronelle Upland Surface is located at only at +3-6 m above sea-level. The Citronelle Upland Surface occurs *north* of the Pleistocene surface units. Therefore, a Western Highlands designation would be inappropriate in our area.

REFERENCES CITED

Froede, C. R., Jr., Rucker, B. R., and Gillam, R. L., 2006, Eolian development of the Naval Live Oaks dune escarpment, Santa Rosa Peninsula, Florida (USA): *Southeastern Geology,* v. 44, p.85-92.

Neuendorf, K. K. E., Mehl, J. P., Jr., and Jackson, J. A., 2005, Glossary of Geology, Fifth Edition, American Geological Institute, Alexandria, VA., 779 p.

Otvos, E. G., 1997, Northeastern Gulf Coastal Plain Revisited. Neogene and Quaternary Units and Events- Old and New Concepts, Second Day, Stop 2: *Guidebook, Gulf Coast Association of Geological Societies Annual Meeting*, New Orleans, New Orleans, 143 p.

Otvos, E. G., 2004, Prospects for interregional correlations using Wisconsin and Holocene aridity episodes, northern Gulf of Mexico coastal plain: *Quaternary Research,* v. 61, p. 105-118.

Otvos, E. G., 2005, Gulf Coast Geology, *Field Trip 4,* Stop 7, *in*: Geological Society of America 54th Annual Meeting of the Southeastern Section, M. A. Meylan, Editor, p. 63-115.

SOUTHEASTERN GEOLOGY
V. 44, No. 4, February 2007, p. 206-210

REPLY TO ERVIN G. OTVOS: "QUATERNARY COASTAL DEVELOPMENT IN NW FLORIDA: MISCONCEPTIONS RELATED TO EOLIAN PROCESSES"

CARL R. FROEDE JR.

United States Environmental Protection Agency
Region 4
61 Forsyth Street
Atlanta, GA 30303-8960

BRIAN R. RUCKER AND RICHARD L. GILLAM

INTRODUCTION

My co-authors and I appreciate the opportunity to address and clarify issues raised by Dr. Otvos regarding our recently published paper (Froede and others, 2006). Apparently, we differ in many ways with him over relevant data and its interpretation. Since many of Otvos' difficulties appear to be with information from the Florida Geological Survey, we will simply note those areas and address only the issues directly pertinent to our analysis. While we recognize Dr. Otvos' experience and expertise, we respectfully disagree with his assertions regarding our work.

LATE QUATERNARY GEOLOGICAL DEVELOPMENT AND STRATIGRAPHIC UNITS - LATE PLEISTOCENE

Otvos stated that our work was deficient because it did not prominently feature his recent publications. It was not our intention to slight his work and we incorporated and cited them accordingly. We did not attempt to reconcile Otvos' more recent work (e.g., Otvos, 2004, 2005) with that of the Florida Geological Survey. The geologic map that we used for the Naval Live Oaks Area was obtained from the survey's web-page (please see our original Figure 2). If Otvos believes that this geologic map is inaccurate, then he should convince the Florida Geological Survey to revise it - especially if they are ignoring his thirty years of relevant coastal research.

Otvos misrepresents our chronology. In brief, the Santa Rosa Peninsula was developed during the Pleistocene, as shown in our original Figure 2. Quartz sand dunes also formed along the Peninsula during this Epoch. The southeastward migration of the Naval Live Oaks Dune would have been initiated with the close of the Pleistocene and the rise of sea level position. We believe that Holocene sea level changes both below and above the present eustatic position also contributed to the southeastward migration of the dune. Even a possible 2.0 m rise in sea level above the present position (see Balsillie and Donoghue, 2004; Fairbridge, 1961, 1976, 1984; Finkl, 1995; Kearney, 2001) would not have made much difference on wind channeling across Pensacola Bay. The northerly wind would transport quartz sand particles up the exposed escarpment and across the top of the dune ridge. We believe that the modern north-to-south predominant wind direction (presented in our original Figure 3) is generally consistent with wind patterns in the past, although we do not know if intensity levels were higher than presently recorded. Various paleo-Indian cultures lived along the Santa Rosa Peninsula (as we originally reported) and we believe that they and the subsequent European inhabitants probably had an impact on its geomorphology, although detailed investigations have not yet been performed. Initial archeological work out on the western Florida Shelf indicates that paleo-Indians may have lived in this area as far back as the late Pleistocene (Garrison, 1992).

Our geologic reconstruction of the history of the Santa Rosa Peninsula did not attempt to integrate Otvos' luminescence age-dates to the divisions previously defined by the Florida Geological Survey. We do not question the applicability, reliability, or relevancy of luminescence as an age-dating technique.

How Old is the Dune?

Otvos believes that the Naval Live Oaks Dune and escarpment are late Pleistocene in age. In his 1997 guidebook, he identifies the Naval Live Oaks Dune escarpment as the "Wisconsinian(?) dune hill on Pensacola Bay" (Otvos, 1997, p. 123). This assumed age was not based on any supporting data provided in his guidebook. In 2004, Otvos reported luminescence age-dates for various quartz sand dunes along the Santa Rosa Peninsula (Otvos, 2004). Two of the samples were analyzed using thermoluminescence techniques (Samples 2 and 3), one was analyzed using the optically stimulated luminescence method (Sample 4), and a location (i.e., B-6) was presented in his Figure 1 that was reported to be a Sangamon barrier with a single age-date of 116 ka (Otvos, 2004). No additional information was conveyed in the document regarding the Sangamon barrier (e.g., age-dating method, standard deviation, lat/long coordinates, quartz properties). In 2005, Otvos (p. 107) identified the Naval Live Oaks Dune as the "Wisconsin dune ridge with Sangamon barrier sand exposure" and he cited a luminescence age date of 116 ka for the lower bluff interval.

He also identified several stratified layers exposed at the Naval Live Oaks Dune escarpment:

> ... thin inclined, gray paleosol horizons that separate individual dune parcels became visible. Slumping still obscures the interface with the overlying very dark-to-pale yellowish-orange, similarly cross-stratified, partially oxidized Wisconsin eolian sands. Secondary oxide/hydroxide-precipitation structures are common. (2005, p. 107)

Once again no data was supplied to defend the idea that the dune escarpment is completely Wisconsinian. From our perspective, only one of the stratified layers has been age-dated (by a single sample) to defend Otvos' dune age assumption.

In our examination of the Naval Live Oaks Dune we noted a significant accumulation of quartz sand at the top of the dune escarpment. This sand was clearly derived from the exposed cliff scarp as it retains the same lithologic properties. The geomorphology of the dune adjacent to Butcherpen Cove suggests a southeastward migration (please see our original Figure 1). Surface wind patterns from two nearby airports were also analyzed and they indicate that the predominant wind direction is from the north. All of these data indicate that the dune has been slowly migrating to the south-southeast and it continues to do so today. While the lower section of the dune escarpment is late Pleistocene (or possibly even older) the upper portion reflects dune migration through the Holocene.

Sample Size For Defining the Geologic History of the Santa Rosa Peninsula

Otvos places a great deal of interpretative weight on what we believe to be an unrepresentative number of samples and sample locations. He reported four luminescence samples from various sand dunes along the entire 32-kilometer-long Santa Rosa Peninsula (Otvos, 2004). From these four sample locations he reconstructs the geologic history of the Peninsula along with wind direction, aridity episodes, wet periods, and changing sea level positions (Otvos, 2004, 2005). We believe that Otvos' geologic assessment of the history of the peninsula extends well beyond the scope of his data.

The age range of the four luminescence samples also causes us some concern. They extend from the Holocene (6.87 ± 0.7 ka) to the Sangamon (116 ka). In fact, Otvos' (2004) age-dates appear to indicate an age progression opposite to what is expected from longshore drift. We are not familiar enough with luminescence dating to determine what factors might create problems with this methodology and further investigation is likely warranted. However, even if the dates are valid, we fail to see any statistical relevance to a four-sample data set with

Table 1. Climatic wind data for the Pensacola Naval Air Station from 1930 to 1996 period (NOAA, 1998). Prevailing wind direction (DIR) is reported in compass points and mean wind speed (SPD) is reported in meters per second. This information is consistent with the wind rose data that we presented in our original Figure 3. Many of the monthly mean wind velocities for this 66-year period exceed Bagnold's (1954) threshold value (i.e., 4.27 m/s) for sand movement. The southward migration of sand up the escarpment and across the top of the dune is supported by decades of wind data.

	JAN	FEB	MAR	APR	MAY	JUN	JUL	AUG	SEP	OCT	NOV	DEC	ANN
DIR	N	N	N	N	N	N	ESE	ESE	ESE	SE	SE	SE	N
SPD	4.47	4.92	4.92	5.36	4.47	4.47	3.58	3.13	4.02	4.02	4.02	4.47	4.47

such a wide range in values used to define the geologic age and history of the entire Santa Rosa Peninsula.

PRESENT COASTAL CLIMATE: WIND EROSION AS CAUSE FOR DUNE MIGRATION AND SCARP DEVELOPMENT?

We would agree with Otvos that the mainland coastal scarps likely formed with the Holocene sea level rise. This same eustatic event truncated the northwestern end of the late Pleistocene age Naval Live Oaks Dune. We believe it was during this same period when channelized northerly wind began to transport dune sands southward on top of the existing dune ridge increasing both its size and elevation.

We used the terms "escarpment" and "cliff scarp" to convey the steepness and size of the dune face exposed adjacent to the water's edge. The terms are clear within the context of the paper (please see our original Figure 5). Words such as "scarp" and "dune face" fail to relate the large-scale steep sand surface exposed along Butcherpen Cove. We apologize if that context was not clear to Otvos.

We examined surface wind data that was collected hourly by the National Weather Service over a seven year period from several nearby regional airports. Our wind data set is consistent with past records for this same area (Table 1). Otvos questions our use of this data set based on his examination of cross-bedded dunes on the "south shores" of the adjacent Santa Rosa Island. We believe our Holocene extrapolation of the surface wind data is supported by the geomorphology of the Naval Live Oaks Dune and escarpment. The northerly wind velocity at times far exceeds Bagnold's (1954) threshold value to transport sand up the escarpment (as we previously reported). The accumulation of sand atop the dune demonstrates this ongoing process (Figure 1).

We apologize for any confusion caused by the use of "Naval Live Oaks Area" vs. "Naval Live Oaks Reservation." Although the National Park Service originally referred to our study area as the Naval Live Oaks Reservation (National Park Service, 1978), it has in subsequent years been known by both appellations. A quick Internet search using both terms will confirm our position.

Otvos states that lateral sand ripples on the dune escarpment dismiss the south-southeastward migration of the dune. The wind rose diagrams that we presented do not reflect a continual north-to-south wind direction. Obviously, the wind patterns are seasonal and Otvos is well aware of this. No further comment will be offered.

Otvos claims that the presence of "oxidized orange-gray, yellowish-gray color" sands defends his Pleistocene age for the Naval Live Oaks Dune escarpment. We find this lithostratigraphic suggestion unsupported and believe that his Wisconsin age presumption should be defended using paleontological, palynological, or luminescence dating methods.

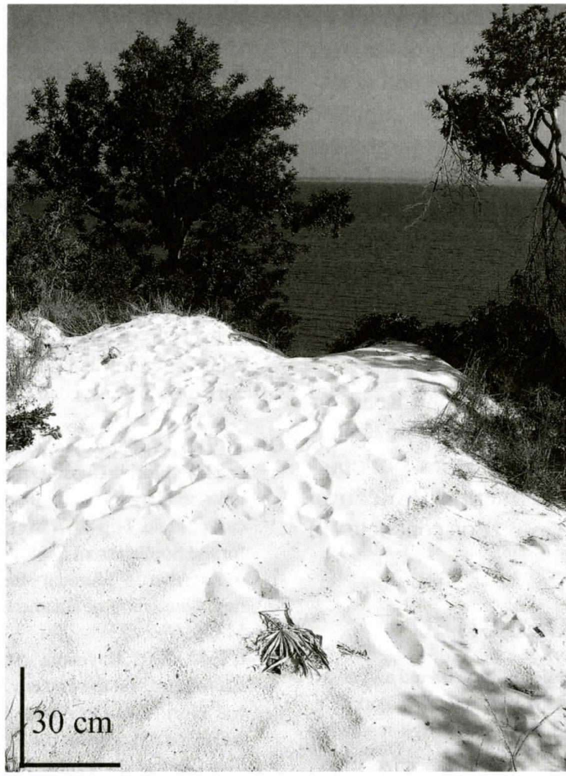

Figure 1. Quartz sand grains continue to accumulate at the top of the dune as northerly winds transport material up the dune escarpment. This particular location is the highest point of the dune (N 30° 22.082; W087° 08.731). The image faces north looking back across Pensacola Bay. Scale bar is 30 cm.

GEOLOGICAL MAPPING AND TERRAIN DESIGNATIONS

Otvos raises numerous stratigraphic and geomorphic questions that essentially reflect discrepancies between his work and that published by the Florida Geological Survey. These arguments do not appear to be germane to our paper and we look forward to their resolution by coastal researchers. Similarly, our delineation between the Western Highlands and Coastal Lowlands was cited from Scott (2005), and we have seen no compelling evidence to reject his work.

CONCLUSIONS

We disagree with Otvos' claim that our work was severely flawed by unsupported conclusions. Our article drew from geologic work reported within the past five years by the Florida Geological Survey. We presented photographic evidence as to the size and scale of the Naval Live Oaks Dune escarpment exposed at Butcherpen Cove. Seven years of wind data collected hourly by the National Weather Service from the closest two airports (many more wind data sets were examined from nearby airports) document a predominant north-to-south surface wind pattern. These winds from the north **continue** to transport sand up the escarpment, adding to the material accumulating atop the highest point of the dune (Figure 1). We encourage anyone interested to visit this site and witness this ongoing process for themselves.

Otvos contends that the Naval Live Oaks Dune is a large Wisconsinian dune that is slowly eroding away (Otvos, 1997, 2005). Our analysis of the feature suggests that while the original dune was developed during the Pleistocene, it has expanded in size and elevation by subsequent south-southeastward migration over the existing dune. Sea level changes and northerly winds throughout the Holocene supplied the forces necessary to develop this prominent topographic feature. We believe that the Naval Live Oaks Dune will continue to migrate slowly southeastward as long as the wind patterns remain consistent in both direction and intensity.

ACKNOWLEDGMENTS

We thank Jerry Akridge and John Reed for their helpful comments and review of our letter. This work neither represents the views or opinions of the U.S. Environmental Protection Agency, nor was this investigation conducted in any official capacity.

REFERENCES CITED

Bagnold, R.A., 1954, The physics of blown sand and desert dunes: William Morrow and Company, New York, NY.

Balsillie, J.H., and Donoghue, J.F., 2004, High resolution sea-level history for the Gulf of Mexico since the last glacial maximum: Report of Investigations 103, Florida Geological Survey, Tallahassee, FL.

Fairbridge, R.W., 1961, Eustatic changes in sea level, *in* Ahrens, L.H., Press, F., Raukawa, K., and Runcorn, S.K., eds., Physics and chemistry of the Earth, v. 4: Pergamon Press, New York, NY, p. 99-185.

Fairbridge, R.W., 1976, Shellfish-eating preceramic Indians in coastal Brazil. Science, v. 191, p. 353-359.

Fairbridge, R.W., 1984, The Holocene sea-level record in south Florida, *in* Gleason, P.J., ed., Environments of south Florida: present and past II: Miami Geological Society, Miami, FL, p. 427-436.

Finkl, C.W., Jr., 1995, Holocene cycles: climate, sea levels, and sedimentation: Journal of Coastal Research Special Issue No. 17, Fort Lauderdale, FL.

Froede, C.R., Jr., Rucker, B.R., and Gillam, R.L., 2006, Eolian development of the Naval Live Oaks Dune escarpment, Santa Rosa Peninsula, Florida (USA): Southeastern Geology, v. 44(2), p. 85-92.

Garrison, E.G., 1992, Recent archaeogeophysical studies of paleoshorelines of the Gulf of Mexico, *in* Johnson, L.L., ed., Paleoshorelines and prehistory: An investigation of method: CRC Press, Boca Raton, FL, p. 103-116.

Kearney, M.S, 2001, Late Holocene sea level variation, *in* Douglas, B.C., Kearney, M.S., and Leatherman, S.P., eds., Sea level rise: history and consequences: Academic Press, New York, NY, p. 13-36.

National Park Service., 1978, General management plan and development concept plan; Gulf Islands National Seashore; Mississippi–Florida: Denver Service Center, Denver, CO.

NOAA, 1998, Climatic wind data for the United States: National Climatic Data Center, Asheville, NC, Accessed from: www5.ncdc.noaa.gov/documentlibrary/pdf/wind1996.pdf.

Otvos, E. G., 1997, Northeastern Gulf Coastal Plain revisited, Neogene and Quaternary units and events - old and new concepts, *in* Stephens, B., and Easley, D.H., eds., Louisiana to northwest Florida field trip guidebook: Gulf Coast Association of Geological Societies Annual Meeting, New Orleans Geological Society, New Orleans, LA.

Otvos, E. G., 2004, Prospects for interregional correlations using Wisconsin and Holocene aridity episodes, northern Gulf of Mexico coastal plain: Quaternary Research, v. 61, p. 105-118.

Otvos, E. G., 2005, Revisiting the Mississippi, Alabama, and NW Florida Coast–Dated Quaternary Coastal Plain units and landforms: Evidence for a revisited sea-level curve, Field Trip 4, *in* Meylan, M.A., ed., Guidebook for the Southeastern Section of the Geological Society of America 54th Annual Meeting: Department of Geology, University of Southern Mississippi, Hattiesburg, MS, p. 63-115.

Scott, T. M., 2005, Revisions to the geomorphology of Florida focusing on the Eastern Panhandle and North-Central Florida, *in* Copeland, R., compiler, Geomorphic influence of scarps in the Suwannee River Basin: Field Trip Guidebook No. 44: Southeastern Geological Society, Tallahassee, FL, p. 18-36.

SOUTHEASTERN GEOLOGY
Duke University
Box 90233
Durham, NC 27708-0233

Returned Service Requested

BELK LIBRARY
SERIALS DEPT
APPALACHIAN STATE UNIVERSITY
PO BOX 32026
BOONE NC 28608